

# Aspects of superradiant scattering off Kerr black holes

**José Sá**

Mestrado em Física

Departamento de Física e Astronomia

2017

## **Orientador**

[João Rosa](#), Professor Auxiliar Convidado, [Faculdade de Ciências da Universidade do Porto](#)

## **Coorientador**

[Orfeu Bertolami](#), Professor Catedrático, [Faculdade de Ciências da Universidade do Porto](#)

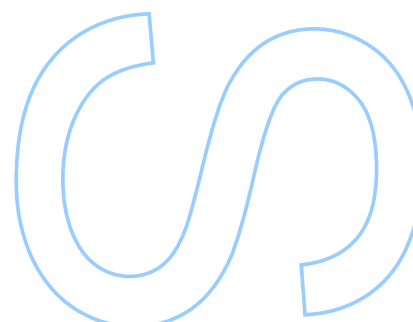
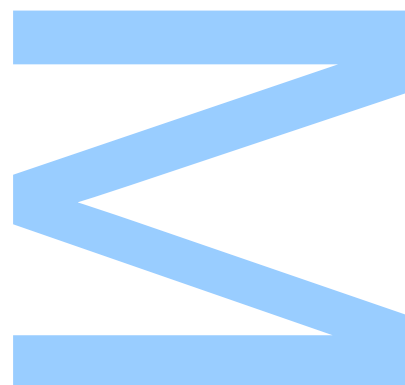




Todas as correções determinadas  
pelo júri, e só essas, foram efetuadas.

O Presidente do Júri,

Porto, \_\_\_\_/\_\_\_\_/\_\_\_\_



UNIVERSIDADE DO PORTO

MASTER'S THESIS

---

# Aspects of superradiant scattering off Kerr black holes

---

*Author:*

José SÁ

*Supervisor:*

João ROSA

*Co-supervisor:*

Orfeu BERTOLAMI

*A thesis submitted in fulfilment of the requirements  
for the degree of Master of Science*

*at the*

Faculdade de Ciências da Universidade do Porto  
Departamento de Física e Astronomia

September 2017

# *Acknowledgements*

Some text...

UNIVERSIDADE DO PORTO

# *Abstract*

Faculdade de Ciências da Universidade do Porto

Departamento de Física e Astronomia

Master of Science

**Aspects of superradiant scattering off Kerr black holes**

by José Sá

The Thesis Abstract is written here (and usually kept to just this page). The page is kept centered vertically so can expand into the blank space above the title too...

UNIVERSIDADE DO PORTO

## *Resumo*

Faculdade de Ciências da Universidade do Porto

Departamento de Física e Astronomia

Mestre de Ciência

**Aspects of superradiant scattering off Kerr black holes**

por José Sá

Tradução em português do “Abstract” escrito em inglês mais a cima. A página é centrada vertical e horizontalmente, podendo expandir para o espaço superior da página em branco ...

# Contents

<b>Acknowledgements</b>	<b>i</b>
<b>Abstract</b>	<b>ii</b>
<b>Resumo</b>	<b>iii</b>
<b>Contents</b>	<b>iv</b>
<b>List of Figures</b>	<b>vi</b>
<b>List of Tables</b>	<b>vii</b>
<b>Abbreviations</b>	<b>viii</b>
<b>1 Superradiance</b>	<b>1</b>
1.1 Introduction . . . . .	1
1.2 Klein paradox as a first example . . . . .	3
1.2.1 Bosons . . . . .	3
1.2.2 Fermions . . . . .	4
<b>2 Kerr black hole</b>	<b>7</b>
2.1 General Relativity . . . . .	7
2.2 Spacetime symmetries . . . . .	9
2.3 Kerr-Child coordinates . . . . .	11
2.4 Boyer-Linquist coordinates . . . . .	14
2.5 Ergoregion and the Penrose process . . . . .	17
<b>3 Teukolsky's master equation</b>	<b>20</b>
3.1 Newman-Penrose formalism . . . . .	20
3.1.1 Kinnersley tetrad . . . . .	21
3.1.2 Maxwell equations . . . . .	23
3.2 Spin-Weighted Spheroidal Harmonics . . . . .	30
3.3 Analytic radial approximations . . . . .	33
3.4 Amplification factor ${}_sZ_{\ell m}$ . . . . .	37
<b>4 Numerical methods</b>	<b>42</b>

4.1	Eigenvalues . . . . .	42
4.1.1	Leaver method . . . . .	43
4.1.2	Spectral method . . . . .	44
4.2	Amplification factor . . . . .	47
<b>5</b>	<b>Superradiant scattering of plane waves</b>	<b>53</b>
5.1	Harmonics decomposition . . . . .	54
5.2	Scattering theory . . . . .	56
5.3	Phase shifts . . . . .	57
<b>6</b>	<b>Discussion and future work</b>	<b>61</b>
<b>A</b>	<b>Tetrad techniques</b>	<b>62</b>
A.1	Noncoordinate representation . . . . .	62
A.2	Spin connection . . . . .	63
<b>B</b>	<b>Additional Newman-Penrose definitions and computations</b>	<b>65</b>
B.1	Spin coefficients . . . . .	65
<b>C</b>	<b>Spin-weighted spherical harmonics</b>	<b>68</b>
<b>D</b>	<b>Eigenvalue small-<math>c</math> expansion</b>	<b>71</b>
	<b>Bibliography</b>	<b>73</b>



# List of Figures

2.1	Contour plots of the surface $r(x, y, z)/a$ for constant values of 0, 1/2, 1, 3/2, in the Kerr-Child coordinates. The left plot is the intersection of the $y = 0$ plane with the 3D representation (right) that spotlights the ring singularity. Dashed curves representing orthogonal constant $\theta(x, y, z)$ hypersurfaces become asymptotically affine. . . . .	13
2.2	Illustration of the Schwarzschild (A,C) and Kerr (B,D) null equatorial in-falling geodesics given by Eqs. (2.26), for $r(0) = 20M$ , with emphasis on $L \neq 0$ . Even starting with opposite angular momentum, the Kerr geodesic (D) is forced to co-rotate with the BH once crossed the ergoregion (dotted). .	17
2.3	Illustration of the Penrose process, with ergoregion (dotted) and event horizon surfaces parameterized in Kerr-Child cartesian coordinates. . . . .	18
4.1	Showcasing discontinuities in the values of ${}_{\pm 1}\mathcal{E}_{\ell 1}$ for $m = 1, 2$ when using incorrect implementation of the Leaver method. Real values of the eigenvalues are shown as dashed lines ( $m = 1, 2, 3$ ) of the same color. . . . .	43
4.2	Eigenvalues for $\ell = 1$ (left) and $\ell = 2$ (right) for typical values of $c$ , using the spectral method. . . . .	46
4.3	Plots of all spin-weighted spheroidal harmonics ${}_{-1}S_{\ell m}(\theta, 0)$ with $\ell = 1$ (left) and $\ell = 2$ (right) for $s = -1$ and $c = 0.4$ . This plot shares the same legend coloring as the above (Figure 4.2). Dotted curves represent the values of the ${}_{-1}Y_{\ell m}$ , when $c \rightarrow 0$ . . . . .	46
4.4	Amplification factor of an extremal BH ( $\mathcal{J} = 0.9999$ ) for modes with $\ell = 1$ . In figure, superradiance occurs only for $m = 1$ as predicted. . . . .	49
4.5	Log plot demonstrating error propagation for ${}_{\pm 1}Z_{53}$ when computing the factor using both numerical solutions for the radial part of $\phi_0$ and $\phi_2$ . . . . .	50
4.6	MoreZPlots . . . . .	52
5.1	Eigenvalues for $\ell = 1$ (left) and $\ell = 2$ (right) for typical values of $c$ , using the spectral method. . . . .	58
5.2	Eigenvalues for $\ell = 1$ (left) and $\ell = 2$ (right) for typical values of $c$ , using the spectral method. . . . .	59
5.3	Eigenvalues for $\ell = 1$ (left) and $\ell = 2$ (right) for typical values of $c$ , using the spectral method. . . . .	60

# List of Tables

3.1	Newman-Penrose fields that obey the Teukolsky master equation for different spin-weights [24]	29
3.2	Solutions near horizon far horizon [25]	40

# Abbreviations

<b>BH</b>	Black Hole
<b>BL</b>	Boyer-Linquist
<b>EF</b>	Eddington-Finkelstein
<b>GR</b>	General Relativity
<b>GW</b>	Gravitational Wave
<b>NP</b>	Newman-Penrose
<b>QFT</b>	Quantum Field Theory
<b>SWSH</b>	Spin-Weighted Spheroidal Harmonic

# Chapter 1

## Superradiance

### 1.1 Introduction

The first direct observation of gravitational waves (GWs) by the Laser Interferometer Gravitational Wave Observatory (LIGO) was in 2015 and later announced in 2016. The recorded event matched the predictions of General Relativity (GR) for a binary system of black holes (BHs) merging together in an inward spiral into a single BH [1]. These observations demonstrated not only the existence of GWs but also existence of binary stellar-mass BH systems and that these systems could merge in a time less than the known Universe age. Since then, two more similar events were detected, which assured the inauguration of a new era of GW cosmology.

Naturally, this sparked new interest in the study of binary systems and GW-related phenomena. One of these phenomena is the possibility of amplification in waves scattered off rotating and/or charged BHs, which can occur under certain conditions for scalar, electromagnetic (EM) and gravitational bosonic waves. Such effect is one of many that encompass a wide range of phenomena generally known as *superradiance*.

(WHAT IS THE QUESTION TRYING TO BE ANSWERED)

Historically, the first appearance of the concept of superradiance was in 1954, in a publication by Dicke [2]. Almost two decades later, Zel'dovich [3, 4] showed that an absorbing cylinder rotating with an angular velocity  $\Omega$  could amplify an incident wave,  $\psi \sim e^{-i\omega t + im\phi}$ , with frequency  $\omega$  if

$$\omega < m\Omega \tag{1.1}$$

were satisfied, where  $m$  is the usual azimuthal number of the monochromatic plane wave relative to the rotation axis. In his work, he noticed that superradiance was related with dissipation of rotational energy from the absorbing object, possibly due to spontaneous pair creation at the surface. Hawking later showed that the presence of strong electromagnetic or gravitational fields could indeed generate bosonic and fermionic pairs spontaneously. This result was possible by the efforts of Starobinsky and Deruelle [5–8], which also laid the groundwork necessary for the discovery of BH evaporation.

Among other possible cases of radiation amplification, the phenomena worked out throughout this work is an example of *rotational superradiance*. As the name suggests, it occurs in the presence of “rotating” objects, as is the famous example of Zel’dovich cylinder. The condition Eq. (1.1) also appears in the context of general relativity, but in this case  $\Omega$  represents the angular velocity of a Kerr BH event horizon. This geometry is the simplest solution for a static but non-stationary BH, which breaks spherical symmetry. In Chapter 2 we describe many features of the Kerr BH, the most important for this work being the existence of a *ergoregion* where is possible for a infalling particle (or wave) to have negative energy when measured from a static observer in asymptotic flat space. As a result, under certain conditions it is possible for a particle to extract energy from the BH through the *Penrose process*, which is a counterpart to wave amplification.

In case of superradiance, it is was shown by Teukolsky that all types of wave perturbations on Kerr background are described using the same master equation [9]. This generalization is only possible by recurring to the Newman-Pensore (NP) formalism, which is a form of spinor calculus in GR [10], introduced in Chapter 3. Certain modes in bosonic waves (scalar, electromagnetic, gravitational) can be amplified while others are partially or totally absorbed by the BH, while fermionic waves have no such property. Therefore we will focus primarily on EM waves in the case of a neutral rotating BH, due to the close parallel to GW perturbations, which needs less algebraic computations to achieve to the same equation. However, this study provides a close parallel to the gravitational case as it provide insight to the same physical process.

The effects of superradiance can be computed for each mode by solving the radial part of Teukolsky’s equation using approximated methods. Since no other analytical methods which solve this problem have been found, the only other way of tackling the problem is by taking a numerical approach. All steps necessary to implement this method are explained in detail in Chapter 4, including some results.

(TALK ABOUT CHAPTER 5)

## 1.2 Klein paradox as a first example

Radiation amplification can be traced to the birth of Quantum Mechanics, in the beginning of the 20th century. First studies of the Dirac equation by Klein [11] revealed the possibility of electrons propagating in a region with a sufficiently large potential barrier without the expected dampening from non-relativistic tunnel effect. Due to some confusion, this result was wrongly interpreted by some authors as fermionic superradiance, as if the current reflected by the barrier could be greater than the incident current. The problem was named *Klein paradox* by Sauter [12] and this misleading result was due to an incorrect calculation of the group velocities of the reflected and transmitted waves.

Today, it is known that fermionic currents cannot be amplified for this particular problem [11, 13], a result that was correctly obtained by Klein in his original paper. On the contrary, superradiant scattering can indeed occur for bosonic fields.

### 1.2.1 Bosons

The equation that governs bosonic wave function is the Klein-Gordon equation, which for a minimally coupled electromagnetic potential takes the form

$$(D^\nu D_\nu - \mu^2)\Phi = 0, \quad (1.2)$$

where the usual partial derivative becomes  $D_\nu = \partial_\nu + ieA_\nu$  and  $\mu$  is the boson mass.

The problem is greatly simplified by considering flat space-time in (1+1)-dimensions and a step potential  $A_t(x) = V\theta(x)$ , for constant  $V > 0$  and wave solutions  $\Phi = e^{-i\omega t}\phi$ . For  $x < 0$ , the solution can be divided as incident and reflected, taking the form

$$\phi_{\text{inc}}(x) = \mathcal{J}e^{ikx}, \quad \phi_{\text{refl}}(x) = \mathcal{R}e^{-ikx}, \quad (1.3)$$

in which the dispersion relation states that  $k = \sqrt{\omega^2 - \mu^2}$ . For  $x > 0$ , the transmitted wave is naturally given by

$$\psi_{\text{inc}}(x) = \mathcal{T}e^{iqx}, \quad (1.4)$$

but in this case the root sign for the momentum must be carefully chosen so that the group velocity sign of the transmitted wave matches that of the incoming wave [13], *i.e.*

$$\left. \frac{\partial \omega}{\partial p} \right|_{p=q} = \frac{q}{\omega - eV} > 0, \quad (1.5)$$

therefore we must have that

$$q = \text{sgn}(\omega - eV) \sqrt{(\omega - eV)^2 - \mu^2}. \quad (1.6)$$

After obtaining the continuity relations at the barrier,  $x = 0$ , we follow by computing the ratios of the transmitted and reflected currents relative to the incident one, which yield

$$\frac{j_{\text{refl}}}{j_{\text{inc}}} = - \left| \frac{\mathcal{R}}{\mathcal{J}} \right|^2 = - \left| \frac{1-r}{1+r} \right|^2, \quad \frac{j_{\text{trans}}}{j_{\text{inc}}} = \text{Re}(r) \left| \frac{\mathcal{T}}{\mathcal{J}} \right|^2 = \frac{4 \text{Re}(r)}{|1+r|^2}, \quad (1.7)$$

written as a function of the coefficient

$$r = \frac{q}{k} = \text{sgn}(\omega - eV) \sqrt{\frac{(\omega - eV)^2 - \mu^2}{\omega^2 - \mu^2}}. \quad (1.8)$$

Hence, in the case of strong potential limit,  $eV > \omega + \mu > 2\mu$ , we may have  $r < 0$  real and the reflected current is larger (in magnitude) than the incident wave and therefore we have amplification.

### 1.2.2 Fermions

Dirac noticed that the Klein-Gordon equation masked internal degrees of freedom, so he devised his own equation which describes fermions. Considering that scalar potentials do not have any impact on spin orientation [14], we need only to consider half of the spinor components in the Dirac equation

$$(i\gamma^\nu D_\nu - \mu)\Psi = 0, \quad (1.9)$$

where  $\mu$  is the fermion mass, for which a valid representation of the gamma matrices is

$$\gamma^0 = \begin{pmatrix} 1 & 0 \\ 0 & -1 \end{pmatrix}, \quad \gamma^1 = \begin{pmatrix} 0 & 1 \\ -1 & 0 \end{pmatrix}. \quad (1.10)$$

Probing wave solutions  $\Psi = e^{-i\omega t}\psi$ , the incident and reflected solutions are

$$\psi_{\text{inc}}(x) = \mathcal{I} e^{ikx} \begin{pmatrix} 1 \\ k \\ \frac{\omega + \mu}{\omega + \mu} \end{pmatrix}, \quad \psi_{\text{refl}}(x) = \mathcal{R} e^{-ikx} \begin{pmatrix} 1 \\ -k \\ \frac{\omega + \mu}{\omega + \mu} \end{pmatrix}, \quad (1.11)$$

while for  $x > 0$ , the transmitted wave function is written as

$$\psi_{\text{trans}}(x) = \mathcal{T} e^{iqx} \begin{pmatrix} 1 \\ q \\ \frac{\omega - eV + \mu}{\omega - eV + \mu} \end{pmatrix}, \quad (1.12)$$

where we followed the same procedure as before, obtaining the same results from Eq. (1.5) through (1.7). Due to the structure of the spinor components, the coefficient in Eq. (1.8) is modified to

$$r = \text{sgn}(\omega - eV) \frac{\omega + \mu}{\omega - eV + \mu} \sqrt{\frac{(\omega - eV)^2 - \mu^2}{\omega^2 - \mu^2}}, \quad (1.13)$$

and now, in the same region,  $\omega > \mu$ , superradiance does not occur.

Even though superradiance and spontaneous pair creation are two distinct phenomena, this result is usually interpreted using the latter, from a Quantum Field Theory (QFT) stand point. All incident particles are completely reflected, as well as some extra due to pair creation at the barrier as a result of stimulation by the incident radiation and the presence of a strong electromagnetic field, while the resultant anti-particles are transmitted in the opposite direction, accounting for the change of sign in the transmitted current in Eq. (1.7), owing to the opposite charge they carry. This also explains the undamped transmission part.

One may think that this difference between bosons and fermions arises from the potential barrier shape, but work by other authors [12, 13, 15] shows that only the difference between the asymptotic values of the potential at infinity is essential for the process. The difference comes from intrinsic properties of these particles. The amount of fermion pairs produced in a given state, *i.e.* for a given  $\omega$ , is limited by Pauli's exclusion principle, while such limitation does not occur for bosons [16]. Additionally, fermionic current densities are always positive definite, while bosons can change sign because of the ambiguity in the wave function describing positive and negative energy solutions.



---

The minimum necessary energy for this to occur,  $2\mu$ , leaves evidence that superradiance is accompanied with spontaneous pair creation and some sort of dissipation by the battery maintaining the strong electromagnetic potential, in order to maintain energy balance.

## Chapter 2

# Kerr black hole

### 2.1 General Relativity

General Relativity is the theory of space, time and gravitation developed by Einstein in 1915. It introduces a new viewpoint on gravity and its relation with the fabric of spacetime, a *manifold* that bounds our three spatial dimensions with time. The concept challenged our deeply ingrained and intuitive notions of nature, partially because the mathematical background needed to understand the precise formulation of the theory was unfamiliar to much of the physics community at the time. This formulation corresponds to a field theory with the dynamical object of study being the metric of spacetime,  $g = g_{\mu\nu}dx^\mu dx^\nu$ , connecting geometry with mass and energy through Einstein's field equations. The theory inherits diffeomorphism invariance, *i.e.* remains the same theory by an active change of coordinates, which was at the core of definition of manifolds.

Immediately after, in 1916, Schwarzschild found the first solution, describing a static spherical isolated object. Then, the theory was left aside because of the numerous coupled nonlinear equations, but the astronomical discovery of compact and highly energetic objects in the 1950s bred new interest into the somewhat dormant GR, mainly because it was thought that these quasars and compact X-ray sources had suffered some form of gravitational collapse or that strong gravitational fields were present. Soon after, the modern theory of gravitational collapse was developed in the mid-1960s, including other BH solutions, for example Kerr's.

The theory of GR can be elegantly described in the form of the Hilbert action,

$$S_H = \frac{1}{16\pi} \int d^4x \sqrt{-g} R, \quad (2.1)$$

where  $g = \det(g_{\mu\nu})$  and  $R = g_{\alpha\beta}R^{\alpha\beta}$  corresponds to the Ricci scalar. Naturally, the first solutions corresponded to pure gravity, usually designated as vacuum solutions, which obey

$$R_{\mu\nu} = 0. \quad (2.2)$$

Despite their simplicity, they enjoy some very fascinating nontrivial properties. One of which is the existence of an event horizon, a surface that separates two causally disconnected regions of spacetime.

The underlying technique behind the study of superradiance is the linearization of Einstein and/or Maxwell equations around known BHs in stationary equilibrium. These perturbations will obey a series of partial differential equations whose dynamical variables are components of the Weyl tensor,  $C_{\mu\nu\rho\sigma}$ , or the Maxwell field tensor,  $F_{\mu\nu}$ . Thanks to the NP formalism we will be able to decouple and separate the equations for both GWs and EM waves, revealing decoupled variables which contain all the information needed about the nontrivial perturbations, instead of working with all components of the field tensors.

For the gravitational case, a straightforward way of obtaining a linearized theory is to consider a background stationary BH solution,  $g_{\mu\nu}^B$ , and then expanding the field equations (2.2) using the metric

$$g_{\mu\nu} = g_{\mu\nu}^B + h_{\mu\nu}^P, \quad (2.3)$$

keeping only terms that are  $\mathcal{O}(h_{\mu\nu}^B)$ . The indices  $B$  and  $P$  refer to the background and perturbations, respectively. As a result we are left with a wave equation in the given background.

In this work we will focus on (massless, neutral) electromagnetic waves and perturbations are performed including EM interactions through the Maxwell action

$$S_{EM} = -\frac{1}{4} \int d^4x \sqrt{-g} F_{\alpha\beta} F^{\alpha\beta}, \quad (2.4)$$

where  $F_{\mu\nu}$  is the Maxwell tensor. Variation of both actions,  $\delta(S_H + S_{EM}) = 0$ , result in two field equations

$$\nabla_\mu F^{\mu\nu} = 0, \quad (2.5)$$

$$R_{\mu\nu} - \frac{R}{2}g_{\mu\nu} = 8\pi T_{\mu\nu}. \quad (2.6)$$

The first equation is just the usual of Maxwell equation in curved spacetime. The latter are the Einstein field equations, reflecting the backreaction of the electromagnetic waves into the geometry through the presence of the EM stress-energy tensor

$$T_{\mu\nu} = F_{\mu\alpha}F_\nu{}^\alpha - \frac{1}{4}g_{\mu\nu}F^2. \quad (2.7)$$

These equations completely describe the system, but the problem is analytically untreatable, so we will resort to perturbation theory, considering the field  $A^\mu$  to be small. This is a very good approximation, as the gravitational field near a stellar-mass BHs is considerably stronger than the radiation emitted by nearby astrophysical sources. As the stress-energy tensor is quadratic in the fields,  $T_{\mu\nu} \sim \mathcal{O}(A^2)$ , then we can ignore the backreaction and the field equations for the metric  $g_{\mu\nu}$  reduce to Eq. (2.2).

## 2.2 Spacetime symmetries

It was generally accepted that a perfectly spherical symmetrical star would collapse to a Schwarzschild BH, although at the time the effect of a slightest amount of angular momentum on a gravitational collapse was not known. Finding a metric with intrinsic rotation could give insight into such a problem. Due to the lack of spherical symmetry, the problem became much harder, and took roughly 50 years after Schwarzschild's discovery to find a metric for a rotating body. Imposing symmetries to the final metric was essential to solve the field equations.

If we represent our spacetime and corresponding fields by  $(\mathcal{M}, g_{\mu\nu}, \psi)$ , then the pull-back  $f^*$  of the diffeomorphism  $f : \mathcal{M} \rightarrow \mathcal{M}$  would give us the same physical system  $(\mathcal{M}, f^*g_{\mu\nu}, f^*\psi)$ . Since diffeomorphisms are just active coordinate transformations, such concept may raise some confusion, as we do not seem to obtain any new information to work with. Almost all physical theories are coordinate invariant, as is Newtonian mechanics and Special Relativity, but in such theories there is a preferable coordinate system,

while the same does not hold true for GR. An analogy can be made with the path integral formalism in QFT, where special consideration is taken when summing all field configurations in order to not overcount indistinguishable configurations, as is the case of gauge field theories. A similar ambiguity can occur in GR, where two apparently different solutions can be related by a diffeomorphism and are actually “the same”, so we must be careful when deriving and analyzing any geometries.

Despite the added complexity of Einstein’s field equations, it is still possible to find exact nontrivial solutions in a systematic way by considering spacetimes with symmetries with the use of Killing vector fields. A vector field  $\xi$  that obeys

$$(\mathcal{L}_\xi g)_{\mu\nu} = 0 \quad (2.8)$$

is called a Killing field. Locally, this expression reduces to  $\nabla_\mu \xi_\nu + \nabla_\nu \xi_\mu = 0$ .

A *stationary* solution implies the existence of a Killing vector  $k$  that is asymptotically timelike,  $k^2 > 0$ , therefore allowing us to normalize our vector such that  $k^2 \rightarrow 1$ . Unlike the case of the static spacetime, a stationary metric does not show invariance under reversal of the time coordinate, which is natural considering a system with angular momentum. Furthermore, a solution is also *axisymmetric* if there is an asymptotically spacelike Killing field  $m$  whose integral curves are closed. A solution is stationary and axisymmetric if both symmetries are present, along with commuting fields,  $[k, m] = 0$ , *i.e.* rotations about the axis of symmetry commute with time translations. The commutativity of the fields implies the existence of a set of coordinates,  $(t, r, \theta, \varphi)$ , such that

$$k = \frac{\partial}{\partial t}, \quad m = \frac{\partial}{\partial \varphi}. \quad (2.9)$$

As a direct implication of this choice of chart, components of the metric stay independent of  $(t, \varphi)$ , in virtue of Eq. (2.8),

$$(\mathcal{L}_m g)_{\mu\nu} = \frac{\partial g_{\mu\nu}}{\partial \varphi} = 0, \quad (2.10)$$

with the same holding true for  $k$ , hence we can write  $g_{\mu\nu} = g_{\mu\nu}(r, \theta)$ .

One of the major applications of Killing vectors is to find conserved charges associated with the motion along a geodesic spanned by the field. These quantities are defined by taking the geodesics to regions of space that are asymptotically flat, where the geometry

does not affect the observer. In the case of the Kerr solution, we have two Killing vectors,  $k$  and  $m$ , which are naturally associated with the total mass  $M$  and angular momentum  $J$  of the BH, respectively. This is usually done by evaluating the Komar integrals [17, 18], which can be written in a covariant way as

$$M = \frac{1}{8\pi} \int_{S_\infty^2} \star dk^b = -\frac{1}{4} \lim_{r \rightarrow \infty} \int_0^\pi d\theta \sqrt{-g} g^{t\alpha} g^{r\beta} g_{t[\alpha, \beta]} , \quad (2.11)$$

$$J = -\frac{1}{16\pi} \int_{S_\infty^2} \star dm^b = \frac{1}{8} \lim_{r \rightarrow \infty} \int_0^\pi d\theta \sqrt{-g} g^{t\alpha} g^{r\beta} g_{\varphi[\alpha, \beta]} , \quad (2.12)$$

where the usual notation  $k^b \equiv g_{\mu\nu} k^\mu dx^\nu$  transforms a vector into a one-form and the operator  $\star : \Omega^p(\mathcal{M}) \rightarrow \Omega^{4-p}(\mathcal{M})$  is the Hodge dual map for  $p$ -forms. In order to complete the integration in the last step are assumed (2.9) and (2.10), keeping  $(t, r)$  constant. According to the widely accepted *no-hair conjecture* [19], these two quantities completely define a stationary (neutral) BH.

## 2.3 Kerr-Child coordinates

Naturally, Kerr was not the only one looking for such solution. Many presented other geometries to approximately describe a rotating star. Most of the solutions were one-parameter modifications to Schwarzschild that were not asymptotically flat. Simply using stationary and axisymmetric symmetries and then solving Einstein equations clearly did not suffice.

Kerr's success originated in of Petrov's classification of spacetimes, which used the algebraic properties of the Weyl tensor to distinguish the solutions in 3 types, with some subcases. He assumed that his solution would have the same classification as Schwarzschild's, associated with the geometry of isolated central objects, such as stars and BHs. From this assumption, using GR spinor techniques and only then imposing the Killing vectors in Eq. (2.9) was possible to find a new solution. Kerr's metric appear in his original paper [20] in the form

$$\begin{aligned} g = & \left(1 - \frac{2Mr}{\rho^2}\right) (dv - a \sin^2 \theta d\chi)^2 \\ & - 2(dv - a \sin^2 \theta d\chi)(dr - a \sin^2 \theta d\chi) \\ & - \rho^2(d\theta^2 + \sin^2 \theta d\chi^2) , \end{aligned} \quad (2.13)$$

where  $a$  is a parameter,  $M$  is the BH mass and  $\rho^2 = r^2 + a^2 \cos^2 \theta$ . Naturally the time Killing vector is  $\partial_v$  and  $\partial_\chi$  is the axial field, entailing that  $J = aM$ .

Taking the limit of  $a \rightarrow 0$ , we reduce the metric to the Schwarzschild solution in ingoing Eddington-Finkelstein (EF) coordinates,  $(v, r, \theta, \chi)$ , which are useful to study ingoing (to the horizon) geodesics and remove the horizon coordinate singularity. When a given metric has singularities it is not trivial to identify if they are physical singularities or an artifact resultant of choice of chart, removable by a better choice of coordinates. That being said, this raises the difficulty of finding the essential singularities. The best way to look for these singularities is to compute curvature scalar quantities, and if they diverge in one particular chart, then they diverge in all charts. Since any BH is just a vacuum solution, then the Ricci scalar vanishes,  $R = 0$ , so we resort to the Kretschmann scalar,

$$R_{\alpha\beta\gamma\delta}R^{\alpha\beta\gamma\delta} = \frac{48M(r^2 - a^2 \cos^2 \theta) [(r^2 - a^2 \cos^2 \theta)^2 - 16r^2 M^2 a^2 \cos^2 \theta]}{(r^2 + a^2 \cos^2 \theta)^6}, \quad (2.14)$$

that clearly diverges for  $\rho^2 = 0$ . The Schwarzschild singularity,  $r = 0$ , is replaced with the Kerr singularity  $(r, \theta) = (0, \pi/2)$ . It is not clear what is the geometry of the Kerr singularity if we interpret  $r$  and  $\theta$  as being part of the ordinary spherical coordinates. Although the metric is singular, we can draw some insight considering  $(r, \theta)$  constant and then the limit of  $r \rightarrow 0$  through the equatorial plane,

$$g|_{\text{singularity}} \sim dv^2 - a^2 d\chi^2. \quad (2.15)$$

Hence the metric is reduced to the line element of the circle,  $S^1$ , confirming a *ring singularity* of radius  $a$ . This result implies that we may only reach the singularity,  $\rho^2 = 0$ , by approaching the Kerr BH through the equatorial plane.

The Kerr-Child theory provides the “cartesian” form [21],

$$g = d\tilde{t}^2 - dx^2 - dy^2 - dz^2 - \frac{2Mr^3}{r^4 + a^2 z^2} \left[ d\tilde{t} + \frac{r(xdx + ydy) + a(ydx - xdy)}{r^2 + a^2} + \frac{z}{r} dz \right]^2, \quad (2.16)$$

which is particularly useful to understand the singularity geometry. In this metric,  $r$  is no longer a coordinate but a function of this chart coordinates  $(\tilde{t}, x, y, z)$ . We can relate the

The Kerr-Child metric to the original Kerr solution, using

$$\tilde{t} = v - r, \quad x + iy = (r - ia)e^{i\chi} \sin \theta, \quad z = r \cos \theta, \quad (2.17)$$

which implies that  $r(x, y, z)$  is implicitly given by

$$r^4 - (x^2 + y^2 + z^2 - a^2)r^2 - a^2z^2 = 0. \quad (2.18)$$

This condition deserves a more in-depth analysis. For increasing  $r$ , the surfaces obeying Eq. (2.18) approximates perfect spheres as the geometry gets more and more flat. Minkowsky flat space is immediately also guaranteed for  $M = 0$ . On the other hand, as we approach the singularity on  $z = 0$  and  $x^2 + y^2 = a^2$ , rotation effects deform the surfaces into oblate spheroids ( $\theta \neq \pi/2$  for the strict inequality). Such remarks are visually demonstrated in Figure 2.1.

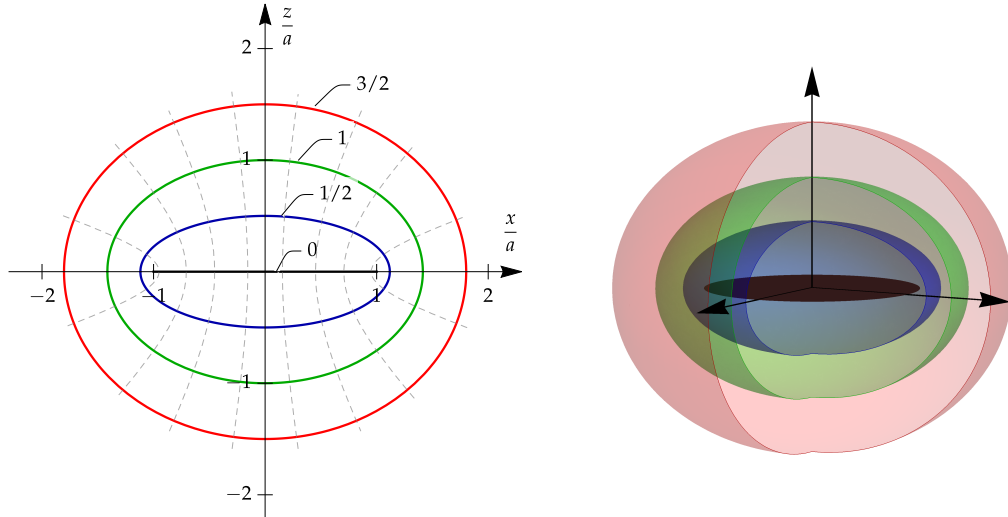


FIGURE 2.1: Contour plots of the surface  $r(x, y, z)/a$  for constant values of 0, 1/2, 1, 3/2, in the Kerr-Child coordinates. The left plot is the intersection of the  $y = 0$  plane with the 3D representation (right) that spotlights the ring singularity. Dashed curves representing orthogonal constant  $\theta(x, y, z)$  hypersurfaces become asymptotically affine.

Even though the Kerr-Child metric takes  $r > 0$  values, there is no mathematical reason to restrict  $r$  strictly to positive values. Thus, hypersurfaces of constant  $r$  can also be represented by  $-r$ . This means that this chart can be analytically extended to regions where  $r < 0$ . It is possible to obtain a *maximally extended* solution by analytic continuation and a proper collage of charts. This gives mathematical access to new spacetime regions, even though most of them show unphysical properties.



## 2.4 Boyer-Linquist coordinates

Considering the problem in hand, the most suitable coordinates for work with the Newman-Penrose (NP) formalism, are the Boyer-Linquist (BL) coordinates [22],

$$g = \left(1 - \frac{2Mr}{\rho^2}\right) dt^2 + 2a \sin^2 \theta \frac{(r^2 + a^2 - \Delta)}{\rho^2} dt d\varphi - \frac{(r^2 + a^2)^2 - \Delta a^2 \sin^2 \theta}{\rho^2} \sin^2 \theta d\varphi^2 - \frac{\rho^2}{\Delta} dr^2 - \rho^2 d\theta^2, \quad (2.19)$$

where we define  $\Delta = r^2 - 2Mr + a^2$ . In order to show that these correspond to the same solution, the change of coordinates

$$dv = d(t + r_*), \quad d\chi = d\varphi + \frac{a}{\Delta} dr, \quad (2.20)$$

takes us back to the original Kerr form (2.13). The coordinate  $v$  is given by the known ingoing EF transformation, defined by the Regge-Wheeler coordinate, also named *tortoise* coordinate, which is very useful to construct null directions. In the case of the Kerr BL metric, it holds that

$$\frac{dr_*}{dr} = \frac{r^2 + a^2}{\Delta}. \quad (2.21)$$

These coordinates are usually referred as “Schwarzschild like”, as they lead to the spherical static case in standard curvature coordinates when setting  $a = 0$ . Time inversion symmetry is characteristic of the static Schwarzschild spacetime, but the same does not hold for Kerr’s. Nevertheless, this specific form is invariant under the inversion  $(t, \varphi) \rightarrow (-t, -\varphi)$ , also known as the *circular condition*, an intuitive notion from physical systems with angular momentum. This discrete symmetry eliminates most of the off-diagonal components of the BL metric,  $g_{tr} = g_{\varphi r} = g_{t\theta} = g_{\varphi\theta} = 0$ , making it the simplest to perform calculations.

To study the possible horizons of the Kerr BH, we will consider  $\mathbf{n} = (dr)^\sharp \equiv (g^{\mu\nu} \nabla_\nu r) \partial_\mu$  which defines a normal vector to constant radial hypersurfaces. It is easy to show that  $\mathbf{n}^2 = g^{rr}$ , which implies that  $\mathbf{n}$  is null when  $\Delta = 0$ , defining null hypersurfaces at

$$r_\pm = M \pm \sqrt{M^2 - a^2}, \quad (2.22)$$

singularities of  $g_{rr}$  which we know to be removable. As a consequence, for a static observer a massless particle on an ingoing null geodesic would spiral around the BH for a infinite time, as the coordinate  $t \rightarrow \infty$ , never reaching  $r = r_+$ . This surface is the event horizon of the Kerr BH, as it separates two causally disconnected regions of spacetime, *i.e* any information from inside this surface will never reach any asymptotic observer. The expression for the event horizon surface also raises limitations for the amount of angular momentum a physical BH can have. We must have

$$|a| < M, \quad (2.23)$$

otherwise  $\Delta$  would lack any real roots and would lead to an essential *naked singularity*, reachable in a finite observable time, which is forbidden by the *Weak Cosmic Censorship* conjecture.

The surface at  $r = r_-$ , on the other hand, is called a Cauchy horizon. In GR, a spacelike surface containing all initial conditions of spacetime (Cauchy surface) would suffice to predict all past and future events, but a Cauchy horizon separates the domain of validity of such initial conditions. Despite no information ever escaping the event horizon, it is still possible to predict events inside  $r_- < r < r_+$ , but such thing it is not guaranteed after crossing the Cauchy horizon. Due to this and some other unphysical features (for example, closed timelike curves and instabilities under perturbations), we need only to focus on the region outside the event horizon  $r > r_+$ , since only information on that region is physically reachable from an asymptotic observer's point of view.

Event tough most of the Kerr BH basic properties were demonstrated, there is still no result so far showing some kind of rotation. First, consider the quantity  $\xi \cdot u = \xi_\alpha u^\alpha$ , where  $u^\alpha$  is the four-velocity of a point-particle and  $\xi^\alpha$  is any Killing field. Taking into account the geodesic equation,  $u^\beta \nabla_\beta u^\alpha = 0$ , it is easy to show that this quantity is conserved along geodesics,

$$u^\beta \nabla_\beta (\xi_\alpha u^\alpha) = u^\alpha u^\beta \nabla_\beta \xi_\alpha = \frac{u^\alpha u^\beta}{2} (\nabla_\alpha \xi_\beta + \nabla_\beta \xi_\alpha) = 0, \quad (2.24)$$

due to Killing Eq. (2.8). As a result, geodesics of a free particle in Kerr geometry will be characterized by two constants

$$E = k^\beta g_{\alpha\beta} \frac{dx^\alpha}{d\tau}, \quad -L = m^\beta g_{\alpha\beta} \frac{dx^\alpha}{d\tau}, \quad (2.25)$$

where  $\tau$  is the affine parameter for the geodesic. These quantities can be interpreted as the energy and angular momentum per mass of the particle, respectively. Due to the circular form of the BL metric, the metric components of the coordinates  $(t, \varphi)$  define a product decomposition, providing the separation of the previous equations,

$$\begin{aligned} \dot{t} &= \frac{1}{\Delta} \left[ (r^2 + a^2 + \frac{2Ma^2}{r})E - \frac{2Ma}{r}L \right], \\ \dot{\varphi} &= \frac{1}{\Delta} \left[ \frac{2Ma}{r}E + \left(1 - \frac{2M}{r}\right)L \right], \end{aligned} \quad (2.26)$$

specified for the equatorial plane  $\theta = \pi/2$ . The final equation for the geodesic is provided by the line element (2.19), which becomes also a first order ODE, after the substitution of  $\dot{t}$  and  $\dot{\varphi}$ .

Consider now a zero angular momentum observer (ZAMO) infalling radially, with  $L = 0$ , then we can get the angular velocity  $\Omega$ , as measured at infinity

$$\Omega = \frac{\dot{\varphi}}{\dot{t}} = -\frac{g_{t\varphi}}{g_{\varphi\varphi}} = \frac{2aM}{r^3 + a^2(2M + r)}. \quad (2.27)$$

Asymptotically we obtain  $\Omega \rightarrow 0$ , but for a finite distance, observers are forced to co-rotate with the BH. Particularly, at the event horizon,  $r = r_+$ , one finds that

$$\Omega_H = \frac{a}{2Mr_+} = \frac{J}{2M(M^2 + \sqrt{M^4 - J^2})}. \quad (2.28)$$

A special linear combination of Killing vector fields,

$$\xi = k + \Omega_H m, \quad (2.29)$$

is also a Killing vector field, but this one is particularly important because it is also a null vector normal to the event horizon, defining it as a Killing horizon of  $\xi$ . Due to the BL chart singularity, the normal vector to radial surfaces,  $n$ , is the zero vector at  $r = r_+$ , but using ingoing EF coordinates we obtain

$$n|_{r=r_+} = (g^{rv}\partial_v + g^{rr}\partial_r + g^{r\chi}\partial_\chi)|_{r=r_+} = -\frac{2Mr_+}{(\rho^2)|_{r=r_+}} \left( \partial_v + \frac{a}{2Mr_+}\partial_\chi \right) \propto \xi. \quad (2.30)$$

Since null geodesics on the outer horizon follow curves generated by the Killing vector  $\xi$ , the integral curves of this vector obey  $\xi^\alpha \partial_\alpha (\varphi - \Omega_H t) = 0$ , resulting in  $\varphi = \Omega_H t + \text{const.}$

Therefore, we say that the BH is “rotating” with angular velocity  $\Omega_H$ .

## 2.5 Ergoregion and the Penrose process

One of the main characteristic that distinguishes Kerr BHs from other spherical solutions is the existence of an *ergoregion*. In this region the Killing vector  $k$  becomes spacelike,  $k^2 = g_{tt} < 0$ , which is bounded by the hypersurface

$$r_{\text{ergo}}(\theta) = M + \sqrt{M^2 - a^2 \cos^2 \theta}. \quad (2.31)$$

This region lies outside the event horizon if  $a \neq 0$ , then being defined as  $r_+ < r < r_{\text{ergo}}(\theta)$ . Notice that a static observer moves in a timelike curve with  $(r, \theta, \varphi)$  constant, *i.e.* with tangent vector proportional to  $k$ , therefore such observer cannot exist inside the ergoregion because the time Killing vector becomes spacelike, otherwise it would violate causality. We can see that  $u^2 = g_{\alpha\beta}u^\alpha u^\beta = g_{tt}(u^t)^2 + 2g_{t\varphi}u^t u^\varphi + g_{\varphi\varphi}(u^\varphi)^2 > 0$  only occurs when  $g_{t\varphi}u^\varphi > 0$ , as all other terms are positive. Inside the ergoregion,  $g_{t\varphi} > 0$ , therefore all observers are forced to rotate in the same direction as the BH.

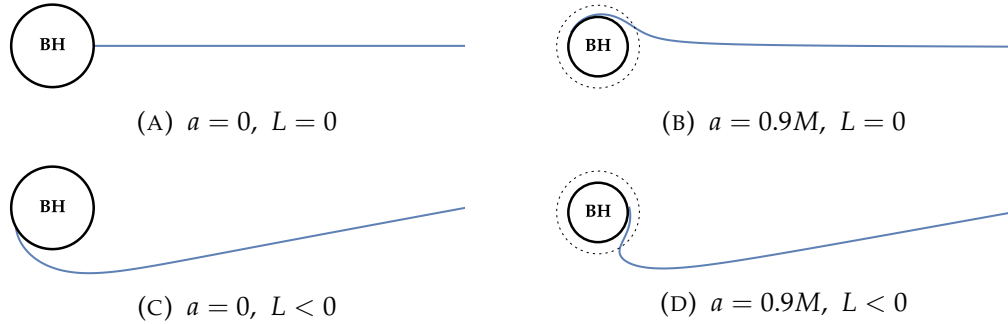


FIGURE 2.2: Illustration of the Schwarzschild (A,C) and Kerr (B,D) null equatorial infalling geodesics given by Eqs. (2.26), for  $r(0) = 20M$ , with emphasis on  $L \neq 0$ . Even starting with opposite angular momentum, the Kerr geodesic (D) is forced to co-rotate with the BH once crossed the ergoregion (dotted).

Despite BHs being always thought as “perfect absorbers” due to the existence of a causal boundary, the ergoregion allows energy extraction from the BH, through the Penrose process, an intrinsic feature of rotating BHs. Much like spontaneous pair creation and amplification at discontinuities are related but distinct effects, the Penrose process allows for a better understating of the phenomena of superradiance in GR.

Considering a particle with rest mass  $\mu$  and four-momentum  $p^\alpha = \mu u^\alpha$ , we may identify the constant of motion

$$E = k \cdot p = \mu(g_{tt}p^t + g_{t\varphi}p^\varphi). \quad (2.32)$$

as it's energy measured by a stationary observer at infinity, due to relations (2.25). As shown above, the Killing vector is asymptotically timelike but is spacelike inside the ergoregion, thus  $g_{tt} < 0$ . For a future-directed geodesic,  $p^0 = \mu u^0 > 0$ , the energy beyond the ergosurface needs not to be positive. Suppose, that by some means such particle manages to decay inside the ergoregion into two other particles, with momenta  $p_1$  and  $p_2$ . Contracting with  $k$ , implies that  $E = E_1 + E_2$ . Supposing that the first of the particles has negative energy,  $E_1 < 0$ , then

$$E_2 = E + |E_1| > E. \quad (2.33)$$

It can be shown that the particle with negative energy (bounded) must fall into the BH while the other may escape the ergoregion, with greater energy than the particle sent in. Energy is conserved by making the BH absorb the particle with negative energy, therefore resulting in a net energy extraction.

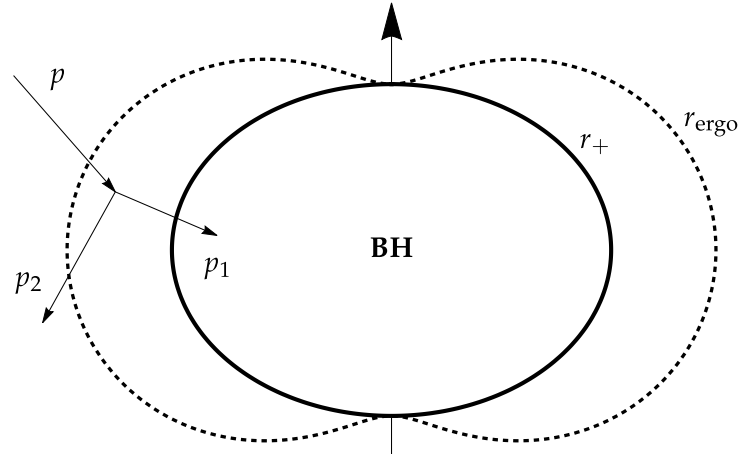


FIGURE 2.3: Illustration of the Penrose process, with ergoregion (dotted) and event horizon surfaces parameterized in Kerr-Child cartesian coordinates.

To understand the limits of the Penrose process, we use the fact that a stationary observer near the horizon must follow orbits of  $\xi$ , given by Eq. (2.29). Although a particle may have negative energy as measured by an asymptotic observer, the stationary one at

the horizon must measure a positive energy, as both he and the particle must follow the same orbits, which implies that  $\xi \cdot p_1 \leq 0$ . The BH will have a variation of mass  $\delta M = E_1$  and angular momentum  $\delta J = L_1$ , where  $L_1 = -m \cdot p_1$  is the particle's angular momentum. As a result,

$$\delta J \leq \frac{2M \left( M^2 + \sqrt{M^4 - J^2} \right)}{J} \delta M, \quad (2.34)$$

which is equivalent to  $\delta \left( M^2 + \sqrt{M^4 - J^2} \right) \geq 0$ . This quantity is usually refereed as the “area” of the event horizon  $A = 4\pi(r_+^2 + a^2) = 8\pi \left( M^2 + \sqrt{M^4 - J^2} \right)$ . Energy extraction from the Penrose process is limited by the requirement that the horizon area must always increase, which is a special case of the second law of BH mechanics.

We can tie the superradiance process with this particle counterpart using a simple and general argument. Asymptotically, we may think of waves as a collective of quantum (photons, gravitons, ...), each carrying  $\hbar\omega$  of energy and  $\hbar m$  of angular momentum [23], where  $m$  labels a mode with definite angular momentum. Therefore, when a given quanta is absorbed, the variation of the BH mass and angular momentum is given by

$$\delta J = \frac{m}{\omega} \delta M. \quad (2.35)$$

The condition for superradiance (1.1) appears explicitly in the second law of BH mechanics (2.34), which guarantees that  $\delta M(1 - \Omega_H m/\omega) > 0$ , *i.e.* confirming energy extraction from the BH when superradiance occurs, while the lack of superradiance increases the mass of the BH.

## Chapter 3

# Teukolsky's master equation

### 3.1 Newman-Penrose formalism

The study of gravitational and electromagnetic perturbations in a BH background was performed long before Kerr found his solution, for other spacetimes such as Schwarzschild's. Despite its simplicity, the procedure involved was already algebraically tedious. In the Kerr case, the metric was far more complicated, making the problem almost untreatable.

Fortunately, the NP formalism [10] provides an alternative method of studying perturbations. This formalism results from a natural introduction of spinor techniques in GR, after the choice of a null complex tetrad basis,

$$e_a = (e_a)^\mu \frac{\partial}{\partial x^\mu} \quad (a = 1, 2, 3, 4) , \quad (3.1)$$

where all quantities will be projected, *i.e.* for the Weyl tensor we define

$$C_{abcd} = (e_a)^\alpha (e_b)^\beta (e_c)^\gamma (e_d)^\delta C_{\alpha\beta\gamma\delta} . \quad (3.2)$$

Penrose believed that the light-cone was the essential element of the spacetime, thus it was of importance to find null directions. The basis consisted in two real vectors,  $\mathbf{l}$  and  $\mathbf{n}$ , and two complex conjugate vectors  $\mathbf{m}$  and  $\bar{\mathbf{m}}$ . Besides satisfying

$$\mathbf{l}^2 = \mathbf{n}^2 = \mathbf{m}^2 = \bar{\mathbf{m}}^2 = 0 , \quad (3.3)$$

orthogonality conditions of NP formalism require

$$\mathbf{l} \cdot \mathbf{m} = \mathbf{l} \cdot \bar{\mathbf{m}} = \mathbf{n} \cdot \mathbf{m} = \mathbf{n} \cdot \bar{\mathbf{m}} = 0 . \quad (3.4)$$

Still we are left with the ambiguity raised by multiplication of scalar functions to each vector, therefore it is customary to impose normalization conditions to the basis,

$$\mathbf{l} \cdot \mathbf{n} = 1 , \quad \mathbf{m} \cdot \bar{\mathbf{m}} = -1 . \quad (3.5)$$

This formalism is a special case of tetrad calculus, where we can identify the new basis as  $(\mathbf{l}, \mathbf{n}, \mathbf{m}, \bar{\mathbf{m}})$ . The “metric” for manipulating tetrad indices,  $\eta_{ab}$ , is defined by all restrictions provided above,

$$g^{\mu\nu} = \eta^{ab} (e_a)^\mu (e_b)^\nu = \mathbf{l}^\mu \mathbf{n}^\nu + \mathbf{n}^\mu \mathbf{l}^\nu - \mathbf{m}^\mu \bar{\mathbf{m}}^\nu - \bar{\mathbf{m}}^\mu \mathbf{m}^\nu . \quad (3.6)$$

Additionally these vectors define new directional derivatives. We will depart shortly from standard notation, by redefining these derivatives as

$$\mathbb{D} = \nabla_{\mathbf{l}} , \quad \mathbb{\Delta} = \nabla_{\mathbf{n}} , \quad \mathbb{\delta} = \nabla_{\mathbf{m}} , \quad \bar{\mathbb{\delta}} = \nabla_{\bar{\mathbf{m}}} . \quad (3.7)$$

More details and definitions on the tetrad formalism can be found in [Appendix A](#).

### 3.1.1 Kinnersley tetrad

The Riemann tensor may have up to twenty non-vanishing components. We know that ten of these are present in the symmetric Ricci tensor, that is intrinsically connected to matter and energy. The other components are pure gravitational degrees of freedom and are encoded in the Weyl tensor. It becomes the most useful object when the Ricci tensor vanishes, such as for vacuum solutions and source-free gravitational waves. In order to remove the Ricci tensor degrees of freedom, the tensor must be constructed as trace-free,

$$\eta^{ad} C_{abcd} = C_{1bc2} + C_{1bc2} - C_{3bc4} - C_{4bc3} = 0 . \quad (3.8)$$

Together with the other symmetries inherited from the Riemann tensor, for instance the first Bianchi identity,  $C_{a[bcd]} = 0$ , it is possible to show that some of these NP components vanish while others remain related, leaving us with ten degrees of freedom. As a result,



in the NP formalism the Weyl tensor can be represented by five complex scalars, usually chosen as

$$\begin{aligned}\psi_0 &= -C_{1313} = -C_{\alpha\beta\gamma\delta} l^\alpha m^\beta l^\gamma m^\delta, & \psi_1 &= -C_{1213} = -C_{\alpha\beta\gamma\delta} l^\alpha n^\beta l^\gamma m^\delta, \\ \psi_2 &= -C_{1342} = -C_{\alpha\beta\gamma\delta} l^\alpha m^\beta \bar{m}^\gamma n^\delta, & \psi_3 &= -C_{1242} = -C_{\alpha\beta\gamma\delta} l^\alpha n^\beta \bar{m}^\gamma n^\delta, \\ \psi_4 &= -C_{2424} = -C_{\alpha\beta\gamma\delta} n^\alpha \bar{m}^\beta n^\gamma \bar{m}^\delta.\end{aligned}\quad (3.9)$$

The complex conjugates can be obtained by doing the replacement  $3 \rightleftharpoons 4$ , by exchanging  $m$  with  $\bar{m}$  and vice-versa. The Weyl tensor has a unique decomposition in terms of a linear combination of NP scalars and tensorial product of two-forms. This decomposition has the general form,

$$\begin{aligned}\frac{1}{4} C_{\mu\nu\rho\sigma} &= -\psi_0 V_{\mu\nu} V_{\rho\sigma} - \psi_1 (V_{\mu\nu} W_{\rho\sigma} + W_{\mu\nu} V_{\rho\sigma}) \\ &\quad - \psi_2 (U_{\mu\nu} V_{\rho\sigma} + V_{\mu\nu} U_{\rho\sigma} + W_{\mu\nu} W_{\rho\sigma}) \\ &\quad - \psi_3 (U_{\mu\nu} W_{\rho\sigma} + W_{\mu\nu} U_{\rho\sigma}) - \psi_4 U_{\mu\nu} U_{\rho\sigma} + \text{c.c.}\end{aligned}\quad (3.10)$$

where  $U_{\mu\nu} = l_{[\mu} m_{\nu]}$ ,  $V_{\mu\nu} = \bar{m}_{[\mu} n_{\nu]}$ ,  $W_{\mu\nu} = l_{[\mu} n_{\nu]} - m_{[\mu} \bar{m}_{\nu]}$ . It is clear that the values that these five complex scalars take is completely dependent on the choice of tetrad frame.

BH solutions are “type D” spacetimes according to Petrov’s classification, which was a major restriction necessary to the discovery of Kerr’s metric. For these spacetimes it is possible to find two different doubly-degenerate principal directions of the Weyl tensor, which we choose to be the real vectors of the tetrad,  $l$  and  $n$  [24]. These yield

$$C_{\mu\alpha\beta[v} l_{\rho]} l^\alpha l^\beta = 0, \quad C_{\mu\alpha\beta[v} n_{\rho]} n^\alpha n^\beta = 0. \quad (3.11)$$

In NP formalism terms, this implies, respectively,

$$\psi_0 = \psi_1 = 0, \quad \psi_3 = \psi_4 = 0. \quad (3.12)$$

Finding the principal directions may not be trivial, but we can apply successive local transformations of the six-parameter Lorentz group in order to rotate the tetrad vectors. This procedure allows for the simplification of the Weyl tensor by vanishing NP scalars, “locking” the orientation of the tetrad frame. The Weyl scalar  $\psi_2$  becomes invariant under boosts in the principal directions, usually refereed as “type III” rotations [24]. These keep the light-cone structure intact by maintaining the direction of  $l$  and  $n$  unchanged (up to

multiplication of scalar functions), being useful to change between ingoing and outgoing frames [25]. Kinnersly solved the type D vacuum field equations [26], finding a suitable tetrad

$$\begin{aligned}\mathfrak{l} &= \left( \frac{r^2 + a^2}{\Delta}, 1, 0, \frac{a}{\Delta} \right), \\ \mathfrak{n} &= \frac{1}{2\rho^2} (r^2 + a^2, -\Delta, 0, a), \\ \mathfrak{m} &= \frac{1}{\sqrt{2}\bar{\rho}^2} (ia \sin \theta, 0, 1, i \csc \theta),\end{aligned}\tag{3.13}$$

where  $\bar{\rho} = r + ia \cos \theta$  and  $\rho^2 \equiv |\bar{\rho}|^2 = \bar{\rho}\bar{\rho}^*$ .

The NP formalism provides a full set of first-order coupled differential equations, relating the NP scalars components of the Weyl and Maxwell tensors. These equations result from the second Bianchi identity,  $C_{\mu\nu[\rho\sigma;\lambda]} = 0$ , and the Maxwell equations. In order to write these equations explicitly we need to define the *spin coefficients* using the connection  $\gamma_{abc} = (e_a)^\mu (e_b)_\mu{}^\nu (e_c)_\nu$ , which replaces the Christoper symbols in this formalism.

To study GWs, instead of perturbing the background metric, the NP formalism provides a natural way of performing perturbations by modification of the tetrad,  $\mathfrak{l} = \mathfrak{l}^B + \mathfrak{l}^P$ ,  $\mathfrak{n} = \mathfrak{n}^B + \mathfrak{n}^P$ , etc., and also the NP scalars,  $\psi_a = \psi_a^B + \psi_a^P$ , maintaining only first-order terms [27]. The formalism reveals decoupled equations for  $\psi_0^P$  and  $\psi_4^P$ , which implies that these dynamic variables are the only independent degrees of freedom of the GWs.

### 3.1.2 Maxwell equations

We focus with more detail on EM perturbations with a fixed background because they involve a simpler procedure and then we will tie with the same master equation that also describes GW perturbations.

In the NP formalism, all Maxwell equations,  $F_{[\mu\nu;\rho]} = 0$  and Eq. (2.5), reduce to

$$F_{[ab|c]} = 0, \quad \eta^{bc} F_{ab|c} = 0\tag{3.14}$$

(see Appendix A). The Maxwell tensor  $F_{\mu\nu}$  has a total of six components which encodes the vector quantities of the electric and the magnetic fields. We may reduce the equation

using three complex NP scalars,

$$\begin{aligned}\phi_0 &= F_{13} = F_{\alpha\beta} l^\alpha m^\beta, & \phi_1 &= \frac{1}{2}(F_{12} + F_{43}) = \frac{1}{2}F_{\alpha\beta} (l^\alpha n^\beta + \bar{m}^\alpha m^\beta), \\ \phi_2 &= F_{42} = F_{\alpha\beta} \bar{m}^\alpha n^\beta.\end{aligned}\tag{3.15}$$

Considering all possible combinations of NP indices in (3.14), we gather eight equations, double the amount of necessary relations. This occurs because the conjugates  $\phi_0^*, \phi_1^*, \phi_2^*$  are coupled in these equations. Eliminating every term of the form  $F_{23|a}$  or  $F_{14|b}$ ,

$$\phi_{2|1} = \phi_{1|4}, \tag{3.16a}$$

$$\phi_{1|2} = \phi_{2|3}, \tag{3.16b}$$

$$\phi_{1|1} = \phi_{0|4}, \tag{3.16c}$$

$$\phi_{0|2} = \phi_{1|3}. \tag{3.16d}$$

We may expand explicitly the left-hand side of Eq. (3.16a),

$$\begin{aligned}\phi_{2|1} &= \phi_{2,1} - \eta^{ab}(\gamma_{a41}F_{b2} + \gamma_{a21}F_{4b}) \\ &= \phi_{2,1} - (\gamma_{241}F_{12} + \gamma_{121}F_{42}) + (\gamma_{341}F_{42} + \gamma_{421}F_{43}) \\ &= \phi_{2,1} + 2F_{42} \left( \frac{\gamma_{341} + \gamma_{211}}{2} \right) + 2\gamma_{421} \left( \frac{F_{12} + F_{43}}{2} \right) \\ &= \mathbb{D}\phi_2 + 2\varepsilon\phi_2 - 2\pi\phi_1,\end{aligned}\tag{3.17}$$

where we used the antisymmetry of the spin connection,  $\gamma_{abc} = -\gamma_{bac}$ . The right-hand side yields

$$\begin{aligned}\phi_{1|4} &= \phi_{1,4} - \frac{1}{2}\eta^{ab}(\gamma_{a14}F_{b2} + \gamma_{a24}F_{1b} + \gamma_{a44}F_{b3} + \gamma_{a34}F_{4b}) \\ &= \phi_{1,4} - \frac{1}{2}(\gamma_{144}F_{23} + \gamma_{134}F_{42} + \gamma_{214}F_{12} + \gamma_{234}F_{41}) \\ &\quad + \frac{1}{2}(\gamma_{314}F_{42} + \gamma_{414}F_{42} + \gamma_{324}F_{14} + \gamma_{424}F_{13}) \\ &= \phi_{2,1} - \gamma_{244}F_{13} + \gamma_{314}F_{42} \\ &= \bar{\mathfrak{D}}\phi_1 - \lambda\phi_0 + \tau\phi_2.\end{aligned}\tag{3.18}$$

The spin coefficients  $\varepsilon, \pi, \lambda, \tau$ , along with other NP definitions are found in Appendix B.1.

If we repeat the same expansion for the other Maxwell equations, we gather the set

$$\mathbb{D}\phi_2 - \bar{\delta}\phi_1 = -\lambda\phi_0 + 2\pi\phi_1 + (\varrho - 2\varepsilon)\phi_2, \quad (3.19a)$$

$$\Delta\phi_1 - \delta\phi_2 = \nu\phi_0 - 2\mu\phi_1 + (2\beta - \tau)\phi_2, \quad (3.19b)$$

$$\mathbb{D}\phi_1 - \bar{\delta}\phi_0 = (\pi - 2\alpha)\phi_0 + 2\varrho\phi_1 - \kappa\phi_2, \quad (3.19c)$$

$$\Delta\phi_0 - \delta\phi_1 = (2\gamma - \mu)\phi_0 - 2\tau\phi_1 + \sigma\phi_2. \quad (3.19d)$$

The Kinnersley tetrad guarantees that  $\kappa = \sigma = \lambda = \nu = 0$ , decoupling all equations above. After substitution of all spin coefficients,

$$\left(\mathbb{D} + \frac{1}{\bar{\rho}^*}\right)\phi_2 = \left(\bar{\delta} + \frac{2ia\sin\theta}{\sqrt{2}(\bar{\rho}^*)^2}\right)\phi_2, \quad (3.20a)$$

$$\left(\Delta - \frac{\Delta}{\rho^2\bar{\rho}^*}\right)\phi_1 = \left[\bar{\delta} + \frac{1}{\sqrt{2}\bar{\rho}}\left(\cot\theta - \frac{ia\sin\theta}{\bar{\rho}^*}\right)\right]\phi_2, \quad (3.20b)$$

$$\left(\mathbb{D} + \frac{2}{\bar{\rho}^*}\right)\phi_1 = \left[\bar{\delta} + \frac{1}{\sqrt{2}\bar{\rho}^*}\left(\cot\theta - \frac{ia\sin\theta}{\bar{\rho}^*}\right)\right]\phi_0, \quad (3.20c)$$

$$\left[\Delta + \frac{\Delta}{2\rho^2}\left(\frac{1}{\bar{\rho}^*} - \frac{2(r-M)}{\Delta}\right)\right]\phi_0 = \left(\delta + \frac{2ia\sin\theta}{\sqrt{2}\bar{\rho}\bar{\rho}^*}\right)\phi_1. \quad (3.20d)$$

An important consequence of the symmetries of the Kerr spacetime allows for a wave decomposition of the form  $\phi_0, \phi_1, \phi_2 \sim e^{-i\omega t + im\varphi}$ . Therefore, the four differential operators group into radial ( $\mathbb{D}, \Delta$ ) and angular ( $\delta, \bar{\delta}$ ). The procedure for separation of the Maxwell equations can be further simplified by introducing new operators

$$\begin{aligned} \mathcal{D}_n &= \partial_r - \frac{iK}{\Delta} + 2n\frac{r-M}{\Delta}, & \mathcal{D}_n^\dagger &= \partial_r + \frac{iK}{\Delta} + 2n\frac{r-M}{\Delta}, \\ \mathcal{L}_n &= \partial_\theta - Q + n\cot\theta, & \mathcal{L}_n^\dagger &= \partial_\theta + Q + n\cot\theta, \end{aligned} \quad (3.21)$$

where we define the functions  $K = (r^2 + a^2)\omega - ma$ ,  $Q = a\omega\sin\theta - m\csc\theta$ . In this definition,  $n$  is any integer. These operators are related to the tetrad by

$$\mathbb{D} = \mathcal{D}_0, \quad \Delta = -\frac{\Delta}{2\rho^2}\mathcal{D}_0^\dagger, \quad \delta = \frac{1}{\sqrt{2}\bar{\rho}}\mathcal{L}_0^\dagger, \quad \bar{\delta} = \frac{1}{\sqrt{2}\bar{\rho}^*}\mathcal{L}_0, \quad (3.22)$$

as a result of the substitutions  $\partial_t \rightarrow -i\omega$ ,  $\partial_\varphi \rightarrow im$ . We may use the fact that  $\mathcal{D}_n$  and  $\mathcal{L}_n$  act mostly as radial and angular derivatives, respectively, to deduce the properties

$$\mathcal{D}_n \Delta = \Delta \mathcal{D}_{n+1}, \quad (3.23a)$$

$$\mathcal{L}_n \sin \theta = \sin \theta \mathcal{L}_{n+1}, \quad (3.23b)$$

$$\left( \mathcal{D}_n + \frac{q}{\bar{\rho}^*} \right) \frac{1}{(\bar{\rho}^*)^p} = \frac{1}{(\bar{\rho}^*)^p} \left( \mathcal{D}_n + \frac{q-p}{\bar{\rho}^*} \right), \quad (3.23c)$$

$$\left( \mathcal{L}_n + \frac{iaq \sin \theta}{\bar{\rho}^*} \right) \frac{1}{(\bar{\rho}^*)^p} = \frac{1}{(\bar{\rho}^*)^p} \left( \mathcal{L}_n + \frac{i(q-p)a \sin \theta}{\bar{\rho}^*} \right), \quad (3.23d)$$

$$\left( \mathcal{D}_n + \frac{q}{\bar{\rho}^*} \right) \left( \mathcal{L}_n + \frac{iaq \sin \theta}{\bar{\rho}^*} \right) = \left( \mathcal{L}_n + \frac{iaq \sin \theta}{\bar{\rho}^*} \right) \left( \mathcal{D}_n + \frac{q}{\bar{\rho}^*} \right), \quad (3.23e)$$

for any integers  $p, q, n$ , holding also for either  $\mathcal{D}_n^\dagger$  or  $\mathcal{L}_n^\dagger$ .

In order to achieve the separable form, we still need to perform a replacement of the Maxwell NP scalars by new dynamical variables

$$\Phi_0 = \phi_0, \quad \Phi_1 = \sqrt{2}\bar{\rho}^* \phi_1, \quad \Phi_2 = 2(\bar{\rho}^*)^2 \phi_2, \quad (3.24)$$

and using properties (3.23c) and (3.23d), we go from Eqs. (3.20) to

$$\left( \mathcal{D}_0 - \frac{1}{\bar{\rho}^*} \right) \Phi_2 = \left( \mathcal{L}_0 + \frac{ia \sin \theta}{\bar{\rho}^*} \right) \Phi_1, \quad (3.25a)$$

$$\Delta \left( \mathcal{D}_0^\dagger + \frac{1}{\bar{\rho}^*} \right) \Phi_1 = - \left( \mathcal{L}_1^\dagger - \frac{ia \sin \theta}{\bar{\rho}^*} \right) \Phi_2, \quad (3.25b)$$

$$\left( \mathcal{D}_0 + \frac{1}{\bar{\rho}^*} \right) \Phi_1 = \left( \mathcal{L}_1 - \frac{ia \sin \theta}{\bar{\rho}^*} \right) \Phi_0, \quad (3.25c)$$

$$\Delta \left( \mathcal{D}_1^\dagger - \frac{1}{\bar{\rho}^*} \right) \Phi_0 = - \left( \mathcal{L}_0^\dagger + \frac{ia \sin \theta}{\bar{\rho}^*} \right) \Phi_1. \quad (3.25d)$$

Now we may use the commutation relation (3.23e) together with (3.23a) to separate the equations for  $\Phi_0$  and  $\Phi_2$ . In order to obtain the first equation, we must first apply the operator  $(\mathcal{L}_0^\dagger + ia \sin \theta / \bar{\rho}^*)$  to Eq. (3.25c) and then use the commutation relation to substitute Eq. (3.25d). Similarly, applying  $(\mathcal{L}_0 + ia \sin \theta / \bar{\rho}^*)$  to Eq. (3.25b) we obtain the final equation. This yield

$$\left[ \Delta \mathcal{D}_1 \mathcal{D}_1^\dagger + \mathcal{L}_0^\dagger \mathcal{L}_1 + 2i\omega(r + ia \cos \theta) \right] \Phi_0 = 0, \quad (3.26)$$

$$\left[ \Delta \mathcal{D}_0^\dagger \mathcal{D}_0 + \mathcal{L}_0 \mathcal{L}_1^\dagger - 2i\omega(r + ia \cos \theta) \right] \Phi_2 = 0. \quad (3.27)$$

Still, there is another way of combining equations, *i.e* Eq. (3.25b) with (3.25d) and the remaining two form the set

$$\mathcal{L}_0 \mathcal{L}_1 \Phi_0 = \mathcal{D}_0 \mathcal{D}_0 \Phi_2, \quad (3.28)$$

$$\mathcal{L}_0^\dagger \mathcal{L}_1^\dagger \Phi_2 = \Delta \mathcal{D}_0^\dagger \mathcal{D}_0^\dagger \Delta \Phi_0. \quad (3.29)$$

Thus, we went from four first-order differential equations relating three NP scalars to four second-order differential equations, two of each decoupled, eliminating the need for the scalar  $\Phi_1$ . The last two equations imply that each of the complex NP scalars contains all the information necessary to describe an EM wave (two polarizations). One may think that we only need one of each group of equations to solve all perturbations, but no closed form solution has yet been found. Thus the problem has to be tackled using approximations or numerical methods, recurring to all last four equations (3.26–3.29), as we will see below.

Due to the nature of the operators  $\mathcal{D}_n$  and  $\mathcal{L}_n$ , we may separate the equations for  $\Phi_0 \sim R_{+1}(r)S_{+1}(\theta)$  and  $\Phi_2 \sim R_{-1}(r)S_{-1}(\theta)$  into two pairs of equations,

$$\left( \Delta \mathcal{D}_0 \mathcal{D}_0^\dagger + 2i\omega r \right) \Delta R_{+1} = \lambda \Delta R_{+1}, \quad (3.30a)$$

$$\left( \mathcal{L}_0^\dagger \mathcal{L}_1 - 2a\omega \cos \theta \right) S_{+1} = -\lambda S_{+1}, \quad (3.30b)$$

and

$$\left( \Delta \mathcal{D}_0^\dagger \mathcal{D}_0 - 2i\omega r \right) R_{-1} = \lambda R_{-1}, \quad (3.31a)$$

$$\left( \mathcal{L}_0 \mathcal{L}_1^\dagger + 2a\omega \cos \theta \right) S_{-1} = -\lambda S_{-1}, \quad (3.31b)$$

where  $\lambda$  is a separation constant. We use the property (3.23a) in to obtain Eq. (3.30a). The constant  $\lambda$  must be real, as the angular differential operators  $\mathcal{L}_n$  are also real. Notice that we do not distinguish the separation constants of both equations. Performing the transformation  $\theta \rightarrow \pi - \theta$ , the angular operators transforms as  $\mathcal{L}_0^\dagger \mathcal{L}_1 \rightarrow \mathcal{L}_0 \mathcal{L}_1^\dagger$ . Then if  $S_{+1}(\theta)$  is a solution for Eq. (3.30b) for a given separation constant  $\lambda$ , this implies that  $\tilde{S}_{-1}(\theta) = S_{+1}(\pi - \theta)$  is a solution for Eq. (3.31b) for the same constant. In other words, the separation constant must be the same for both equations. Also, solutions  $R_{-1}$  and  $\Delta R_{+1}$  obey the same complex conjugate equations due to  $\mathcal{D}_n^\dagger = (\mathcal{D}_n)^*$ .

The second-order equations relating  $\Phi_0$  and  $\Phi_2$  can be separated in the same fashion. Naturally, the separation constant will differ from the eigenvalue Eqs. (3.30) and (3.31). Using the same substitutions made previously, we divide each equation by the corresponding ansatz to obtain

$$\frac{\mathcal{L}_0 \mathcal{L}_1 S_{+1}}{S_{-1}} = \frac{\Delta \mathcal{D}_0 \mathcal{D}_0 R_{-1}}{\Delta R_{+1}} = \mathcal{B}, \quad (3.32)$$

$$\frac{\mathcal{L}_0^\dagger \mathcal{L}_1^\dagger S_{-1}}{S_{+1}} = \frac{\Delta \mathcal{D}_0^\dagger \mathcal{D}_0^\dagger \Delta R_{+1}}{R_{-1}} = \mathcal{B}. \quad (3.33)$$

The separation constant  $\mathcal{B}$  is real and equal for both equations. This claim rests on the same arguments as for the eigenvalue  $\lambda$ . We also make the angular functions  $S_{-1}$ ,  $S_{+1}$  equally normalized. We may observe the latter by assuming two different separation constants  $\mathcal{B}_1, \mathcal{B}_2$ . Then, we have

$$\begin{aligned} (\mathcal{B}_1)^2 \int_0^\pi d\theta \sin \theta (S_{-1})^2 &= \int_0^\pi d\theta \sin \theta (\mathcal{L}_0 \mathcal{L}_1 S_{+1})(\mathcal{L}_0 \mathcal{L}_1 S_{+1}) \\ &= \int_0^\pi d\theta \sin \theta (\mathcal{L}_0^\dagger \mathcal{L}_1^\dagger \mathcal{L}_0 \mathcal{L}_1 S_{+1}) S_{+1} \\ &= \mathcal{B}_1 \mathcal{B}_2 \int_0^\pi d\theta \sin \theta (S_{+1})^2, \end{aligned} \quad (3.34)$$

where we used integration by parts twice. Thus  $(\mathcal{B}_1)^2 = \mathcal{B}_1 \mathcal{B}_2 = \mathcal{B}^2$ . We can compute the coefficient by computing the operation

$$\begin{aligned} \mathcal{L}_0^\dagger \mathcal{L}_1^\dagger \mathcal{L}_0 \mathcal{L}_1 &= \mathcal{L}_0^\dagger (\mathcal{L}_0 \mathcal{L}_1^\dagger - 4a\omega \cos \theta) \mathcal{L}_1 \\ &= \mathcal{L}_0 \mathcal{L}_1^\dagger (-\lambda + 2a\omega \cos \theta) - 4a\omega \cos \theta \mathcal{L}_0^\dagger \mathcal{L}_1 + 4a\omega \sin \theta \mathcal{L}_1 \\ &= -\lambda \mathcal{L}_0 \mathcal{L}_1^\dagger + 2a\omega \left[ \cos \theta \mathcal{L}_0 \mathcal{L}_1^\dagger - \sin \theta (\mathcal{L}_1 + \mathcal{L}_1^\dagger) \right] \\ &\quad - 4a\omega \cos \theta \mathcal{L}_0^\dagger \mathcal{L}_1 + 4a\omega \sin \theta \mathcal{L}_1 \\ &= (-\lambda + 2a\omega \cos \theta) \mathcal{L}_0 \mathcal{L}_1^\dagger + 4a\omega Q \sin \theta \\ &= (-\lambda + 2a\omega \cos \theta)(-\lambda - 2a\omega \cos \theta) + 4a\omega(-a\omega \sin^2 \theta + m) \\ &= \lambda^2 - 4a^2\omega^2 + 4a\omega m = \mathcal{B}^2, \end{aligned} \quad (3.35)$$

applied on the angular function  $S_{+1}$ . The commutation relations between the angular operators can be found directly or by noticing that  $[e_a, e_b] = \eta^{cd}(\gamma_{cba} - \gamma_{cab})e_d$ . Then using Eq. (3.30b) it is possible to eliminate the second-order angular operators. To obtain  $\mathcal{B}^2$ , the same procedure could be done for  $S_{-1}$  or the radial functions.

It will be more profitable to study Eqs. (3.26) and (3.27) as a special case of the Teukolsky master equation [9] which describes all the linearized perturbations around the Kerr BH. The generality of this equation is the primary reason for the focus on the EM case. The treatment for GWs differs in the perturbation formalism only in algebraic complexity, resulting in the same master equation. With the Teukolsky master equation we can proceed considering general perturbations, but there are several numerical and analytical details that make EM waves and GWs differ later on [28].

The general equation reads

$$\begin{aligned} & \frac{1}{\Delta^s} \frac{\partial}{\partial r} \left( \Delta^{s+1} \frac{\partial \Upsilon_s}{\partial r} \right) + \frac{1}{\sin \theta} \frac{\partial}{\partial \theta} \left( \sin \theta \frac{\partial \Upsilon_s}{\partial \theta} \right) - \left[ \frac{(r^2 + a^2)^2}{\Delta} - a^2 \sin^2 \theta \right] \frac{\partial^2 \Upsilon_s}{\partial t^2} \\ & - \frac{4Mar}{\Delta} \frac{\partial^2 \Upsilon_s}{\partial t \partial \varphi} - \left( \frac{a^2}{\Delta} - \frac{1}{\sin^2 \theta} \right) \frac{\partial^2 \Upsilon_s}{\partial \varphi^2} + 2s \left[ \frac{M(r^2 - a^2)}{\Delta} - r - ia \cos \theta \right] \frac{\partial \Upsilon_s}{\partial t} \\ & + 2s \left[ \frac{a(r - M)}{\Delta} + \frac{i \cos \theta}{\sin^2 \theta} \right] \frac{\partial \Upsilon_s}{\partial \varphi} - (s^2 \cot^2 \theta - s) \Upsilon_s = 0, \end{aligned} \quad (3.36)$$

where  $s$  is the field *spin weight* and each field quantity  $\Upsilon_s$  is related to the NP scalars as shown in the Table 3.1. Depending on the spin weight, the equation may describe massless scalar ( $s = 0$ ) or Dirac fields ( $s = \pm \frac{1}{2}$ ), as well as electromagnetic ( $s = \pm 1$ ) or gravitational waves ( $s = \pm 2$ ). Substituting the spin-weight for the EM waves we obtain Eqs. (3.26) and (3.27).

$s$	$\Upsilon_s$
+1	$\Phi_0 = \phi_0$
-1	$\Phi_2 = 2(\bar{\rho}^*)^2 \phi_2$
+2	$\Psi_0 = \psi_0$
-2	$\Psi_4 = 4(\bar{\rho}^*)^4 \psi_4$

TABLE 3.1: Newman-Penrose fields that obey the Teukolsky master equation for different spin-weights [24]

Obviously, Teukolsky's equation is explicitly independent of  $t$  and  $\varphi$ , thus  $\Upsilon_s$  accepts a decomposition in  $e^{-i\omega t + im\varphi}$ , which we already assumed in the EM case to separate the equations. Stationarity and axisymmetry of the spacetime geometry guarantees this form. The azimuthal wave number  $m$  must be an integer, due to periodic boundary conditions on the BL coordinate  $\varphi$ . We may separate all perturbations in a completely general mode



decomposition

$$\Upsilon_s = \int d\omega e^{-i\omega t} \left( \sum_{\ell, m} e^{im\varphi} {}_sS_{\ell m}(\theta) {}_sR_{\ell m}(r) \right). \quad (3.37)$$

The integer  $\ell$  plays a role in labelling all possible solutions for the eigenvalue problem of both radial and angular equations,

$$\frac{1}{\Delta^s} \frac{d}{dr} \left( \Delta^{s+1} \frac{d {}_sR_{\ell m}}{dr} \right) + \left[ \frac{K^2 - 2is(r-M)K}{\Delta} + 4is\omega r - {}_s\mathcal{F}_{\ell m} \right] {}_sR_{\ell m} = 0, \quad (3.38)$$

$$\frac{1}{\sin\theta} \frac{d}{d\theta} \left( \sin\theta \frac{d {}_sS_{\ell m}}{d\theta} \right) + \left[ a^2\omega^2 \cos^2\theta - 2sa\omega \cos\theta - \frac{(m+s\cos\theta)^2}{\sin^2\theta} + s + {}_s\mathcal{A}_{\ell m} \right] {}_sS_{\ell m} = 0. \quad (3.39)$$

The radial and angular eigenvalues are related to the separation constant on Eqs. (3.30) and (3.31) through

$${}_s\mathcal{F}_{\ell m} = {}_s\mathcal{A}_{\ell m} - 2ma\omega + a^2\omega^2 \underset{(s=\pm 1)}{=} \lambda - s(s+1). \quad (3.40)$$

Due to the form of the angular equation, the eigenvalues  ${}_s\mathcal{F}_{\ell m}$ ,  ${}_s\mathcal{A}_{\ell m}$  as well as the function  ${}_sS_{\ell m}(\theta)$  depends also on the coupling  $a\omega$ . Clearly, the same does not hold for the radial function  ${}_sR_{\ell m}(r)$ .

### 3.2 Spin-Weighted Spheroidal Harmonics

To shed some light into the explicit form of  ${}_s\mathcal{A}_{\ell m}$ , we will need to dive into the eigenvalue problem for the angular equation. We may transform Eq. (3.39) into a more familiar form using the change of coordinate  $z = \cos\theta$  and renaming the dimensionless parameter  $c = a\omega$ , obtaining

$$\frac{d}{dz} \left[ (1-z^2) \frac{d {}_sS_{\ell m}}{dz} \right] + \left[ (cz)^2 - 2csz - \frac{(m+sz)^2}{1-z^2} + s + {}_s\mathcal{A}_{\ell m} \right] {}_sS_{\ell m} = 0. \quad (3.41)$$

We may also use freely  ${}_sS_{\ell m}(\cos\theta) \equiv {}_sS_{\ell m}(\theta)$ . We will consider  $c$  real as we are analyzing superradiance of EM waves in vacuum, although we could generalize the spin-weighted spheroidal harmonic (SWSH) equation to imaginary  $c$  values to describe waves in a particular medium.

Spherically symmetric problems allow for a decomposition using spherical harmonics  $Y_{\ell m}(\theta, \varphi)$  of angular dependent functions with finite boundary conditions. These have innumerable applications in physics such as the hydrogen atom or the description of anisotropies in the cosmic microwave background. By setting  $s = 0$  and  $c = 0$  (spherical), then it is clear that the solutions for Eq. (3.41) are given by the associated Legendre polynomials,  $P_\ell^m(z)$ . Therefore,  ${}_sS_{\ell m}$  is a generalization of a spherical harmonic [29], with

$${}_0S_{\ell m}(\theta, \varphi) \underset{(c=0)}{=} Y_{\ell m}(\theta, \varphi), \quad {}_0\mathcal{A}_{\ell m} \underset{(c=0)}{=} \ell(\ell+1), \quad (3.42)$$

where  ${}_sS_{\ell m}(\theta, \varphi) \equiv e^{im\varphi} {}_sS_{\ell m}(\theta)$ . The values of  $\ell$  are non-negative integers, with the restriction of  $\ell \geq |m|$ . We require that spin-weighted spheroidal harmonics (SWSHs) are similarly normalized to unity and also a complete set of orthogonal functions, for any spin-weight and coupling  $c$ ,

$$\int_0^\pi d\theta \sin \theta {}_sS_{\ell m}(\theta) {}_{s'}S_{\ell' m'}(\theta) = \int_{-1}^1 dz {}_sS_{\ell m}(z) {}_{s'}S_{\ell' m'}(z) = \frac{1}{2\pi} \delta_{\ell\ell'} \delta_{mm'}. \quad (3.43)$$

Perturbations of any type in Schwarzschild spacetime are written using spin-weighted *spherical* harmonics,  ${}_sY_{\ell m}(\theta, \varphi)$ , which are still spherical harmonics ( $c = 0$ ). Due to the shared symmetries with spherical harmonics it is possible to find a closed form for  $s \neq 0$  harmonics. We can raise and lower spin-weight with the use of the operators commonly denoted as  $\bar{\partial}$  and  $\partial$  (see Appendix C), respectively, applied on  $Y_{\ell m}$ ,

$$\begin{aligned} (\bar{\partial})^s Y_{\ell m} &= \sqrt{\frac{(\ell+s)!}{(\ell-s)!}} {}_sY_{\ell m}, \\ (-1)^s (\partial)^s Y_{\ell m} &= \sqrt{\frac{(\ell+s)!}{(\ell-s)!}} {}_{-s}Y_{\ell m}, \end{aligned} \quad (3.44)$$

limited by  $|s| \leq \ell$ . Eqs. (3.32) and (3.33) are closely related to former, as applications of the operators  $\mathcal{L}_s^\dagger$  and  $\mathcal{L}_s$  generalize  $\bar{\partial}$  and  $\partial$ , respectively.

Thus, for the non-spherical symmetry we could in principle obtain all SWSHs if we knew the closed form for  ${}_0S_{\ell m}$  and its eigenvalues. The problem lies in the fact that no such decomposition of elementary function was found. This require us to follow numerical and approximate methods to find the values of  ${}_sS_{\ell m}$ .

The major advances on the study of the eigenvalues of the SWSHs was performed

by Leaver in 1985 . Working out the asymptotical and critical behavior of the equation, we observe the equation diverges at the poles,  $z = \pm 1$ , where it takes the form  $(1 \mp z) {}_sS_{\ell m}'(z) \sim \mp \frac{1}{4}(m \pm s)^2 {}_sS_{\ell m}(z)$ . In order to guarantee that a SWSH is everywhere analytical, Leaver proposed the series expansion at  $z = -1$ ,

$${}_sS_{\ell m}(z) = e^{cz}(1+z)^{k_-}(1-z)^{k_+} \sum_{p=0}^{\infty} a_p(1+z)^p, \quad (3.45)$$

where  $k_{\pm} = \frac{1}{2}|m \pm s|$ . The exponential in the ansatz accounts for the large  $z$  behavior of the equation. Substituting in the angular equation, we obtain a three-term recurrence relation between the expansion coefficients  $a_p$  and the boundary condition at  $z = -1$ ,

$$\alpha_p a_{p+1} + \beta_p a_p + \gamma_p a_{p-1} = 0, \quad \alpha_0 a_1 + \beta_0 a_0 = 0, \quad (3.46)$$

where

$$\begin{aligned} \alpha_p &= -2(1+p)(1+2k_+ + p), \\ \beta_p &= (k_- + k_+ + p - s)(1 + k_- + k_+ + p + s) \\ &\quad - 2c(1 + 2k_- + 2p + s) - c^2 - {}_s\mathcal{A}_{\ell m}, \\ \gamma_p &= 2c(k_- + k_+ + p + s). \end{aligned} \quad (3.47)$$

We then find an equation for the eigenvalue  ${}_s\mathcal{A}_{\ell m}$  with explicit dependence on  $m, s$  and  $c$ , by combining the previous relations into a continued fraction,

$$\beta_0 = \frac{\alpha_0 \gamma_1}{\beta_1 -} \frac{\alpha_1 \gamma_2}{\beta_2 -} \frac{\alpha_2 \gamma_3}{\beta_3 -} \dots \left( \equiv \frac{\alpha_0 \gamma_1}{\beta_1 - \frac{\alpha_1 \gamma_2}{\beta_2 - \frac{\alpha_2 \gamma_3}{\beta_3 - \dots}}} \right). \quad (3.48)$$

We can also consider the  $r$ -th inversion of Eq. (3.48),

$$\beta_r - \frac{\alpha_{r-1} \gamma_r}{\beta_{r-1} -} \frac{\alpha_{r-2} \gamma_{r-1}}{\beta_{r-2} -} \dots \frac{\alpha_1 \gamma_2}{\beta_1 -} \frac{\alpha_0 \gamma_1}{\beta_0} = \frac{\alpha_r \gamma_{r+1}}{\beta_{r+1} -} \frac{\alpha_{r+1} \gamma_{r+2}}{\beta_{r+2} -} \dots. \quad (3.49)$$

These equations involve an infinite fraction that depends explicitly on  $c, m, s$ , which leads to suspicion that this leads to an infinite spectrum. This is in a close parallel to the spherical case, where we have a infinite number of harmonics, although no proof has been found. If we notice that  $\gamma_p \propto c$ , then the zero order expansion of the eigenvalue expansion in  $c \ll 1$  leads to  $\beta_r = 0$ . In the spherical geometry, this corresponds to truncating

the series at  $r$ , as  $\gamma_p = 0$  for any  $p$ . Thus, the eigenvalue root depends explicitly on the integer  $r$ , entailing the discretization of the spectra

$${}_s\mathcal{A}_{\ell m} = \ell(\ell + 1) - s(s + 1) + \mathcal{O}(a\omega), \quad (3.50)$$

where we identified  $\ell = r + k_+ + k_-$ . Since  $r \geq 0$ , then we must have  $\ell \geq \max\{|m|, |s|\}$ , *i.e.* the leading contribution for the monopole expansion is the dipole for EM waves and the quadrupole for GWs. Changing  $r$  for  $\ell$  corresponds simply to a relabeling of the eigenfunctions in order to match the values of the spectra when  $c = 0$  and also when  $s = 0$ .

It will be useful to expand  ${}_s\mathcal{A}_{\ell m}$  in high order terms in order to obtain the series coefficients for the eigenvalue (see Appendix D). Up to sixth order, only the zero-order term depends on the sign of the spin weight, in agreement with Eq. (3.40). In the general angular equation, inversion of spin corresponds to inversion of poles, *i.e.* stays invariant under the transformation  $(s, z) \rightarrow (-s, -z)$ . Under this transformation, the eigenvalue must obey  $s + {}_s\mathcal{A}_{\ell m} = -s + {}_{-s}\mathcal{A}_{\ell m}$ , thus it is beneficial to define

$${}_s\mathcal{A}_{\ell m} = {}_s\mathcal{E}_{\ell m} - s(s + 1), \quad (3.51)$$

to also exploit the symmetry of spin inversion in numerical computations. This way, we can simply write that  $\tilde{\lambda} = \pm 1 \mathcal{E}_{\ell m}$ .

### 3.3 Analytic radial approximations

Like the angular equation, in general it is not possible to solve the radial Eq. (3.38) by known analytical methods. The only apparent line of attack would be to numerical solve the equation, but it will be important to find the asymptotic form of  ${}_sR_{\ell m}$  at infinity as well as its near-horizon behavior. For both methods it will prove beneficial to change the variables into dimensionless quantities,

$$x = \frac{r - r_+}{r_+}, \quad \tau = \frac{r_+ - r_-}{r_+}, \quad \bar{\omega} = (2 - \tau)(\bar{\omega} - m\bar{\Omega}_H), \quad (3.52)$$

where every barred frequency is normalized relative to the BH horizon,  $\bar{\omega} \equiv \omega r_+$ . Due to (2.23), we have that  $0 \leq \tau \leq 1$ . Using this coordinate,  $x \rightarrow 0$  represents the BH horizon.

The radial equation now reads

$$\begin{aligned} & \frac{1}{[x(x+\tau)]^s} \frac{d}{dx} \left( [x(x+\tau)]^{s+1} \frac{d {}_s R_{\ell m}}{dx} \right) + \\ & + \left[ \frac{\mathcal{K}^2 - is(2x+\tau)\mathcal{K}}{x(x+\tau)} + 4is(1+x)\bar{\omega} - {}_s \mathcal{F}_{\ell m} \right] {}_s R_{\ell m} = 0, \end{aligned} \quad (3.53)$$

where we normalize  $\mathcal{K} = K/r_+ = \omega + x(x+2)\bar{\omega}$ . In this method, it will be sufficient to use a spherical approximation for the harmonics eigenvalues,  ${}_s \mathcal{F}_{\ell m} = \ell(\ell+1) - s(s+1) + \mathcal{O}(a\omega)$ , for small enough frequencies.

The near-horizon approximation corresponds to considering only small distances compared to the perturbations characteristic wavelength,  $r - r_+ \ll \omega^{-1}$  ( $\bar{\omega}x \ll 1$ ). Because superradiant scattering occurs when  $\omega \lesssim \Omega_H$ , we also neglect terms  $\mathcal{O}(\omega x)$ . In this limit,  $\mathcal{K} \simeq \bar{\omega}$ . The resultant equation remains singular at the horizons  $x = 0$  and  $x = -\tau$ . Thus, making the substitution  ${}_s R_{\ell m}(x) \simeq x^\alpha (x+\tau)^\beta F(x)$ , the function  $F(x)$  is analytical if  $\alpha + \beta = -s$  and also if  $\alpha = -\frac{1}{2}s \pm (\frac{1}{2}s + i\bar{\omega}/\tau)$ . Boundary conditions at the horizon requires that a physical observer measures a negative radial group velocity of the signal. In order words, we require the wave to travel into the black hole and never outwards. Since  $x^{\pm i\bar{\omega}/\tau} \simeq e^{\pm i\kappa r_*}$ , where  $\kappa = \omega - m\Omega_H$ , then the ingoing solution requires  $\alpha = -s - i\bar{\omega}/\tau$ . The near-horizon solution gives

$${}_s R_{\ell m}(x) \simeq A x^{-s-i\bar{\omega}/\tau} (x+\tau)^{i\bar{\omega}/\tau} {}_2F_1 \left( -\ell, \ell+1, 1-s - \frac{2i\bar{\omega}}{\tau}; -\frac{x}{\tau} \right), \quad (3.54)$$

where  $F(x) = {}_2F_1(a, b, c; x)$  is the hypergeometric function.

Asymptotically, we consider  $x \gg \tau$ , where  $\mathcal{K} \sim x^2\bar{\omega}$ . The resultant equation, allows to substitute a power law  ${}_s R_{\ell m}(x) \sim x^\alpha e^{-i\bar{\omega}x} M(x)$ . In order for  $M(x)$  to be analytic everywhere, then we must have  $\alpha^2 + (2s+1)\alpha = {}_s \mathcal{F}_{\ell m}$ . We are left with Kummer's differential equation for  $M(x)$ , where  $\alpha = \ell - s$  or  $\alpha = -1 - \ell - s$ . The general solution is the combination

$$\begin{aligned} {}_s R_{\ell m}(x) & \sim C e^{-i\bar{\omega}x} x^{\ell-s} {}_1F_1(1+\ell-s, 2\ell+2; -2i\bar{\omega}x) \\ & + D e^{-i\bar{\omega}x} x^{-1-\ell-s} {}_1F_1(-\ell-s, -2\ell; -2i\bar{\omega}x), \end{aligned} \quad (3.55)$$

where  ${}_1F_1(a, b; x)$  are Olver's confluent hypergeometric functions and  $B, C$  are integration constants.

Althought useful, these solutions do not provide enough physical insight. Another way

of obtaining the same assymptotic behavior is by transforming the radial equation into a Schrodinger-like potential problem

$$\left[ \frac{d^2}{dr_*^2} + V_{\text{eff}} \right] {}_sU_{\ell m} = 0, \quad (3.56)$$

where  ${}_sU_{\ell m} = \sqrt{\Delta^s(r^2 + a^2)} {}_sR_{\ell m}$  and the tortoise coordinate  $r_*$  was defined in Eq. (2.21).

We write the potential as a function of the radial coordiante,

$$V_{\text{eff}} = \frac{K^2 - 2is(r - M)K + \Delta(4is\omega r - {}_s\mathcal{F}_{\ell m})}{(r^2 + a^2)^2} - G^2 - \frac{dG}{dr_*} \quad (3.57)$$

where  $G = s(r - M)/(r^2 + a^2) + r\Delta/(r^2 + a^2)^2$ . Even tought  $r_*$  is related to the radial coordinate through an non-invertable relation, we use this coordinate to remove all the  $\Delta$  singularities from the diferential equation.

Taking  $r \rightarrow \infty$  ( $r_* \rightarrow \infty$ ), the potential becomes

$$V_{\text{eff}} \sim \omega^2 + \frac{2is\omega}{r}, \quad (3.58)$$

with assymptotic solution  ${}_sU_{\ell m} \sim r^{\pm s} e^{\mp i\omega r_*}$ . The combination of both solutions corresponds to

$${}_sR_{\ell m}(r) \sim A_{\text{in}} \frac{e^{-i\omega r_*}}{r} + A_{\text{out}} \frac{e^{i\omega r_*}}{r^{2s+1}}. \quad (3.59)$$

The ingoing and outgoing wave coefficients can be related to the integration coefficients  $B, C$  by expanding the hypergeometric function in (3.55) at infinity,

$$\begin{aligned} A_{\text{in}} &= \left[ C(-2i\bar{\omega})^{-\ell+s-1} \frac{\Gamma(2\ell+2)}{\Gamma(\ell+s+1)} + D(-2i\bar{\omega})^{\ell+s} \frac{\Gamma(-2\ell)}{\Gamma(-\ell+s)} \right] r_+, \\ A_{\text{out}} &= \left[ C(2i\bar{\omega})^{-\ell-s-1} \frac{\Gamma(2\ell+2)}{\Gamma(\ell-s+1)} + D(2i\bar{\omega})^{\ell-s} \frac{\Gamma(-2\ell)}{\Gamma(-\ell-s)} \right] (r_+)^{2s+1}. \end{aligned} \quad (3.60)$$

We may notice the ratio of gamma functions with negative integer valued arguments, which can be misinterpreted as a divergence due to existing poles of  $\Gamma$ . This is a mere artifact of the asymptotic expantion for general confluent hypergeometric arguments. A way to circumvent this problem is to consider Euler's reflection formula for any value of

$\ell$  and then take the limit to the integer set,

$$\lim_{\ell \in \mathbb{Z}} \frac{\Gamma(-2\ell)}{\Gamma(-\ell \pm s)} = \frac{\Gamma(\ell \mp s + 1)}{\Gamma(2\ell + 1)} \lim_{\ell \in \mathbb{Z}} \frac{\sin(\ell\pi) \cos(\mp s\pi)}{\sin(2\ell\pi)} = \frac{(-1)^{\ell+s}}{2} \frac{(\ell \mp s)!}{(2\ell)!}. \quad (3.61)$$

At the event horizon  $r = r_+$ ,  $r_* \rightarrow -\infty$  and  $\Delta = 0$ . The effective radial potential is simplified to a constant

$$V_{\text{eff}} \simeq \left( \kappa - is \frac{r_+ - M}{2Mr_+} \right)^2. \quad (3.62)$$

Due to the logarithmic behavior of  $r_*$  at the horizon, the solution takes the form  ${}_sU_{\ell m} \sim e^{\pm i\kappa r_*} (r - r_+)^{\pm s/2} \sim \Delta^{\pm s/2} e^{\pm i\kappa r_*}$ . The boundary conditions at  $r = r_+$  state that the horizon solution must only have the ingoing solution

$${}_sR_{\ell m} \simeq A_{\text{hole}} \Delta^{-s} e^{-i\kappa r_*}. \quad (3.63)$$

Expanding solution (3.54), the integration constants relate through  $A_{\text{hole}} = (r_+)^{-s} A$ .

With both approximations it is possible to extend the solutions of small frequency waves to overlapping regions and perform a matching of coefficients, which can be used to find how much of the wave is reflected/amplified. The near region  $r - r_+ \ll \omega^{-1}$  and the asymptotic region  $r - r_+ \gg r_+$  overlap when  $\omega r_+ \ll 1$  ( $\bar{\omega} \ll 1$ ). The overlapping region becomes larger as  $\omega r_+$  becomes smaller. We proceed by expanding the far region solution (3.55) at the horizon,  $x = 0$ , where the lowest order terms are simply

$${}_sR_{\ell m} \simeq C x^{\ell-s} + D x^{-1-\ell-s}. \quad (3.64)$$

On the other hand, expanding the near region solution (3.55) at infinity we get

$$\begin{aligned} {}_sR_{\ell m} \sim & A \tau^{-\ell} \frac{\Gamma(2\ell + 1)}{\Gamma(\ell + 1)} \frac{\Gamma(1 - s - 2i\omega/\tau)}{\Gamma(\ell + 1 - s - 2i\omega/\tau)} x^{\ell-s} \\ & + A \tau^{\ell+1} \frac{\Gamma(-2\ell - 1)}{\Gamma(-\ell)} \frac{\Gamma(1 - s - 2i\omega/\tau)}{\Gamma(-\ell - s - 2i\omega/\tau)} x^{-\ell-1-s}. \end{aligned} \quad (3.65)$$

The matching is possible because the solutions when expanded in regions in the limit of their validity are given in terms of two monomials of  $x^{\ell-s}$  and  $x^{-1-\ell-s}$ . A combination of

these results yields

$$\frac{D}{C} = \frac{(-1)^{\ell+1}}{2} \frac{(\ell!)^2}{(2\ell)!(2\ell+1)!} \frac{\Gamma(\ell+1-s-2i\omega/\tau)}{\Gamma(-\ell-s-2i\omega/\tau)} \tau^{2\ell+1}, \quad (3.66)$$

where we used the same identification as in Eq. (3.61) for the  $\Gamma$  functions with negative arguments. With this result it is possible to find the ratio between the incoming and the outgoing energy from the BH.

### 3.4 Amplification factor ${}_sZ_{\ell m}$

Potential barrier problems are heavily associated with reflection and absorption of radiation. Central potentials have waves scattered differently for each mode  $(\omega, \ell, m)$ , depending on the incident angle of the wave. The stress-energy tensor allows to define conserved currents, which can be used to compute the flow of energy and angular momentum. In particular, we will be interested in calculating the asymptotic energy flow going inward and outward of the BH.

Different Killing vectors have distinct currents, due to different possible projections of the stress-energy tensor. These currents are conserved due to  $\nabla_\mu T^{\mu\nu} = 0$  and the Killing Eq. (2.8). The energy flux is defined as

$$dE = T^\mu{}_\nu k^\nu d\Sigma_\mu \quad (3.67)$$

where  $d\Sigma_\mu$  is defined as the 3-surface element. An asymptotically flat geometry such as the Kerr metric has infinity  $r$ -constant hypersurface with induced 3-metric  $h = h_{\alpha\beta} dy^\alpha dy^\beta$ , where  $h_{\alpha\beta} = g_{\alpha\beta}$  for  $y^\alpha \in (t, \theta, \varphi)$ . In BL coordinates, the normal to the surface is the outgoing radial vector  $n = (dr)^\sharp$ , while the other vectors form the tangent basis. By computing the highest order term when  $r \rightarrow \infty$ , the surface element is asymptotically spherically symmetric, given by

$$d\Sigma_\mu = n_\mu \sqrt{\det h} dt d\theta d\varphi \sim n_\mu r^2 \sin \theta dt d\theta d\varphi. \quad (3.68)$$

We are obviously interested in obtaining an expression relating the flow of energy at infinity and the Maxwell NP scalar. Thus, will be convenient to describe the stress-energy tensor using symmetric tetrad combinations and NP scalars and their conjugates. Much like the Weyl and the Maxwell tensor, this composition is uniquely defined by Eqs. (2.7)



and (3.15),

$$2T_{\mu\nu} = \phi_0^* \phi_0 \mathbf{n}_\mu \mathbf{n}_\nu + \phi_2^* \phi_2 \mathbf{l}_\mu \mathbf{l}_\nu + 2\phi_1^* \phi_1 [\mathbf{l}_{(\mu} \mathbf{n}_{\nu)} + \mathbf{m}_{(\mu} \bar{\mathbf{m}}_{\nu)}] \\ - 4\phi_0^* \phi_1 \mathbf{n}_\mu \mathbf{m}_\nu - 4\phi_1^* \phi_2 \mathbf{l}_\mu \mathbf{m}_\nu + 2\phi_0^* \phi_2 \mathbf{m}_\mu \mathbf{m}_\nu + \text{c.c.} \quad (3.69)$$

Energy flow is thus computed by taking the series expansion of

$$r^2 T^r_t = -r^2 \frac{\Delta}{\rho^2} T_{rt} = -r^2 \left( \frac{1}{4} |\phi_0|^2 - |\phi_2|^2 \right) + \mathcal{O} \left( \frac{1}{r} \right), \quad (3.70)$$

recalling definition (3.24) when considering the asymptotic form of  ${}_s R_{\ell m}$  in Eq. (3.59). We can clearly identify the ingoing and outgoing flows as

$$\frac{d^2 E_{\text{in}}}{dt d\Omega} = \lim_{r \rightarrow \infty} \frac{r^2}{4} |\phi_0|^2, \quad \frac{d^2 E_{\text{out}}}{dt d\Omega} = \lim_{r \rightarrow \infty} r^2 |\phi_2|^2, \quad (3.71)$$

In order to obtain the full conservation law we must find the absorbed radiation by the BH. We turn now to the horizon null hypersurface, for which the normal vector  $n$  in BL coordinates is the zero vector, due to  $g^{rr} = 0$ . Similarly, the stress-energy tensor in this tetrad basis is ill-defined since  $\mathbf{l}$  is singular at the horizon, where  $\Delta = 0$ . The Kinnersley tetrad keeps its properties, by applying a boost in the null directions

$$\tilde{\mathbf{l}} = \frac{\Delta}{2(r^2 + a^2)} \mathbf{l}, \quad \tilde{\mathbf{n}} = \frac{2(r^2 + a^2)}{\Delta} \mathbf{n}, \quad (3.72)$$

while removing the singularity at the horizon. The NP field quantities are now given by  $\tilde{\Upsilon}_s = [\Delta/2(r^2 + a^2)]^s \Upsilon_s$ . In addition, we shall use the ingoing EF coordinates, defined in Eq. (2.20), as the chart is the indicated to consider inward future directed waves, because  $(\mathbf{l} \cdot \partial_v)$  is a positive constant,

$$\tilde{\mathbf{l}} = \left( 1, \frac{\Delta}{2(r^2 + a^2)}, 0, \frac{a}{r^2 + a^2} \right), \quad \tilde{\mathbf{n}} = \left( 0, -\frac{r^2 + a^2}{\rho^2}, 0, 0 \right). \quad (3.73)$$

If we set  $r = r_+$ , we obtain that  $\tilde{\mathbf{l}} = \boldsymbol{\xi}$ . This implies that  $\tilde{\mathbf{l}}$  is the normal vector to the event horizon, just like  $\mathbf{n}$ , but they are opposite to each other as  $n^v = g^{rv} < 0$ .

The radial 3-surface element cannot be of the form in Eq. (3.68), since the induced metric at the horizon is now singular,  $\sqrt{\det \bar{h}} = \Delta \rho^2 \sin \theta = 0$ . Special considerations must be taken when taking the induced metric of a null hypersurface. We usually choose  $k = \partial_v$  as one of the surface tangent vectors, due to  $\boldsymbol{\xi} \cdot k = 0$ . Then we compute the

induced metric  $\sigma$  of a 2-surface space spanned by the vectors  $\partial_\theta$  and  $\partial_\chi$ . The general 3-surface element for a null horizon, normal to the inward radial direction, is given by

$$d\Sigma_\mu = \tilde{l}_\mu (\sqrt{\det \sigma} d\theta d\chi) dv = \tilde{l}_\mu 2Mr_+ \sin \theta d\theta d\varphi dt, \quad (3.74)$$

where  $\det \sigma = g_{\theta\theta} g_{\chi\chi} - (g_{\theta\chi})^2$ . In the last equality we used the fact that the jacobian  $\partial(v, \chi)/\partial(t, \varphi) = 1$ . The resultant energy flux going inside the BH is then computed by

$$\frac{d^2 E_{\text{hole}}}{dt d\Omega} = 2Mr_+ T_{\mu\nu} \tilde{l}^\mu k^\nu \quad (r = r_+). \quad (3.75)$$

Generalizing Eq. (3.67), we may define the the flow of angular momentum using the axisymmetric Killing vector,  $dL = -T^\mu{}_\nu m^\nu d\Sigma_\mu$ , and combining previous results to write

$$\frac{d^2 E_{\text{hole}}}{dt d\Omega} - \Omega_H \frac{d^2 L_{\text{hole}}}{dt d\Omega} = 2Mr_+ T_{\mu\nu} \tilde{l}^\mu \tilde{l}^\nu \quad (r = r_+). \quad (3.76)$$

The computation of the flow of the energy into the BH requires finding the ratio between the energy and angular momentum carried by waves. For a scalar wave  $\Phi \sim e^{-i\omega t + im\varphi}$ , we can easily find the ratio by computing  $dL/dE = -T^r{}_\varphi / T^r{}_t = -\partial_\varphi \Phi / \partial_t \Phi = m/\omega$ , using the standard scalar energy-stress tensor [23]. Another simpler argument was made in (2.35), obtaining the same result. Since this ratio holds for any type of perturbation [25],

$$\frac{d^2 E_{\text{hole}}}{dt d\Omega} = \frac{2Mr_+ \omega}{\omega - m\Omega_H} \tilde{\phi}_0 \tilde{\phi}_0^* = \frac{\omega}{8Mr_+ \kappa} |\Delta\phi_0|^2 \quad (r = r_+). \quad (3.77)$$

Double projection of the future-directed inward vector  $\tilde{l}$  onto the energy-stress tensor gives us  $|\tilde{\phi}_0|^2$ , due to the decomposition (3.69). At the horizon, the boosted NP scalar can be written as  $\tilde{\phi}_0 = (\Delta\phi_0)/(4Mr_+)$ , where  $\Delta\phi_0$  is regular at the horizon by construction and also by checking with the boundary solution (3.63).

Now, we are prepared to define the amplification factor as

$${}_s Z_{\ell m} = \frac{dE_{\text{out}}/dt}{dE_{\text{in}}/dt} - 1, \quad (3.78)$$

where we integrated over the polar angles. The factor is defined as the overall gain/loss effect for each mode  $(\omega, \ell, m)$ , therefore it measures how much of the wave was *globally* reflected ( ${}_s Z_{\ell m} = 0$ ), absorbed ( ${}_s Z_{\ell m} < 0$ ) or amplified ( ${}_s Z_{\ell m} > 0$ ). Assuming a single

mode decomposition and remembering that  $\phi_2 = \Phi_2 / (2\bar{\rho}^2) \sim {}_{-1}R_{\ell m} / (2r^2)$ , we show that

$${}_{\pm 1}Z_{\ell m} + 1 = \left| \frac{\lim_{r \rightarrow \infty} (\frac{1}{r} {}_{-1}R_{\ell m})}{\lim_{r \rightarrow \infty} (r {}_{+1}R_{\ell m})} \right|^2 = \left| \frac{A_{\text{out}}(s = -1)}{A_{\text{in}}(s = +1)} \right|^2 \equiv \left| \frac{\mathcal{Z}_{\text{out}}}{\mathcal{Z}_{\text{in}}} \right|^2, \quad (3.79)$$

Naturally, in order to give use to the  $D/C$  ratio from the matching of coefficients, we need to obtain the ratio  $A_{\text{out}}/A_{\text{in}}$  for the same spin weight. We redefine these constants in Table 3.2. Using Eq. (3.32), we can relate the *ingoing* integration constants from both

	$\omega r \gg 1$	$\omega r \ll 1$
${}_1R_{\ell m}$	$\mathcal{Y}_{\text{in}} \frac{e^{-i\omega r_*}}{r} + \mathcal{Y}_{\text{out}} \frac{e^{i\omega r_*}}{r^3}$	$\mathcal{Y}_{\text{hole}} \Delta^{-1} e^{-ikr_*}$
${}_{-1}R_{\ell m}$	$\mathcal{Z}_{\text{in}} \frac{e^{-i\omega r_*}}{r} + \mathcal{Z}_{\text{out}} r e^{i\omega r_*}$	$\mathcal{Z}_{\text{hole}} \Delta e^{-ikr_*}$

TABLE 3.2: Solutions near horizon far horizon [25]

$\phi_0$  and  $\phi_2$ . In the large  $r$  limit, this equation is simplified into  $(\partial_r - i\omega)(\partial_r - i\omega) {}_{-1}R_{\ell m} \sim \mathcal{B} ({}_{{+1}}R_{\ell m})$ , and considering terms only up to  $\mathcal{O}(\frac{1}{r})$  we substitute  $\mathcal{Y}_{\text{in}}$ ,

$${}_{\pm 1}Z_{\ell m} + 1 = \frac{\mathcal{B}^2}{16\omega^4} \left| \frac{\mathcal{Z}_{\text{out}}}{\mathcal{Z}_{\text{in}}} \right|^2, \quad (3.80)$$

where now the expression is only using  $s = -1$  coefficients. Still, the amplification should not depend on the sign of spin-weight, *i.e.* the amplification should be the same for all EM waves, the same holding true for GW perturbations. The *in-out* ratio is given by

$$\begin{aligned} \frac{\mathcal{B}^2}{16\omega^4} \left| \frac{\mathcal{Z}_{\text{out}}}{\mathcal{Z}_{\text{in}}} \right|^2 &= \frac{\mathcal{B}^2}{\ell^2(\ell+1)^2} \left| \frac{1 + \frac{(-1)^{\ell+1}}{2} \frac{D}{C} \frac{\Gamma(\ell)\Gamma(\ell+2)}{\Gamma(2\ell+1)\Gamma(2\ell+2)} (2i\bar{\omega})^{2\ell+1}}{1 - \frac{(-1)^{\ell+1}}{2} \frac{D}{C} \frac{\Gamma(\ell)\Gamma(\ell+2)}{\Gamma(2\ell+1)\Gamma(2\ell+2)} (2i\bar{\omega})^{2\ell+1}} \right|^2 \\ &\simeq 1 - (2\bar{\omega})^{2\ell+1} \frac{\Gamma(\ell)\Gamma(\ell+2)}{\Gamma(2\ell+1)\Gamma(2\ell+2)} \text{Re} \left\{ 2i \frac{D}{C} \right\}, \end{aligned} \quad (3.81)$$

where we approximated the relative normalization  $\mathcal{B} = \lambda + \mathcal{O}(a\omega) = \ell(\ell+1) + \mathcal{O}(a\omega)$ , by considering a small deviation from spherical symmetry.

The  $D/C$  ratio has a non-trivial expression in terms of  $\Gamma$  functions of non-integers arguments. The factorial property of  $\Gamma$  allows the approximation ( $y = -2i\omega/\tau$ )

$$\frac{\Gamma(\ell+1-s+y)}{\Gamma(-\ell-s+y)} = \prod_{n=-\ell-s}^{\ell-s} (n+y) \underset{(s=\pm 1)}{\simeq} (-1)^{\ell+1} \frac{\ell+1}{\ell} y \prod_{n=1}^{\ell} (n^2 - y^2). \quad (3.82)$$

Combining all results, the amplification factor for EM perturbations yields

$${}_{\pm 1}Z_{\ell m} \simeq -4\bar{\omega}(\bar{\omega} - m\bar{\Omega}_H) (2 - \tau)(2\bar{\omega}\tau)^{2\ell} \left[ \frac{(\ell - 1)!(\ell + 1)!}{(2\ell)!(2\ell + 1)!} \right]^2 \prod_{n=1}^{\ell} \left( n^2 + \frac{4\bar{\omega}^2}{\tau^2} \right). \quad (3.83)$$

A very similar expression can be obtained for GW perturbations (see e.g. [30]). The validity of this result is mainly based on the overlapping of the far-region and near-region solutions. When the black hole is extremal,  $\tau = 0$ , the factor is regular and proportional to  ${}_{\pm 1}Z_{\ell m} \propto -(4\bar{\omega}\bar{\omega})^{2\ell+1}$ , while the amplification occurs mostly when  $\ell = m = 1$ , due to the dampening of the quickly growing factorials in the denominator of  ${}_{\pm 1}Z_{\ell m}$ .

We know that the EM fields must be real quantities, therefore physical waves must also include negative valued  $\omega$  in the mode decomposition (3.37). The amplification factor explicitly demonstrates that superradiance occurs when

$$\omega(\omega - m\Omega_H) < 0. \quad (3.84)$$

For  $\omega > 0$ , amplification occurs for  $m > 0$  modes, in the region (1.1), while for  $\omega < 0$ , only modes with  $m < 0$  can be amplified. The circular symmetry of the spacetime guarantees that superradiance phenomena is invariant under the change of  $(\omega, m) \rightarrow (-\omega, -m)$ . In other other words,

$${}_sZ_{\ell, -m}(-\omega) = {}_sZ_{\ell m}(\omega), \quad (3.85)$$

which is clear from the EM case in (3.83).

## Chapter 4

# Numerical methods

In this chapter we will develop the necessary method to compute the necessary coefficients to compute the gain/loss factor, using Mathematica<sup>TM</sup>. We will go beyond the spherical approximation and calculate the SWSHs eigenvalues for any BH angular momentum. With the eigenvalue defined for a particular mode, we will compute the asymptotic radial coefficients, which in turn are used to compute the amplification factor in three different ways.

### 4.1 Eigenvalues

The need for obtaining the eigenvalues  ${}_s\mathcal{E}_{\ell m}$  rests on the dependency to solve the radial equation numerically with no spherical approximation. Additionally, the relative normalization constant  $\mathcal{B}$ , which depends explicitly on the eigenvalue, will be rather important in one of the methods used to calculate the gain/loss factor  ${}_sZ_{\ell m}$  for each mode  $(\omega, \ell, m)$ . There is no reason to differentiate the eigenvalue for given BH angular momentum and a particular frequency, since the parameter dependence of the eigenvalue is  $c = a\omega$ . Considering the focus in superradiant modes, we only will need eigenvalues in the range  $0 < c < 3$ . Even for extremal BHs, the typical frequency value for a superradiant mode,  $\bar{\omega} \sim 1/2$ , so this margin is sufficient even for observing the effects in non-superradiant modes. Due to the circular symmetry,  ${}_s\mathcal{E}_{\ell, -m}(c) = {}_s\mathcal{E}_{\ell m}(-c)$ , instead of computing for negative values of  $c$ , we will consider all integer azimuthal numbers  $|m| \leq \ell$ .

#### 4.1.1 Leaver method

The first method implemented was Leaver's. Consists is using the three recursion relation obtained for SWSHs and correspondent continued fraction (3.48) and it's inversions. Since the problem is now numerical, we have to stop the continued fraction at some particular  $p = N$ . By substitution of the parameters  $s$  and  $m$  and  $c$ , we are left with an equation with  $N$  roots for  ${}_s\mathcal{E}_{\ell m}$ . A root-finding algorithm is a method that allows to approximate roots of some equation  $f(x) = 0$ , by suggestion of a connected region were  $f$  has different signs at the boundary. The method "FindRoot" in Mathematica<sup>TM</sup> allows to distinguish the roots of equation by finding the closest to a particular input value. Firstly, we use the the expansion coefficients for  $c \ll 1$  (Appendix D) to suggest a value of the eigenvalue  ${}_s\mathcal{E}_{\ell m}$  that is close to  $\ell(\ell + 1)$ . We improved on this method by starting the curve at  $c = 0$ , and then obtaining the eigenvalue numerically for small increments in  $c$  and then using the last eigenvalue solution as the initial guess for the next increment. This is particularly useful to generate and save a complete table of eigenvalues for given range and then use interpolation methods to guess eigenvalues for intermediate  $c$  values.

For both methods the obtained curves are well behaved for  $\ell = 1$ , but for bigger  $\ell$  we start to observe some discontinuities, especially when we increase the range of  $c$ . For a

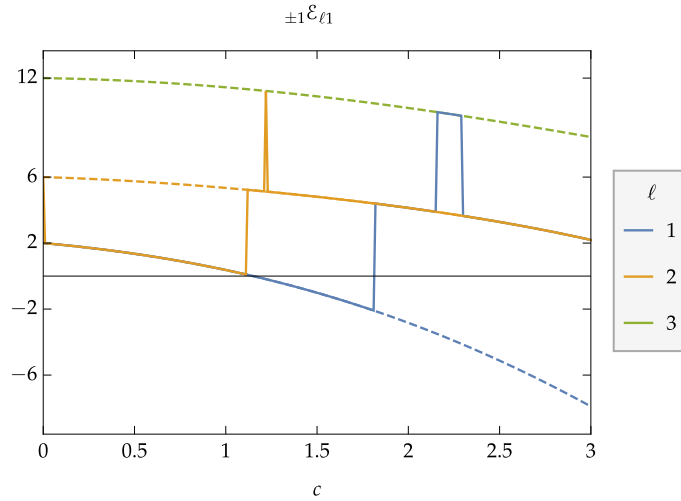


FIGURE 4.1: Showcasing discontinuities in the values of  $\pm 1\mathcal{E}_{\ell 1}$  for  $m = 1, 2$  when using incorrect implementation of the Leaver method. Real values of the eigenvalues are shown as dashed lines ( $m = 1, 2, 3$ ) of the same color.

fixed  $s$  and  $m$ , we have an infinite number of curves labeled by  $\ell$  and in some cases the root finding algorithm selecting roots from adjacent curves, either from the branch  $\ell - 1, \ell + 1$  or even distant values. These solutions cannot ever intersect, otherwise the eigenvalue

would be degenerate and the SWSHs would not be a orthogonal basis of functions. The issue rests on the lack of accuracy when identifying of the  $\ell$ -th root. We lose accuracy when trying to obtaining roots on levels further down in the continued fraction. We solve the problem by considering the inversion (3.49), choosing  $r = \ell + \max\{|m|, |s|\}$ , as the main information in the value taken by the  $\ell$ -th root is in the  $\beta_r$ , with the continuous fractions providing higher order contributions in  $c$ .

Once the eigenvalue root is know, one can find any number of the series expansions coefficients  $a_p$ , for a particular eigenfunction (3.45), by using the three-coefficient recursion relation (3.46).

#### 4.1.2 Spectral method

Due to initial problems with the Leaver method, we decided to use the spectral method. Because the spheroidal Eq. (3.39) can be seen as a perturbed version of the spherical case,  $c = 0$ . We may rewrite the equation using three operators depending on their order in  $c$ ,

$$(\mathcal{H}^{(0)} + \mathcal{H}^{(1)} + \mathcal{H}^{(2)})_s S_{\ell m} = -{}_s \mathcal{E}_{\ell m} {}_s S_{\ell m} \quad (4.1)$$

The zeroth order operator  $\mathcal{H}^{(0)}$ , defines the eigenvalue problem for the spin-weighted spherical harmonics, which will provide the complete non-perturbed basis,  $\mathcal{H}^{(0)} {}_s Y_{\ell m} = -\ell(\ell + 1) {}_s Y_{\ell m}$ . The other two operators are quickly identified from the angular equation as  $\mathcal{H}^{(1)} = -2sc \cos \theta$  and  $\mathcal{H}^{(2)} = c^2 \cos^2 \theta$ . Simple perturbation theory states that

$$\begin{aligned} {}_s \mathcal{E}_{\ell m} &= \ell(\ell + 1) - \int d\Omega ({}_s Y_{\ell m})^* \mathcal{H}^{(1)} {}_s Y_{\ell m} + \mathcal{O}(c^2) , \\ {}_s S_{\ell m} &= {}_s Y_{\ell m} - \sum_{j \neq \ell} \frac{\int d\Omega ({}_s Y_{jm})^* \mathcal{H}^{(1)} {}_s Y_{\ell m}}{j(j + 1) - \ell(\ell + 1)} {}_s Y_{jm} + \mathcal{O}(c^2) . \end{aligned} \quad (4.2)$$

We may include  $\mathcal{H}^{(2)}$  by using a higher order expansion, which can be found in any Quantum Mechanics textbook. The integrals  $\int d\Omega ({}_s Y_{jm})^* \mathcal{H}^{(1)} {}_s Y_{\ell m}$  and  $\int d\Omega ({}_s Y_{jm})^* \mathcal{H}^{(2)} {}_s Y_{\ell m}$  may be computed using Clebsch-Gordon coefficients decomposition generalized for spin-weighted harmonics (C.11). These operators can be written in terms of general matrix

elements in the basis of spin-weighted spherical harmonics,

$$\begin{aligned} h_{j\ell}^{(1)} &= \int d\Omega \cos \theta ({}_s Y_{jm})^* {}_s Y_{\ell m} = \sqrt{\frac{2\ell+1}{2j+1}} \langle \ell, m; 1, 0 | j, m \rangle \langle \ell, -s; 1, 0 | j, -s \rangle, \\ h_{j\ell}^{(2)} &= \int d\Omega \cos^2 \theta ({}_s Y_{jm})^* {}_s Y_{\ell m} = \frac{\delta_{j\ell}}{3} + \frac{2}{3} \sqrt{\frac{2\ell+1}{2j+1}} \langle \ell, m; 2, 0 | j, m \rangle \langle \ell, -s; 2, 0 | j, -s \rangle, \end{aligned} \quad (4.3)$$

remembering that  $\cos \theta$  and  $\cos^2 \theta$  can be rewritten using  ${}_0 Y_{10}(\theta, \varphi)$  and  ${}_0 Y_{20}(\theta, \varphi)$ . The first integral is proportional Leaver series coefficient  $f_1$  defined in Appendix D.

Perturbation theory shows that the SWSHs can be expanded using of spherical harmonics. This should not be a surprising fact as any angular function  $f(\theta, \varphi)$  with a particular spin-weight can be represented using a decomposition using spin-weighted spherical harmonics. Having this idea in mind, we write

$${}_s S_{\ell m}(c; \theta, \varphi) = \sum_j b_j^{(\ell)} {}_s Y_{jm}(\theta, \varphi) \quad \left( \ell, j \geq \max\{|s|, |m|\} \right). \quad (4.4)$$

Replacing the expansion in Eq. (4.1), we can take advantage of the orthogonality of the harmonics,  $\int d\Omega ({}_s Y_{jm})^* {}_s Y_{\ell m} = \delta_{\ell j}$ , by multiplying the the equation by  $({}_s Y_{\ell m})^*$  and integrating the solid angle. The angular equation is replaced by an eigenvalue matrix equation  $\sum_j a_{ij} b_j^{(\ell)} = -{}_s \mathcal{E}_{\ell m} b_i^{(\ell)}$ , such that

$$a_{ij} = \begin{cases} c^2 h_{ii}^{(2)} - 2sc h_{ii}^{(1)} - i(i+1) & i = j \\ c^2 h_{ij}^{(2)} - 2sc h_{ij}^{(1)} & |i-j| = 1 \\ c^2 h_{ij}^{(2)} & |i-j| = 2 \\ 0 & \text{otherwise} \end{cases} \quad \left( i, j \geq \max\{|s|, |m|\} \right), \quad (4.5)$$

where the the eigenvalues of this matrix are  $-{}_s \mathcal{E}_{\ell m}$  and the correspondent eigenvector is given by  $b_j^{(\ell)}$ .

Like the Leaver method, we will have to truncate the matrix at some finite size. From Eq. (4.5), we know that the zeroth order contribution to the  $\ell$ -th eigenvalue will be the element  $a_{\ell\ell}$ . We opted to implement a  $N \times N$  centered submatrix such that  $i, j \geq \ell_{\min} \equiv \max\{|s|, |m|\}$  and truncating the matrix at  $N > \ell + 1 - \ell_{\min}$ , in order to include the  $a_{\ell\ell}$  terms in the approximation. In reality, we must implement a variable  $N \equiv N(c)$ , so that it increases the size of the taken submatrix in order to include extra corrections for larger values of  $c$ . The size of submatrix also increases linearly with  $\ell$ . The best way to



approximate  ${}_s\mathcal{E}_{\ell m}$  would be to not to construct the submatrix including all values of  $\ell_{\min}$  but center the submatrix at  $a_{\ell\ell}$  and increase its size to fine-tune the eigenvalue. Since we will take very large  $\ell$  values, we will use the first method for simplicity.

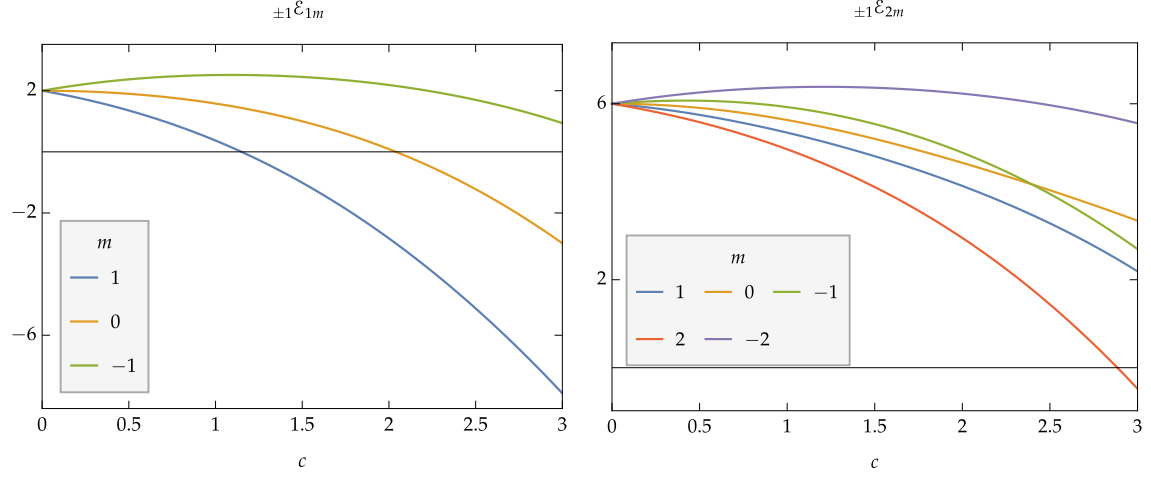


FIGURE 4.2: Eigenvalues for  $\ell = 1$  (left) and  $\ell = 2$  (right) for typical values of  $c$ , using the spectral method.

Optimized numerical methods allow for fast computation of the eigenvalues and eigenvectors of a band-diagonal matrix. The “Eigensystem” method found in Mathematica™ returns a array of eigenvalues and their correspondent normalized eigenvectors, guaranteeing Eq. (3.43). Since the result is positively sorted list of  $-{}_s\mathcal{E}_{\ell m}$ , with  $0 \leq \ell - \ell_{\min} \leq N - 1$ , of which we need to select the negative of the  $(N - \ell + \ell_{\min})$ -th element. We show EM eigenvalues form lower  $\ell$  values in Figure 4.2. This procedure also returns correct eigen-

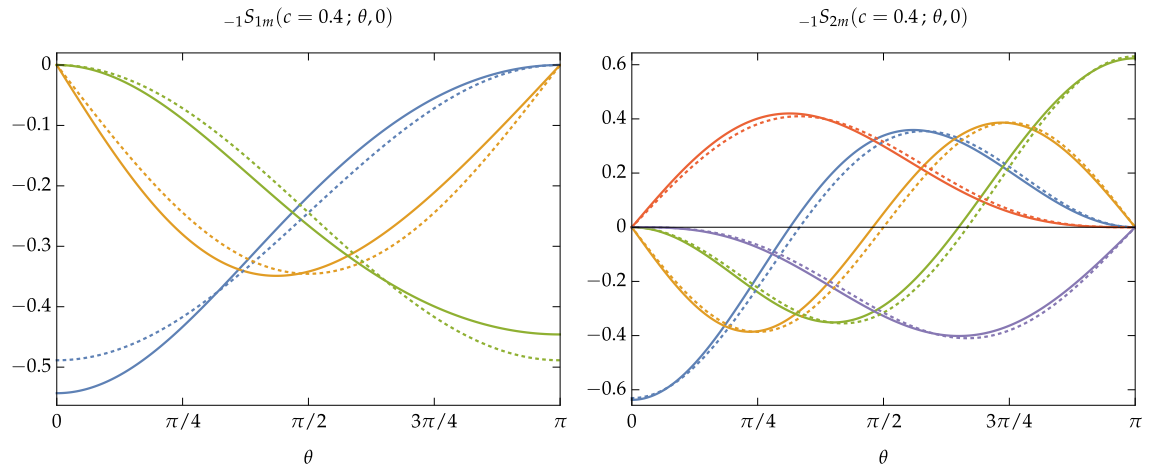


FIGURE 4.3: Plots of all spin-weighted spheroidal harmonics  $-{}_1S_{\ell m}(\theta, 0)$  with  $\ell = 1$  (left) and  $\ell = 2$  (right) for  $s = -1$  and  $c = 0.4$ . This plot shares the same legend coloring as the above (Figure 4.2). Dotted curves represent the values of the  $-{}_1Y_{\ell m}$ , when  $c \rightarrow 0$ .

vector for approximating the eigenfunction using (4.4). In order to ensure that the SWSHs have the same phase convolutions of their spherical counterparts, we must ensure that the correspondent eigenvector has  $b_\ell^{(\ell)} > 0$ , by mapping the obtained vector components as  $b_j^{(\ell)} \mapsto \text{sgn}(b_\ell^{(\ell)}) b_j^{(\ell)}$ . This process is computationally more stressful, since it requires the computing and combining  $N$  different spherical harmonics with the same  $s$  and  $m$ . In the superradiance range, the values of  $c$  can be small ( $< \frac{1}{2}|m|$ ), therefore the SWSHs may not differ greatly from  ${}_sY_{\ell m}(\theta, \varphi)$ , with smaller deviations as  $\ell$  increases (e.g. see Figure 4.3). In this regime, we may use pure spin-weighted spherical harmonics as approximations, as they not change the qualitative behaviour of the  ${}_sS_{\ell m}(\theta, \varphi)$ .

## 4.2 Amplification factor

Finding non-approximate form to the amplification factor  ${}_{\pm 1}Z_{\ell m}$  requires the numerical solving of the radial Eq. (3.53), which is already in an adimensional form. We computed the angular eigenvalues beforehand, which depend on the mode  $(\ell, m)$  as well as the coupling  $c = a\omega$ . Additionally the equation depends on the BH parameters  $(M, J)$  and  $\omega$  explicitly, but it is possible to normalize all variables so that we only need to specify  $(\mathcal{J}, \ell, m, \bar{\omega})$ , where  $\mathcal{J} = a/M = J/M^2$ . We choose to work with barred frequencies because  $\bar{\Omega}_H = \mathcal{J}/2$ , which makes it easier to numerically select superradiant modes.

We need to obtain numerical interpolations for  ${}_{\pm 1}R_{\ell m}$ , by integrating the solution outwards from the horizon, at  $x = 0$ , up to a sufficiently large  $x_\infty \gg |\bar{\omega}|^{-1}$ . The solutions for  $s = \pm 1$  contain the all the EM field information, but they have different asymptotic behaviors. For  $\phi_0$ , Eq. (3.59) tells us that the ingoing coefficient tends to overshadow the outgoing coefficient, while the opposite occurs for  $\phi_2$ . This way seems natural to try to solve the both equations, where we can obtain  $\mathcal{Y}_{\text{in}}$  and  $\mathcal{Z}_{\text{out}}$  separately (Table 3.2).

Knowing the irregularities of the solution at the horizon, we propose the ansatz

$${}_{\pm 1}R_{\ell m} = (r_+)^{\mp 1} x^{\mp 1 - i\omega/\tau} f_{\pm}(x), \quad (4.6)$$

where  $f(x)$  is a new function obeys a regular second-order differential equation. Thus we need to set two initial conditions at the horizon,  $f_{\pm}(0)$  and  $f'_{\pm}(0)$ . We expect to  $|f_{\pm}(x)|$  to become approximately constant to large  $x$ , because this form is written in way that also matches the behavior of the radial function at infinity,  ${}_{\pm 1}R_{\ell m} \sim r^{\mp 1}$ .

Comparing Eq. (4.6) with the asymptotic form at large  $x$  as well as near the horizon, we obtain

$$\begin{aligned} r_+ \tau \frac{y_{\text{in}}}{y_{\text{hole}}} &= \frac{f_+(x_\infty)}{f_+(0)} \exp \left[ -i\bar{\omega}x_\infty - i\bar{\omega}(2-\tau) \log(x_\infty) - i\frac{\omega}{\tau} \log(x_\infty) \right] , \\ \frac{1}{r_+ \tau} \frac{z_{\text{out}}}{z_{\text{hole}}} &= \frac{f_-(x_\infty)}{f_-(0)} \exp \left[ +i\bar{\omega}x_\infty + i\bar{\omega}(2-\tau) \log(x_\infty) - i\frac{\omega}{\tau} \log(x_\infty) \right] . \end{aligned} \quad (4.7)$$

If both solutions are normalized such that  $f_\pm(0) = 1$ , then we have to deal with the relative normalization of  $z_{\text{hole}}/y_{\text{hole}}$ . We can obtain such ratio in terms of known parameters by considering Eq. (3.32) at  $x \simeq 0$ ,

$$(r_+ \tau)^2 \frac{z_{\text{hole}}}{y_{\text{hole}}} = -\frac{\mathcal{B}\tau^2}{2\omega(i\tau + 2\omega)} . \quad (4.8)$$

Therefore to compute the amplification factor we use ( $f_\pm(0) = 1$ )

$${}_{\pm 1}Z_{\ell m} = \frac{\mathcal{B}^2\tau^4}{4\omega^2(\tau^2 + 4\omega^2)} \left| \frac{f_-(x_\infty)}{f_+(x_\infty)} \right|^2 - 1 . \quad (4.9)$$

Another way of dealing with the relative normalization would be to select different initial conditions at the horizon  $x = 0$ . We could cancel the relative normalization of  $z_{\text{hole}}/y_{\text{hole}}$  if we would set any normalization which results in  $f_-(0)/f_+(0) = -\mathcal{B}\tau^2/[2\omega(i\tau + 2\omega)]$ , eliminating the dependence of  $\mathcal{B}, \tau, \omega$  in Eq. (4.9).

The differential equation obtained from substituting (4.6) into Eq. (3.53) is identically zero for  $x = 0$ . Therefore no matter what initial conditions set for  $f_\pm'$  the system would not evolve due to stiffness, which makes the step size of the integrator effectively zero. The usual solution for stiff differential equation is to start the solver a small distance from the horizon  $\epsilon > 0$ . We adjust the initial conditions by substituting the series expansion of  $f_\pm(x) = \sum_{n=0}^{N_H} a_n x^n$  in the radial equation, discarding a terms higher than  $\mathcal{O}(x^{N_H})$  and obtaining the coefficients  $a_n \propto a_0, 1 \leq n \leq N_H$ . Therefore we may set the initial conditions as

$$f_\pm(\epsilon) = f_\pm(0) \sum_{n=0}^{N_H} \left( \frac{a_n}{a_0} \right) \epsilon^n , \quad f'_\pm(\epsilon) = f'_\pm(0) \sum_{n=1}^{N_H} \left( \frac{a_n}{a_0} \right) \epsilon^n , \quad (4.10)$$

$f_\pm(0) = 1$  are the original horizon conditions consider. We found  $\epsilon = 10^{-12}$ ,  $N_H = 6$  and  $x_\infty = 200 \times 2\pi/|\bar{\omega}|$  working perfectly for the “NDSolve” integrator. Effectively we will have  $|f'_\pm(\epsilon)| \simeq \epsilon$ , but this contribution is sufficient to remove stiffness from the system

and has important contributions in case of extremal BHs ( $\mathcal{J} \rightarrow 1$ ).

This previous method requires us to call the integrator twice which is not very effective numerically. Exploring the conservation of the wronskian (conserved current) of Eq. (3.56), we can obtain

$$\frac{dE_{\text{out}}}{dt} - \frac{dE_{\text{in}}}{dt} = \frac{dE_{\text{hole}}}{dt}, \quad (4.11)$$

which simply states total energy conservation. Therefore we can rewrite Eq. (3.78) only using *hole-in* ratio, thus we are able to get the amplification factor with just with the  $s = +1$  solution,

$${}_{\pm 1}Z_{\ell m} = -\frac{\bar{\omega}\tau^2}{\omega} \left| \frac{f_+(0)}{f_+(x_\infty)} \right|^2. \quad (4.12)$$

If we use the *out-hole* ratio in the amplification factor we only need to solve for  $s = -1$ ,

$${}_{\pm 1}Z_{\ell m} = -\left(1 + \frac{\mathcal{B}^2\tau^2}{4\bar{\omega}\omega(\tau^2 + 4\omega^2)} \left| \frac{f_-(x_\infty)}{f_-(0)} \right|^2\right)^{-1}. \quad (4.13)$$

Results from computing the mode  $\ell = m = 1$  at  $\mathcal{J} = 0.9999$ , we obtain a maximum amplification of about 4.36% for a frequency of about  $\omega M \simeq 0.436$ . Modes in the region (3.84) have always  ${}_{\pm 1}Z_{\ell m} > 0$ , but decreases heavily in orders of magnitude as  $\ell$  increases (Figure 4.6).

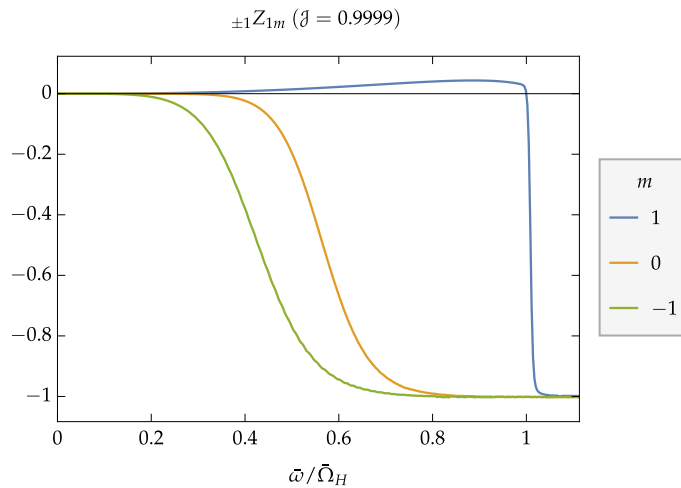


FIGURE 4.4: Amplification factor of an extremal BH ( $\mathcal{J} = 0.9999$ ) for modes with  $\ell = 1$ . In figure, superradiance occurs only for  $m = 1$  as predicted.

Thus we have three ways of computing  ${}_{\pm 1}Z_{\ell m}$ , which only two of them are independent. We rename these different forms in Eqs. (4.12), (4.13), (4.9) as  $Z^{(1)}$ ,  $Z^{(2)}$ ,  $Z^{(3)}$ , respectively. We can rearrange the expressions, so that we have

$$Z^{(3)} = Z^{(1)} \left[ 1 + \frac{1}{Z^{(2)}} \right] - 1. \quad (4.14)$$

It is expected that if the amplification factors based only on a single solution are approximately equal, then the same would be true when considering the third factor, which uses both solutions. But from a better look at Figure 4.5 we can see that this fact is not true, especially in higher values of  $\ell$ . Somehow it appears that we are not able to compute the

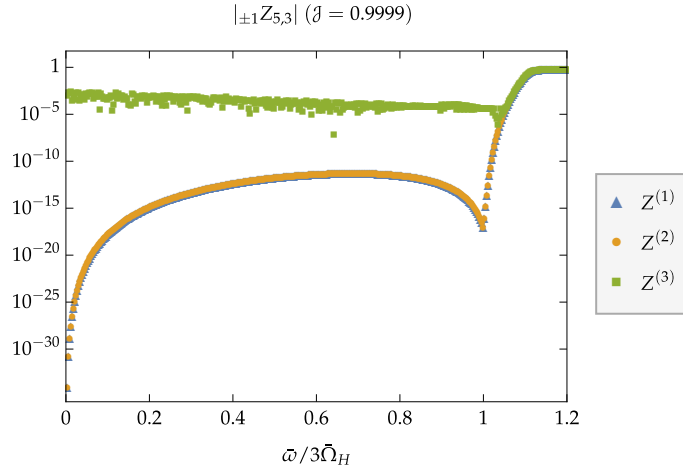


FIGURE 4.5: Log plot demonstrating error propagation for  ${}_{\pm 1}Z_{5,3}$  when computing the factor using both numerical solutions for the radial part of  $\phi_0$  and  $\phi_2$ .

ratio of  $\mathcal{Y}_{\text{in}}$  and  $\mathcal{Z}_{\text{out}}$  with enough accuracy, probably because the large values that  $f_{\pm}(x_{\infty})$  take do not hold the necessary precision to perform the division.

Picking carefully a superradiant frequency. For larger values of  $\ell$  (with small  $m$ ) the gain/loss is practically zero. Still we have huge differences in the order of magnitude of the amplification factor when comparing results from using only one solution and using both. Since two different equations are numerically solved, it will always be a discrepancy,  $Z^{(2)} = Z^{(1)}(1 + \eta)$ , with  $\eta$  very small. The problem is that this error is propagated in absolute value,  $Z^{(3)} \simeq Z^{(1)} - \eta$ . For example, when  $(\mathcal{J}, \ell, m, \bar{\omega}) = (0.9999, 5, 3, 0.1)$  we have  $\eta \simeq -0.003$  and  $Z^{(1)} \sim 10^{-20}$ , which implies that when using both solutions we have a discrepancy of a factor of  $10^{17}$ . Therefore we cannot use the expression  $Z^{(3)}$  to compute the amplification factor, when we have  $\eta \gg Z^{(1)}, Z^{(2)}$ .

We go a step further to increase the numerical precision in this problem by considering higher order terms in the asymptotic expansion of Eq. (3.59). Separately, we will substitute both two asymptotic series in Eq. (3.53), one for the ingoing part and another for the outgoing. Together they have the form

$$_{-1}R_{\ell m}(r) = e^{-i\bar{\omega}x} x^{-1-i(2-\tau)\bar{\omega}} \sum_{n=0}^{N_\infty} I_n x^{-n} + e^{-i\bar{\omega}x} x^{1+i(2-\tau)\bar{\omega}} \sum_{n=0}^{N_\infty} O_n x^{-n}, \quad (4.15)$$

where we identify  $I_0 r_+ = \mathcal{Z}_{\text{in}}/\mathcal{Z}_{\text{hole}}$  and  $O_0/r_+ = \mathcal{Z}_{\text{out}}/\mathcal{Z}_{\text{hole}}$ . Although we have chosen the  $s = -1$  solution, the same procedure can be done for  $s = +1$ , because when using a higher order expansion, both ingoing and outgoing coefficients are present.

Firstly, we directly substitute the series into Eq. (3.53), neglecting terms above  $\mathcal{O}(x^{N_\infty})$  and grouping the exponentials terms, in order to obtain  $I_n \propto I_0$ ,  $O_n \propto O_0$  ( $1 \leq n \leq N_\infty$ ), exactly like the series used above to define boundary conditions at the horizon. Secondly, substitution of the numerical ansatz (4.6) in the LHS of the previous equation, together with it's derivative, we have a system two linear equations, which in the limit of large- $x$  limit allows to determine

$$\frac{1}{r_+} \frac{\mathcal{Z}_{\text{in}}}{\mathcal{Z}_{\text{hole}}} = I_0 \left( f_-(x_\infty), f_-'(x_\infty) \right), \quad r_+ \frac{\mathcal{Z}_{\text{out}}}{\mathcal{Z}_{\text{hole}}} = O_0 \left( f_-(x_\infty), f_-'(x_\infty) \right). \quad (4.16)$$

Lastly, we may use previous expression (4.11) to compute  $_{\pm 1}Z_{\ell m}$  only using one of the coefficient, instead of using Eq. (3.80). This new method solves some of the precision problems from the first method when using both  $\phi_0$  and  $\phi_2$ , for a smaller  $x_\infty = 80 \times 2\pi/|\bar{\omega}|$  and  $N_\infty = 10$ , with the same  $\epsilon = 10^{-12}$ .

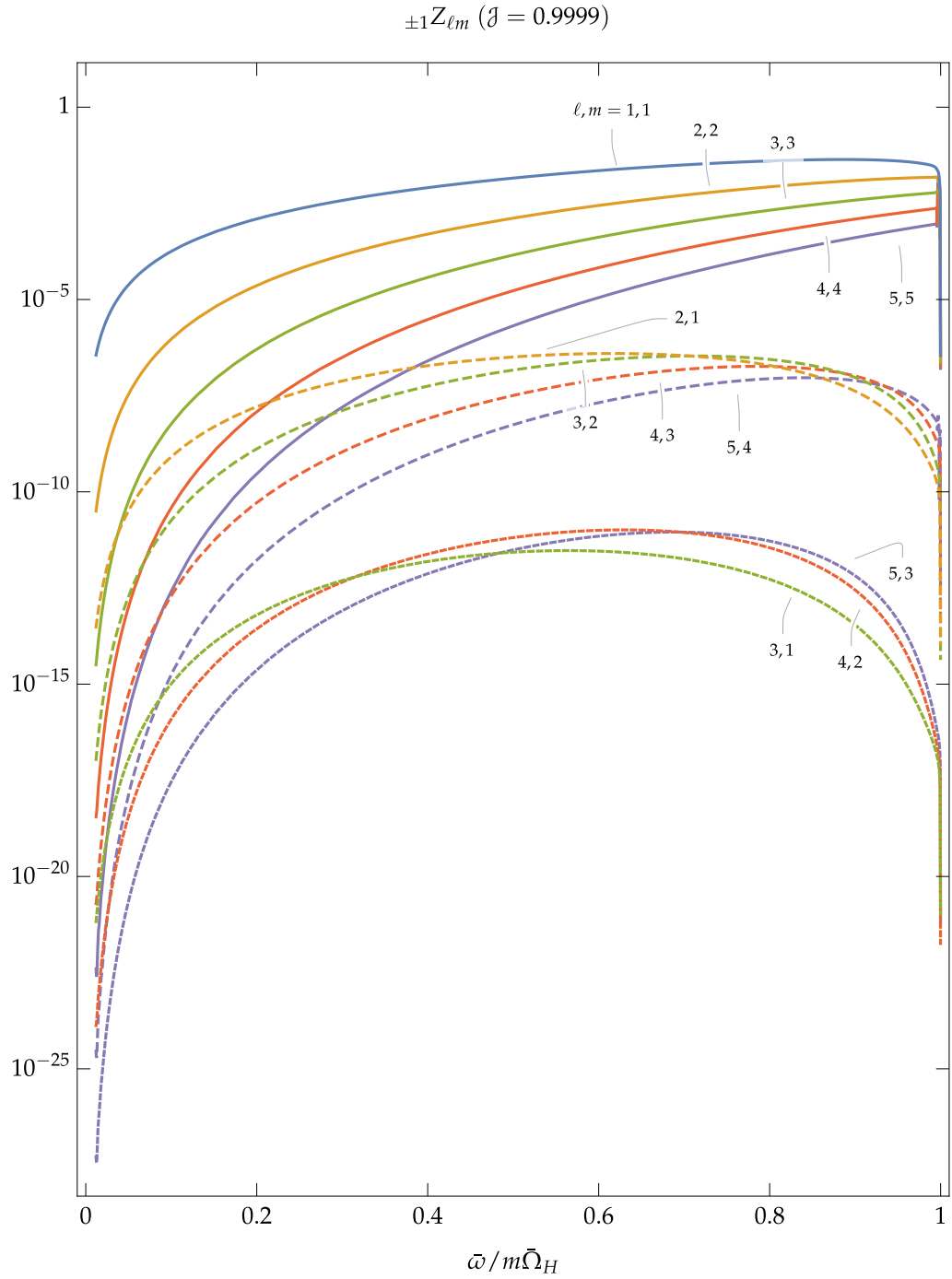


FIGURE 4.6: MoreZPlots

## Chapter 5

# Superradiant scattering of plane waves

The prediction of EM and gravitational radiation amplification was a surprising prediction of Einstein's theory of gravitation in Kerr geometry. A method for direct or indirect observation of this process would provide a probe for rotating BHs and thus it would constitute an important test of GR in regions of extreme gravity. We owe to find in which conditions the scattering an EM wave composed of multiple mode  $(\omega, \ell, m)$  provides information to probe the occurrence of superradiance in a BH. We know that each mode will be independently amplified/attenuated as shown above. The challenge is to predict if superradiant scattering occurred given the wave composed of these modified modes.

Having shown that superradiance occurs for small frequencies we need to find astrophysical sources that emit EM waves. Binary systems of rotating neutron stars and BH may exhibit the necessary conditions for superradiant scattering. These objects, also known as pulsars, possess a strong magnetic field with magnetic dipole moment typically not aligned with the rotation axis. Obviously the magnetic field configuration of a neutron star can be very complicated but its main properties are best described by the *oblique-rotator* model, which considers only the leading order in the multipolar expansion, *i.e.* a magnetic moment dipole

$$\mathbf{m}_P = \frac{m_P}{2} \left[ e^{-i\omega t} \sin \alpha_S (\hat{\mathbf{x}} \pm i\hat{\mathbf{y}}) + \cos \alpha_S \hat{\mathbf{z}} \right] + \text{c.c.}, \quad (5.1)$$

where  $\omega$  is the frequency of rotation. The upper (lower) sign corresponds to a neutron star co-rotating (counter-rotating) with the BH. The moment  $\mathbf{m}_P$  makes an angle  $\alpha_S$  with



respect with the rotation axis, resulting in the precession of the pulsars' magnetic axis, which produces a periodic focused beam of EM radiation. This periodicity is so precise that makes pulsars ideal for measuring time differences in GR tests. Neutron stars usually have a millisecond period producing radiation of a few kHz, which is in range of the superradiant frequencies of a typical stellar mass extremal BH.

(IN NEED OF A FIGURE WITH BH AND PULSAR)

We will focus on scattering of incident plane waves, which means we will consider a source that is far away from the BH. More specifically, we consider incident plane waves from a magnetic dipole source whose electric and magnetic radiation fields, which are found in standard textbook, are given by

$$\begin{aligned} \mathbf{E} &= \frac{\mu_0}{8\pi} \frac{e^{i\omega|\mathbf{r}-\mathbf{r}_S|}}{|\mathbf{r}-\mathbf{r}_S|} \left( \frac{\mathbf{r}-\mathbf{r}_S}{|\mathbf{r}-\mathbf{r}_S|} \times \frac{d^2\mathbf{m}_P}{dt^2} \right) + \text{c.c.} \\ &\simeq -\frac{\mu_0}{8\pi} \frac{e^{i\omega L}}{L} e^{i\mathbf{k}\cdot\mathbf{r}} \left( \hat{\mathbf{r}}_S \times \frac{d^2\mathbf{m}_P}{dt^2} \right) + \text{c.c.}, \end{aligned} \quad (5.2)$$

where  $\mathbf{k} = -\omega\hat{\mathbf{r}}_S$  and  $L = |\mathbf{r}_S|$  is the distance to the source to the BH. This approximation is valid for when  $r = |\mathbf{r}|$  is large compared with the radiation wavelength and the physical dimension of the dipole. Additionally, in the last step we require that  $r \ll L$ . With the similar procedure the magnetic field can be obtain using  $\mathbf{B} \simeq -\hat{\mathbf{r}}_S \times \mathbf{E}$ . Thus, when sufficiently far away from the dipole the radiation can be seen as plane waves propagating in the direction of  $(-\hat{\mathbf{r}}_S) = (\sin\theta_0 \cos\varphi_0, \sin\theta_0 \sin\varphi_0, \cos\theta_0)$ .

## 5.1 Harmonics decomposition

By projecting the complex representation of  $\mathbf{E}$  using the perpendicular directions  $\mathbf{e}_{\hat{\theta}_0}$  and  $\mathbf{e}_{\hat{\phi}_0}$ , we can obtain the two EM field polarizations,

$$\epsilon_\theta = \frac{\mu_0 m_P \omega^2 \sin\alpha_S}{8\pi} \frac{e^{i\omega L}}{L} e^{\pm i\varphi_0} \cos\varphi_0, \quad \epsilon_\varphi = \pm i \frac{\mu_0 m_P \omega^2 \sin\alpha_S}{8\pi} \frac{e^{i\omega L}}{L} e^{\pm i\varphi_0}, \quad (5.3)$$

To use results from previous chapters it is convenient to write the EM degrees of freedom using the NP formalism. There is no need for computing both NP scalars, since we know that the result will very similar. Asymptotically we have  $\mathbf{m} \sim \partial_\theta + i \csc\theta \partial_\varphi$ , thus we may show that  $\phi_0 = (\mathbf{E} + i\mathbf{B}) \cdot (\mathbf{e}_\theta + i\mathbf{e}_\varphi)/\sqrt{2}$  and  $2\phi_2 = (\mathbf{E} + i\mathbf{B}) \cdot (\mathbf{e}_\theta - i\mathbf{e}_\varphi)/\sqrt{2}$ . Together with the dipole field approximation, the validity of this expansion is when  $r_+ \ll r \ll L$ . Following the work done in Chapter 4, we will keep using  $\phi_2$  as our primary scalar as it

is the indicated for studying outgoing radiation. Thus, we may write

$$\phi_2^{(\text{plane})} = -\frac{2\pi i}{3} \left( \epsilon_R e^{-i\omega t + i\mathbf{k}\cdot\mathbf{r}} + \epsilon_L^* e^{i\omega t - i\mathbf{k}\cdot\mathbf{r}} \right) \sum_{m=-1}^{+1} {}_{-1}Y_{1,m}(\theta_0, \varphi_0)^* {}_{-1}Y_{1,m}(\theta, \varphi), \quad (5.4)$$

where  $\hat{\mathbf{k}} \equiv (\theta_0, \varphi_0)$  and  $\hat{\mathbf{r}} \equiv (\theta, \varphi)$  are the directions of incidence and observation, respectively. This result can be easily obtained by explicitly expanding the harmonics sum. The left and right polarizations are defined as

$$\begin{aligned} \epsilon_R &= \frac{\epsilon_\theta - i\epsilon_\varphi}{\sqrt{2}} = \mp \frac{\mu_0 m_P \omega^2 \sin \alpha_S}{2\sqrt{6}\pi} \frac{e^{i\omega L}}{L} {}_{-1}Y_{1,\pm 1}(\theta_0, \varphi_0), \\ \epsilon_L^* &= \frac{\epsilon_\theta^* - i\epsilon_\varphi^*}{\sqrt{2}} = \pm \frac{\mu_0 m_P \omega^2 \sin \alpha_S}{2\sqrt{6}\pi} \frac{e^{-i\omega L}}{L} {}_{-1}Y_{1,\mp 1}(\theta_0, \varphi_0). \end{aligned} \quad (5.5)$$

It may seem that  $\phi_2$  for a plane wave is approximately describe using only  $\ell = 1$  harmonics, but we must not forgot the angular dependence in

$$e^{i\mathbf{k}\cdot\mathbf{r}} = 4\pi \sum_{\ell,m} i^\ell j_\ell(\omega r) Y_{\ell m}(\theta_0, \varphi_0)^* Y_{\ell m}(\theta, \varphi), \quad (5.6)$$

whose decomposition in terms of  $s = 0$  spherical harmonics is well-known [31], where  $j_\ell(z)$  corresponds to the spherical Bessel function of the first kind. Substitution into the result in a superposition of different spin-weight harmonics and after grouping  $\hat{\mathbf{k}}$  and  $\hat{\mathbf{r}}$  terms these can be expanded using Clebsh-Gordon coefficients.

$$\begin{aligned} \phi_2^{(\text{plane})} &= -2\pi \epsilon_R e^{-i\omega t} \sum_{\ell,m} \left( \sum_{n=\ell-1}^{\ell+1} i^{n+1} j_n(\omega r) \frac{2n+1}{2\ell+1} |\langle n, 0; 1, 1 | \ell, 1 \rangle|^2 \right) {}_{-1}Y_{\ell m}(\hat{\mathbf{k}})^* {}_{-1}Y_{\ell m}(\hat{\mathbf{r}}) \\ &\quad + (\epsilon_R \rightarrow \epsilon_L^*, \omega \rightarrow -\omega) \\ &\sim +2\pi \epsilon_R e^{-i\omega t} \sum_{\ell,m} \left( -\frac{1}{2\omega} \frac{e^{i\omega r}}{r} + (-1)^\ell \frac{\ell(\ell+1)}{8\omega^3} \frac{e^{-i\omega r}}{r^3} \right) {}_{-1}Y_{\ell m}(\hat{\mathbf{k}})^* {}_{-1}Y_{\ell m}(\hat{\mathbf{r}}) \\ &\quad + (\epsilon_R \rightarrow \epsilon_L^*, \omega \rightarrow -\omega). \end{aligned} \quad (5.7)$$

The expression for  $\phi_0$  is very similar, changing the coefficients of  $e^{\pm i\omega r}$  accordingly so they obey Eqs. (3.32) and (3.33) when  $r \gg r_+$ , replacing  ${}_{-1}Y_{\ell m}(\hat{\mathbf{r}}) \rightarrow {}_{+1}Y_{\ell m}(\hat{\mathbf{r}})$ .

We have shown that even a simple plane wave is composition of modes with positive and negative frequencies modulated by the left and right polarizations, respectively,

which are proportional to  $_{-1}Y_{1,\pm 1}(\theta_0, \varphi_0)$ . According to condition (3.84), modes with either  $\omega > 0, m > 0$  or  $\omega < 0, m < 0$  can be amplified. The position of the source modulates the incident wave changing its mode composition. Therefore if the plane wave source co-rotates with the BH, when  $\theta_0 \rightarrow 0$  the positive frequencies dominate because  $\epsilon_L^* \rightarrow 0$ , coinciding with the region where  $m > 0$  harmonics predominate. Analogously, when  $\theta_0 \rightarrow \pi$  negative frequencies dominate as  $\epsilon_R \rightarrow 0$ . In the other hand, when considering counter-rotation and the incidence at one of the poles, harmonics with  $m\omega > 0$  have null coefficients so those modes are never amplified [30]. More specifically, when we have exactly  $\theta_0 = 0$  ( $\theta_0 = \pi$ ) the modes  $m = 1$  ( $m = -1$ ) are the only non-zero contributions of the EM wave if and only if the source co-rotates with the BH, while other  $m$  modes vanish.

(CAN BE USED A FIGURE TO SHOW LEFT/RIGHT DOMINANCE)

## 5.2 Scattering theory

We understand that we (US HUMANS) have limited observational capabilities and only have access to given direction of observation for this hypothetical binary system. If it were possible to map the entire scattered wave with enough detail we could in principle extract and compare each mode with the ones of the emitted wave. For this analysis we would only need to know the global gain/loss factor, given by  $_{\pm 1}Z_{\ell m}$ . Therefore we will resort to scattering theory of waves to study the angular effects of superradiance.

Intuitively, it is understood that only a small part of the incident wave will be scattered by the BH. The scattered part together with the incident wave produce a characteristic interference pattern. In order to differentiate the scattered wave we need to remove the background incident plane wave. Scattering theory assumes that we may write

$$\phi_2 - \phi_2^{(\text{plane})} = f(\theta, \varphi) \frac{e^{i\omega(r_* - t)}}{r} + (\omega \rightarrow -\omega, f \rightarrow g), \quad (5.8)$$

where  $\phi_2$  is written similarly with coefficients  $Z_{\text{out}}$  and  $Z_{\text{in}}$  obtained numerically in Chapter 4.

Up to this point we used the approximation of plane wave first introduced in (5.4), which can only be used in flat space. The fact is that this approximation does not take into account the long-range behaviour of Kerr's gravitational field, which goes as  $\mathcal{O}(\frac{1}{r})$  as obtained in (3.58). We know that from the asymptotic form of the radial function that this can be bypassed by a logarithmic phase-correction in the exponential, substituting

$r \rightarrow r_*$ . We can match the ingoing parts of  $\phi_2$  and  $\phi_2^{(\text{plane})}$  so the scattered part only have outgoing part, obtaining

$$f(\theta, \varphi) = -\frac{\pi \epsilon_R}{\omega} \sum_{\ell, m} \left[ (-1)^{\ell+1} \frac{\ell(\ell+1)}{4\omega^2} \frac{\mathcal{Z}_{\text{out}}}{\mathcal{Z}_{\text{in}}} - 1 \right] {}_{-1}Y_{\ell m}(\hat{\mathbf{k}})^* {}_{-1}Y_{\ell m}(\hat{\mathbf{r}}). \quad (5.9)$$

A similar expression is obtained for  $g(\theta, \varphi)$  proportional to  $\epsilon_L^*$ .

The long-range effect of the background is independent of the BH rotation (also in Schwarzschild), *i.e.* we must not mistake the spherical approximation with long-range effects of the effective gravitational potential. Approximation of plane waves as described in (5.4) also discards the effects of the BH rotation, which is the reason at the plane wave is decomposed using spherical harmonics  ${}_{-1}Y_{\ell m}(\hat{\mathbf{r}})$  instead of SWSHs. We can also recall that the mode factor in Eq. (5.9) is very similar the expression (3.80), derived in Chapter 3. We see that for  $a\omega \rightarrow 0$ ,

$$\frac{\mathcal{B}}{4\omega^2} \frac{\mathcal{Z}_{\text{out}}}{\mathcal{Z}_{\text{in}}} \simeq \frac{\ell(\ell+1)}{4\omega^2} \frac{\mathcal{Z}_{\text{out}}}{\mathcal{Z}_{\text{in}}}, \quad (5.10)$$

remembering that  $\mathcal{B} = [(\pm 1 \mathcal{E}_{\ell m})^2 - 4a^2\omega^2 + 4ma\omega]^{1/2}$ . An argument could be made state that the latter expression for the coefficient is the correct instead of the one in Eq. (5.9), but this approximation is good enough when considering superradiant frequencies  $|\omega| \simeq 0.4\Omega_H$  for a typical stellar mass extremal BH (see Figure 4.3).

### 5.3 Phase shifts

If to assume co-rotation of the source with optimal incidence at  $\theta_0 = \varphi_0 = 0$  we will only need to compute  $f(\theta, \varphi)$ , since  $\epsilon_L^* = 0$ . This assumption eases the need to compute modes other than  $m = 1$ . Therefore, truncating the harmonic expansion (5.9) at some  $\ell = \ell_{\text{max}}$  implies that scattering with incidence on axis reduces the number of necessary harmonics in  $\ell_{\text{max}}(\ell_{\text{max}} + 1)$ .

Proceeding with the sum, it appears that the partial wave sum is divergent near  $\theta = 0$ , since the value of increasing  $f(0, 0)$  seems to increase more with each contribution. (see Figure 5.1). This problem is due to the long-range effect of gravitational potential of BHs. Central potentials falling as  $1/r$  (check (3.58)) do not have effect on the global amplitude of the wave but the scattered wave has phase shifts in each of the modes coefficients, producing a divergence at  $(\theta, \varphi) = (\theta_0, \varphi_0)$ . This problem was also studied in classical

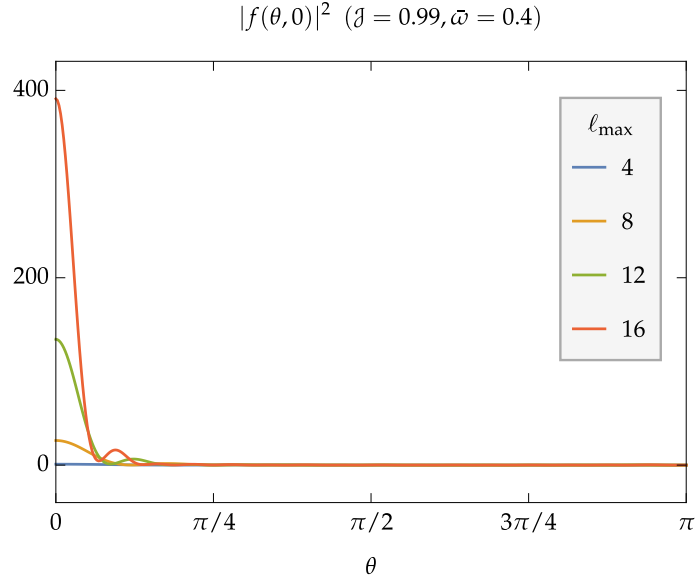


FIGURE 5.1: Eigenvalues for  $\ell = 1$  (left) and  $\ell = 2$  (right) for typical values of  $c$ , using the spectral method.

Coloumb scattering, where  $f(\theta, 0)$  has is known to diverge at  $\theta = \theta_0$ . This result appears strange at first, but we must remember that, being a complete space of functions, the harmonics obey  $\sum_{\ell m} {}_{-1}Y_{\ell m}(\hat{\mathbf{k}})^* {}_{-1}Y_{\ell m}(\hat{\mathbf{r}}) = \delta(\cos \theta - \cos \theta_0) \delta(\varphi - \varphi_0)$ .

In order to regularize the sum for  $f(\theta, \varphi)$ , it is convenient to separate it in two terms,

$$f(\theta, \varphi) = f_N(\theta, \varphi) + f_D(\theta, \varphi), \quad (5.11)$$

$f_N(\theta, \varphi)$  carries all the scattering information about the Newtonian effects of the long-range  $1/r$  (Coulomb) potential. It can be written as

$$f_N(\theta, \varphi) = -\frac{\pi \epsilon_R}{\omega} \sum_{\ell, m} \left( e^{2i\delta_N} - 1 \right) {}_{-1}Y_{\ell m}(\hat{\mathbf{k}})^* {}_{-1}Y_{\ell m}(\hat{\mathbf{r}}), \quad (5.12)$$

where the phase shifts are [32]

$$e^{2i\delta_N} = \frac{\Gamma(\ell + 1 - 2iM\omega)}{\Gamma(\ell + 1 + 2iM\omega)}. \quad (5.13)$$

Assuming an incidence of  $\theta_0 = 0$ , summing the series leads to a similar result as the Rutherford elastic scattering in a Coulomb potential,  $|f_N(\theta, 0)|^2 \sim 1/\sin^4(\theta/2) \sim 1/\theta^4$ , which appears to explain the divergence at  $\theta = 0$ .

On the other hand, the  $f_D(\theta, \varphi)$  encloses all the information regarding the main scattering effects, including superradiance. From Eq. (5.11), simple algebra states that

$$f_D(\theta, \varphi) = -\frac{\pi \epsilon_R}{\omega} \sum_{\ell, m} \left[ \frac{\mathcal{B}}{\ell(\ell+1)} \sqrt{\pm 1 Z_{\ell m} + 1} e^{2i\delta_\ell} - e^{2i\delta_N} \right] {}_{-1}Y_{\ell m}(\hat{\mathbf{k}})^* {}_{-1}Y_{\ell m}(\hat{\mathbf{r}}), \quad (5.14)$$

where we define

$$2\delta_\ell = \arg \left[ (-1)^{\ell+1} \frac{Z_{\text{out}}}{Z_{\text{in}}} \right]. \quad (5.15)$$

In order of this sum to converge two things must occur. First, absolute value of the factor (5.10) must go to 1. Numerically, we find that in the limit of  $\ell/\omega \rightarrow \infty$  superradiant modes are reflected with no change in the amplitude,  $\pm 1 Z_{\ell m} \rightarrow 0$  (check Figure 4.6). Also, from Eq. (3.35) we know that for  $c = a\omega$  constant, increasing  $\ell$  leads to the eigenvalue  $\pm 1 \mathcal{E}_{\ell m} \sim \ell(\ell+1)$ , which cancels the factor in (5.14).

Secondly, the numerically computed phases using (5.15) must converge for the the Newtonian phase shifts (5.13),  $\delta_\ell \rightarrow \delta_N$ . Results appear to indicate that these phases, like  $\delta_N$ , are independent of  $m$ . Also they appear to have the same asymptotic form, apart from a constant value  $\delta_0$ . We attribute this difference to a ambiguity in the definition of the tortoise coordinate, given by

$$r_* = r + \frac{2Mr_+}{r_+ - r_-} \log \left( \frac{r - r_+}{r_+} \right) - \frac{2Mr_-}{r_+ - r_-} \log \left( \frac{r - r_-}{r_-} \right) + \text{const.}, \quad (5.16)$$

which is needed to extract the complex asymptotic coefficients of (3.59). It is expect for this

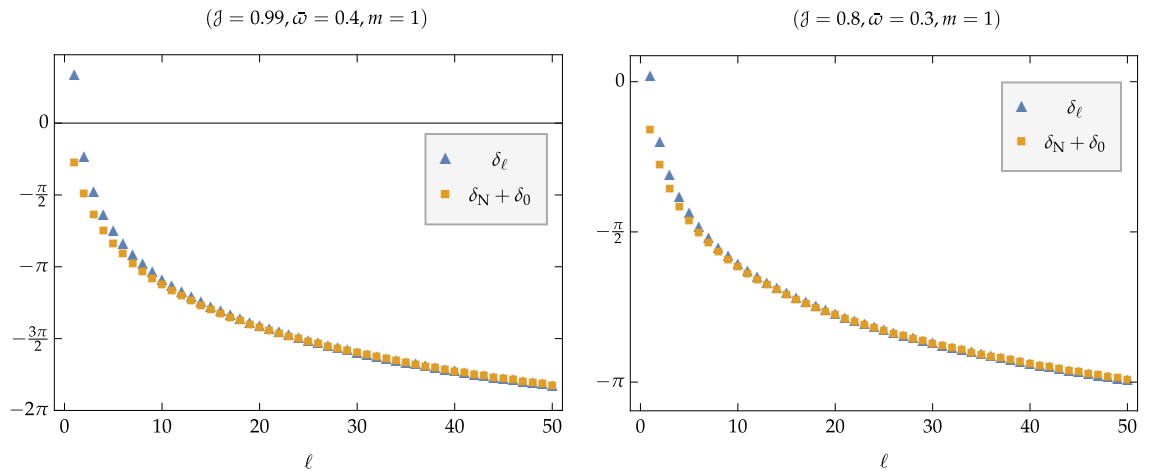


FIGURE 5.2: Eigenvalues for  $\ell = 1$  (left) and  $\ell = 2$  (right) for typical values of  $c$ , using the spectral method.

integration constant to be only dependent on  $a$  and  $M$ , thus for constant  $\bar{\omega}$  the value of  $\delta_0$  should be dependent on  $\mathcal{J}$ . We fit numerically the value of  $\delta_0$  independently for each case. From Figure 5.2 we verify that these phases indeed share the same asymptotic behaviour for large values of  $\ell$ . Effects of superradiance are predominant when  $\ell$  is small and this is reflected in larger deviations of  $\delta_\ell$  from  $\delta_N$ . Decreasing the BH angular momentum,  $\mathcal{J} \rightarrow 1$ , quickly makes the values of  $\delta_\ell$  come closer to  $\delta_N$ . The respective regularized sums for these phases are plotted in Figure 5.3. Comparing with the previous Figure 5.1 it seems

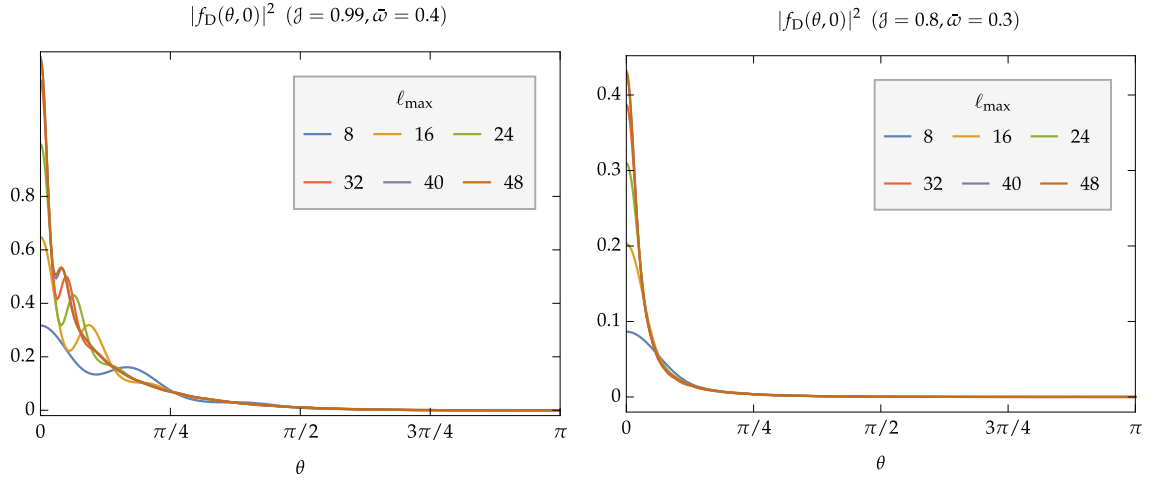


FIGURE 5.3: Eigenvalues for  $\ell = 1$  (left) and  $\ell = 2$  (right) for typical values of  $c$ , using the spectral method.

that the partial wave series for  $|f_D|^2$  is now converging, for values of  $30 < \ell_{\max} < 50$ . The truncation of the series (5.14) at  $\ell = \ell_{\max}$  leads to interference oscillations of characteristic length  $2\pi/\ell_{\max}$ .

The expected values

## **Chapter 6**

### **Discussion and future work**



# Appendix A

## Tetrad techniques

### A.1 Noncoordinate representation

The standard way of expressing quantities in GR was to use a local coordinate basis. This corresponds to use

$$\frac{\partial}{\partial x^\mu} \quad (x^\mu = t, r, \theta, \varphi) \quad (\text{A.1})$$

as our vector basis. One-form basis can be defined the usual way. The tetrad formalism allows for an alternative choice of a *noncoordinate* basis, by introducing a set of linear independent four-vectors,

$$e_a = (e_a)^\mu \frac{\partial}{\partial x^\mu} \quad (a = 1, 2, 3, 4) . \quad (\text{A.2})$$

We will use Greek alphabet  $(\alpha, \beta, \gamma, \dots)$  for the coordinate components and the Latin alphabet  $(a, b, c, \dots)$  for the tetrad components. The tetrad fields also defined directional derivatives, for example for any scalar field  $f$

$$f_{,a} = e_a(f) = (e_a)^\mu \frac{\partial f}{\partial x^\mu} = (e_a)^\mu f_{,\mu} . \quad (\text{A.3})$$

However, this formalism must not be mistaken with as change of coordinates,  $y = \phi(x)$ , such that  $(e_a)^\mu = \partial x^\mu / \partial y^a$ , since those coordinates may not exist. A tetrad frame is a pointwise rotation of the coordinate frame, *i.e.* the concept is related to passive transformations rather than active (diffeomorphisms).

Given any tensor field  $F_{\mu\nu}$ , we can obtain its tetrad components by projecting it onto the tetrad frame,

$$F_{ab} = (e_a)^\mu (e_b)^\nu F_{\mu\nu} . \quad (\text{A.4})$$

We may invert this expression, by defining the inverse tetrad,  $(e^a)_\mu$ , such that

$$(e_a)^\mu (e^b)_\mu = (e_a)^\mu (e^b)^\nu g_{\mu\nu} = \delta_a^b , \quad (\text{A.5})$$

hence invariant quantities remain unchanged,

$$A^2 = A^\mu A_\mu = A^a (e_a)^\mu A_b (e^b)_\mu = A^a A_a . \quad (\text{A.6})$$

We can then substitute the manifold metric for the tetrad “metric”

$$\eta_{ab} = e_a \cdot e_b = g_{\mu\nu} (e_a)^\mu (e_b)^\nu , \quad (\text{A.7})$$

which can be used for raising/lowering tetrad indices,

$$A^a = \eta^{ab} A_b , \quad (\text{A.8})$$

and to contract tetrad components, such as  $\eta_{ab} A^a A^b = A^2$ . This implies that we may return to the original metric using

$$g^{\mu\nu} = \eta^{ab} (e_a)^\mu (e_b)^\nu . \quad (\text{A.9})$$

By analyzing the underlying symmetries of spacetime, one may choose a basis makes the components of  $\eta_{ab}$  constant, which is particularly important for the NP formalism. Going forward, we will assume that this is the case.

## A.2 Spin connection

The analogy with the coordinate basics breaks when applying the a directional derivative of a tetrad components,

$$A_{a,b} = (e_b)^\nu \partial_\nu A_a = (e_b)^\nu \nabla_\nu [(e_a)^\mu A_\mu] = (e_a)^\mu (e_b)^\nu A_{\mu;\nu} + (e_c)^\mu (e_a)_{\mu;\nu} (e_b)^\nu A^c , \quad (\text{A.10})$$

due to extra terms resultant of the tetrad derivatives. Tetrad decompositions,  $A^a$ , are scalars and must not be mistaken as vector fields such as  $(e_a)^\mu$  or  $A^\mu$ . These extra terms can be written using the spin connection

$$\gamma_{cab} = (e_c)^\mu (e_a)_{\mu;\nu} (e_b)^\nu, \quad (\text{A.11})$$

which is antisymmetric in the first two indices,

$$\gamma_{cab} = -\gamma_{acb}, \quad (\text{A.12})$$

due to the metric compatibility of the covariant derivative,  $\nabla_\mu g_{\nu\rho} = 0$ . Nonetheless, this only holds if  $\eta_{ab}$  is constant, otherwise we would have  $\gamma_{abc} + \gamma_{bac} = \eta_{ab,c}$

The other term is called the *intrinsic* derivative of  $A_a$  in the direction of  $e_b$ , being defined as the projection of the tensor  $A_{\mu;\nu}$  in the tetrad frame,

$$A_{a|b} = (e_a)^\mu (e_b)^\nu A_{\mu;\nu} \quad (\text{A.13})$$

If we have a higher rank tensor,  $F_{\mu\nu}$ , we can generalize the intrinsic derivative inverting Eq. (A.10) and generalizing for multiple indices with the use of the spin connection,

$$F_{ab|c} = F_{ab,c} - \eta^{nm} (F_{nb} \gamma_{mac} + F_{an} \gamma_{mbc}). \quad (\text{A.14})$$

Obviously, the spin connection replaces the Christoper symbols,  $\Gamma_{\mu\nu}^\rho$ , in the tetrad formalism, although they are fundamentally different. We will avoid the computation of the Christoper symbols because every equation involving a covariant derivative will become an intrinsic derivative in NP formalism due to tetrad projections. This will become useful during calculations as we generally need  $\frac{1}{2}d^2(d+1)$  computations to fully define the latter, while the spin connection has  $\frac{1}{2}d^2(d-1)$  independent components. For  $d = 4$ , the use of the spin connection implies 16 components less to work with.

## Appendix B

# Additional Newman-Penrose definitions and computations

In this appendix we will present important computations of NP formalism in Kerr background (2.19), using the Kinnersley tetrad defined in (3.13). We will find useful in the one form conversion from the Kinnersley vectors,  $(e_a)^\flat = (e_a)_\mu dx^\mu$ ,

$$\begin{aligned} \mathfrak{l}^\flat &= \frac{1}{\Delta} \left( \Delta, -\rho^2, 0, -a\Delta \sin^2 \theta \right), \\ \mathfrak{n}^\flat &= \frac{1}{2\rho^2} \left( \Delta, \rho^2, 0, -a\Delta \sin^2 \theta \right), \\ \mathfrak{m}^\flat &= \frac{1}{\sqrt{2}\bar{\rho}} \left( ia \sin \theta, 0, -\rho^2, -i(r^2 + a^2) \sin \theta \right), \end{aligned} \tag{B.1}$$

where  $\Delta = r^2 - 2Mr + a^2$ ,  $\bar{\rho} = r + ia \cos \theta$ ,  $\rho^2 = \bar{\rho}\bar{\rho}^*$ .

### B.1 Spin coefficients

The spin connection is defined as the covariant derivative of the tetrad field projected onto the tetrad frame. For example, we write  $\gamma_{412} = \bar{\mathfrak{m}}^\mu \mathfrak{l}_{\mu;\nu} \mathfrak{n}^\nu = \bar{\mathfrak{m}}^\mu \mathfrak{n}^\nu \nabla_\nu \mathfrak{l}_\mu = \bar{\mathfrak{m}}^\mu \Delta \mathfrak{l}_\mu$ . It has 24 components due to the antisymmetry of the first tetrad indices. These can be

encapsulated using 12 complex variables,

$$\begin{aligned}
\kappa &= \gamma_{311} , & \varrho &= \gamma_{314} , & \varepsilon &= \frac{1}{2}(\gamma_{211} + \gamma_{341}) , \\
\sigma &= \gamma_{313} , & \mu &= \gamma_{243} , & \gamma &= \frac{1}{2}(\gamma_{212} + \gamma_{342}) , \\
\lambda &= \gamma_{311} , & \tau &= \gamma_{312} , & \alpha &= \frac{1}{2}(\gamma_{214} + \gamma_{344}) , \\
\nu &= \gamma_{311} , & \pi &= \gamma_{241} , & \beta &= \frac{1}{2}(\gamma_{213} + \gamma_{343}) .
\end{aligned} \tag{B.2}$$

The computation of these coefficients can be done without computation of the Christoffel symbols associated with the covariant derivative. This is cleverly avoided by observing that for any torsion-free connection,  $(e_b)_{[\mu;\nu]} = (e_b)_{[\mu,\nu]}$ . Therefore we define

$$\lambda_{abc} = (e_a)^\mu (e_c)^\nu [(e_b)_{\mu,\nu} - (e_b)_{\nu,\mu}] . \tag{B.3}$$

The computation of the various spin coefficients can be easily performed noticing that  $\lambda_{abc} = \gamma_{abc} - \gamma_{cba}$ , which can be inverted to

$$\gamma_{abc} = \frac{1}{2} (\lambda_{abc} + \lambda_{cab} - \lambda_{bca}) . \tag{B.4}$$

All relevant non-vanishing  $\lambda$ -symbols can be computed by simple coordinate derivatives on the one-form basis,

$$\begin{aligned}
\lambda_{122} &= -\frac{1}{\rho^4} [(r-M)\rho^2 - r\Delta] , & \lambda_{314} &= -\frac{2ia \cos \theta}{\rho^2} , \\
\lambda_{132} &= \frac{i\sqrt{2}ar \sin \theta}{\rho^2 \bar{\rho}} , & \lambda_{324} &= -\frac{ia\Delta \cos \theta}{\rho^4} , \\
\lambda_{213} &= -\frac{\sqrt{2}a^2 \cos \theta \sin \theta}{\rho^2 \bar{\rho}} , & \lambda_{334} &= \frac{(ia + r \cos \theta) \csc \theta}{\sqrt{2}\bar{\rho}^2} , \\
\lambda_{243} &= -\frac{\Delta}{2\rho^2 \bar{\rho}} , & \lambda_{341} &= -\frac{1}{\bar{\rho}} .
\end{aligned} \tag{B.5}$$

All other necessary symbols may be found by the symmetry  $\lambda_{abc} = -\lambda_{cba}$  or by complex conjugation ( $3 \rightleftharpoons 4$ ). For example, for computing the spin coefficient  $\mu$ , we need to use

the relation  $\lambda_{432} = -\lambda_{234} = -(\lambda_{243})^*$ . Assembling all symbols, we obtain

$$\begin{aligned} \kappa = \sigma = \lambda = \nu = 0, \\ \varrho = -\frac{1}{\bar{\rho}}, \quad \mu = -\frac{\Delta}{2\rho^2\bar{\rho}^*}, \quad \tau = -\frac{ia\sin\theta}{\sqrt{2}\rho^2}, \quad \pi = \frac{ia\sin\theta}{\sqrt{2}(\bar{\rho}^*)^2}, \\ \varepsilon = 0, \quad \gamma = \mu + \frac{r-M}{2\rho^2}, \quad \alpha = \pi - \beta^*, \quad \beta = \frac{\cot\theta}{2\sqrt{2}\bar{\rho}}. \end{aligned} \tag{B.6}$$

## Appendix C

# Spin-weighted spherical harmonics

Spin-weight spherical harmonics are a generalization of the standard spherical harmonics found in many well know physical problems such as the hydrogen atom [33–35]. They define a set of eigenfunctions which solves the equation

$$\frac{1}{\sin \theta} \frac{d}{d\theta} \left( \sin \theta \frac{d {}_s Y_{\ell m}}{d\theta} \right) + \left[ s - \frac{(m + s \cos \theta)^2}{\sin^2 \theta} \right] {}_s Y_{\ell m} = -\lambda {}_s Y_{\ell m} , \quad (\text{C.1})$$

with eigenvalues  $\lambda = \ell(\ell + 1) - s(s + 1)$ .

These harmonics are complex functions defined on the  $S^2$ . If take a point in a sphere  $(\theta, \varphi)$ , we can define a right-handed basis at each point,  $\mathbf{e}_\theta = \partial_\theta$  and  $\mathbf{e}_\varphi = 1/\sin \theta \partial_\varphi$ , where  $\mathbf{e}_\theta \cdot \mathbf{e}_\theta = \mathbf{e}_\varphi \cdot \mathbf{e}_\varphi = 1$  and  $\mathbf{e}_\theta \cdot \mathbf{e}_\varphi = 0$ . A given function  $f$  defined on  $S^2$  is said to have spin-weight  $s$  if under the rotation of an angle  $\alpha$  of the tangent vectors to the sphere,

$$\mathbf{e}_\theta \rightarrow \cos \alpha \mathbf{e}_\theta - \sin \alpha \mathbf{e}_\varphi , \quad \mathbf{e}_\varphi \rightarrow \sin \alpha \mathbf{e}_\theta + \cos \alpha \mathbf{e}_\varphi , \quad (\text{C.2})$$

implies that the function transforms as

$$f(\theta, \varphi) \rightarrow e^{is\alpha} f(\theta, \varphi) . \quad (\text{C.3})$$

In the case of spherical symmetry,  $a = 0$ , we may write the Kinnersly angular vector as  $\mathbf{m} = (\mathbf{e}_\theta + i \mathbf{e}_\varphi)/(\sqrt{2}r^2)$ . Under the same transformation, we have  $\mathbf{m} \rightarrow e^{i\alpha} \mathbf{m}$ . From definition (3.15), since we contract the Maxwell tensor with  $\bar{\mathbf{m}}$  once to obtain  $\phi_2$ , we know that  $\phi_2 \rightarrow e^{-i\alpha} \phi_2$ , thus it has spin-weight  $-1$ . On the other hand, for gravitational waves the NP scalars  $\psi_0$  and  $\psi_4$  are double contractions  $\mathbf{m}$  and  $\bar{\mathbf{m}}$  on the Weyl tensor, respectively. Therefore they are  $s = 2$  and  $s = -2$  quantities, respectively.

All spin-weight spherical harmonics can be obtained using raising and lowering operators on the scalar spherical harmonics. In particular we have that  ${}_0Y_{\ell m} = Y_{\ell m}$ . These operators are defined as

$$\begin{aligned}\bar{\partial}f &= -(\sin\theta)^s \left\{ \partial_\theta + \frac{i}{\sin\theta} \partial_\varphi \right\} [(\sin\theta)^{-s}f] = - \left( \partial_\theta + \frac{i}{\sin\theta} \partial_\varphi - s \cot\theta \right) f, \\ \bar{\partial}f &= -(\sin\theta)^{-s} \left\{ \partial_\theta - \frac{i}{\sin\theta} \partial_\varphi \right\} [(\sin\theta)^sf] = - \left( \partial_\theta - \frac{i}{\sin\theta} \partial_\varphi + s \cot\theta \right) f.\end{aligned}\tag{C.4}$$

Is clear from the definition of the operators, that for a function  $f$  is a function with spin-weight  $s$ , then  $\bar{\partial}f$  has spin-weight  $s + 1$  while  $\bar{\partial}f$  has spin-weight  $s - 1$ , due to an extra  $e^{\pm i\alpha}$  factor under the transformation (C.2).

Expanding  $\bar{\partial}\bar{\partial}$  we can found the property that for any function  $f$  with definite spin-weight, we have

$$\frac{1}{2}(\bar{\partial}\bar{\partial} - \bar{\partial}\bar{\partial})f = sf.\tag{C.5}$$

This last equation can also be shown using the properties

$$\begin{aligned}\bar{\partial}{}_sY_{\ell m} &= +\sqrt{\ell(\ell+1) - s(s+1)} {}_{s+1}Y_{\ell m}, \\ \bar{\partial}{}_sY_{\ell m} &= -\sqrt{\ell(\ell+1) - s(s+1)} {}_{s-1}Y_{\ell m}.\end{aligned}\tag{C.6}$$

We can apply multiple raising and lowering operators to obtain any spherical harmonic, given that  $\ell \geq \max\{|m|, |s|\}$ ,

$$\begin{aligned}{}_sY_{\ell m}(\theta, \varphi) &= (-1)^m \sqrt{\frac{2\ell+1}{4\pi}} (\ell+m)!(\ell-m)!(\ell+s)!(\ell-s)! \\ &\times \sum_{k=0}^{\ell-s} \frac{(-1)^m (\sin \frac{\theta}{2})^{m+s+2k} (\cos \frac{\theta}{2})^{2\ell-m-s-2k}}{k!(\ell-m-k)!(\ell-s-k)!(m+s+k)!} e^{im\varphi}\end{aligned}\tag{C.7}$$

For this work, will be useful to list the lowest dipole ( $s = -1, \ell = 1$ ) spherical harmonics

$$\begin{aligned}{}_{-1}Y_{1,\pm 1}(\theta, \varphi) &= -\sqrt{\frac{3}{8\pi}} \sin\theta, \\ {}_{-1}Y_{10}(\theta, \varphi) &= -\sqrt{\frac{3}{16\pi}} (\cos\theta \pm 1) e^{\pm i\varphi},\end{aligned}\tag{C.8}$$



while the  $s = 1$  harmonics can be obtained using properties

$$\begin{aligned} {}_{-s}Y_{\ell m}(\theta, \varphi)^* &= (-1)^{-s+m} {}_sY_{\ell, -m}(\theta, \varphi) , \\ {}_{-s}Y_{\ell m}(\pi - \theta, \varphi + \pi)^* &= (-1)^\ell {}_sY_{\ell m}(\theta, \varphi) . \end{aligned} \quad (\text{C.9})$$

Another possible way of writing the spin-weight spherical harmonics is by using the hypergeometric function,

$$\begin{aligned} {}_sY_{\ell m}(\theta, \varphi) &= (-1)^m \sqrt{\frac{2\ell+1}{4\pi} \frac{(\ell+m)!(\ell-m)!}{(\ell+s)!(\ell-s)!}} \left(\sin \frac{\theta}{2}\right)^{m+s} \left(\cos \frac{\theta}{2}\right)^{2\ell-m-s} \\ &\quad \times {}_2F_1\left(m-\ell, s-\ell, m+s+1; -\tan^2 \frac{\theta}{2}\right) e^{im\varphi} . \end{aligned} \quad (\text{C.10})$$

The product of two spin-weighted spherical harmonics with the same argument can be written as a linear combination of other harmonics, admitting a Clebsh-Gordon decomposition,

$${}_{s'}Y_{j'm'} {}_sY_{jm} = \sum_{S,J,M} C_{SJM} {}_sY_{JM} , \quad (\text{C.11})$$

where

$$\begin{aligned} C_{SJM} &= (-1)^{j+j'-J} \sqrt{\frac{(2j+1)(2j'+1)}{4\pi(2J+1)}} \\ &\quad \times \langle j', m'; j, m | J, M \rangle \langle j', s'; j, s | J, S \rangle \delta_{M, m+m'} \delta_{S, s+s'} , \end{aligned} \quad (\text{C.12})$$

with the restriction that the triangle inequality must hold,  $|j - j'| \leq J \leq j + j'$ .

Since these harmonics are generalizations of the standard  $s = 0$  spherical harmonics, we expect that for each spin-weight  $s$  they form an orthogonal and complete set of functions

$$\begin{aligned} \int d\Omega {}_sY_{\ell'm'}(\theta, \varphi)^* {}_sY_{\ell m}(\theta, \varphi) &= \delta_{\ell\ell'} \delta_{mm'} , \\ \sum_{\ell=|s|}^{\infty} \sum_{m=-\ell}^{\ell} {}_sY_{\ell m}(\theta_0, \varphi_0)^* {}_sY_{\ell m}(\theta, \varphi) &= \delta(\cos \theta - \cos \theta_0) \delta(\varphi - \varphi_0) , \end{aligned} \quad (\text{C.13})$$

so that any spin-weighted  $s$  function  $f(\theta, \varphi)$  can be written as

$$f(\theta, \varphi) = \sum_{\ell=|s|}^{\infty} \sum_{m=-\ell}^{\ell} c_{\ell m} {}_sY_{\ell m}(\theta, \varphi) , \quad (\text{C.14})$$

so each mode coefficient  $c_{\ell m}$  is uniquely defined.

## Appendix D

### Eigenvalue small- $c$ expansion

Using the Leaver continued fraction equation for the eigenvalue, defined in (3.48), is possible to expand the eigenvalue for  $c \ll 1$ ,

$${}_s\mathcal{A}_{\ell m} = \sum_{p=0}^{\infty} f_p c^p. \quad (\text{D.1})$$

Directed substitution into the continued fraction is done in [36, 37], where the coefficients are presented up to  $\mathcal{O}(c^6)$ . Defining

$$h(\ell) = \frac{(\ell^2 - s^2) [\ell^2 - (k_+ - k_-)^2] [\ell^2 - (k_+ + k_-)^2]}{2\ell^3 (\ell^2 - \frac{1}{4})} = \frac{2(\ell^2 - m^2) (\ell^2 - s^2)^2}{\ell^3 (4\ell^2 - 1)} \quad (\text{D.2})$$

we may list the series coefficients below,

$$f_0 = \ell(\ell + 1) - s(s + 1), \quad (\text{D.3a})$$

$$f_1 = -\frac{2ms^2}{\ell(\ell + 1)}, \quad (\text{D.3b})$$

$$f_2 = h(\ell + 1) - h(\ell) - 1 \quad (\text{D.3c})$$

$$f_3 = 2ms^2 \left[ \frac{h(\ell)}{(\ell - 1)\ell^2(\ell + 1)} - \frac{h(\ell + 1)}{\ell(\ell + 1)^2(\ell + 2)} \right], \quad (\text{D.3d})$$

$$f_4 = 4m^2s^4 \left[ \frac{h(\ell + 1)}{\ell^2(\ell + 1)^4(\ell + 2)^2} - \frac{h(\ell)}{(\ell - 1)^2\ell^4(\ell + 1)^2} \right] + \frac{h(\ell + 1)^2}{2(\ell + 1)} - \frac{h(\ell)^2}{2\ell} \\ + \frac{(\ell - 1)h(\ell - 1)h(\ell)}{2\ell(2\ell - 1)} + \frac{h(\ell)h(\ell + 1)}{2\ell(\ell + 1)} - \frac{(\ell + 2)h(\ell + 1)h(\ell + 2)}{2(\ell + 1)(2\ell + 3)}, \quad (\text{D.3e})$$

$$\begin{aligned}
f_5 = & 8m^3s^6 \left[ \frac{h(\ell)}{(\ell-1)^3\ell^6(\ell+1)^3} - \frac{h(\ell+1)}{\ell^3(\ell+1)^6(\ell+2)^3} \right] \\
& + 2ms^2 \left[ \frac{3h(\ell)^2}{2(\ell-1)\ell^3(\ell+1)} - \frac{3h(\ell+1)^2}{2\ell(\ell+1)^3(\ell+2)} + \frac{(3\ell+7)h(\ell+1)h(\ell+2)}{2\ell(\ell+1)^3(\ell+3)(2\ell+3)} \right. \\
& \left. - \frac{(3\ell-4)h(\ell-1)h(\ell)}{2(\ell-2)\ell^3(\ell+1)(2\ell-1)} - \frac{(7\ell^2+7\ell+4)h(\ell)h(\ell+1)}{2(\ell-1)\ell^3(\ell+1)^3(\ell+2)} \right] \quad (D.3f)
\end{aligned}$$

$$\begin{aligned}
f_6 = & \frac{16m^4s^8}{\ell^4(\ell+1)^4} \left[ \frac{h(\ell+1)}{(\ell+1)^4(\ell+2)^4} - \frac{h(\ell)}{(\ell-1)^4\ell^4} \right] \\
& + \frac{4m^2s^4}{\ell^2(\ell+1)^2} \left[ \frac{3h(\ell+1)^2}{(\ell+1)^3(\ell+2)^2} - \frac{3h(\ell)^2}{(\ell-1)^2\ell^3} - \frac{(3\ell^2+14\ell+17)h(\ell+1)h(\ell+2)}{(\ell+1)^3(\ell+2)(\ell+3)^3(2\ell+3)} \right. \\
& + \frac{(11\ell^4+22\ell^3+31\ell^2+20\ell+6)h(\ell)h(\ell+1)}{(\ell-1)^2\ell^3(\ell+1)^3(\ell+2)^2} + \frac{(3\ell^2-8\ell+6)h(\ell-1)h(\ell)}{(\ell-2)^2(\ell-1)\ell^3(2\ell-1)} \left. \right] \\
& + \frac{h(\ell+1)^3}{2(\ell+1)^2} - \frac{h(\ell)^3}{2\ell^2} - \frac{(\ell-1)^2h(\ell-1)^2h(\ell)}{4\ell^2(2\ell-1)^2} + \frac{(\ell-1)(7\ell-3)h(\ell-1)h(\ell)^2}{4\ell^2(2\ell-1)^2} \\
& + \frac{(2\ell^2+4\ell+3)h(\ell)^2h(\ell+1)}{4\ell^2(\ell+1)^2} - \frac{(2\ell^2+1)h(\ell)h(\ell+1)^2}{4\ell^2(\ell+1)^2} \\
& - \frac{(\ell+2)(7\ell+10)h(\ell+1)^2h(\ell+2)}{4(\ell+1)^2(2\ell+3)^2} + \frac{(\ell+2)^2h(\ell+1)h(\ell+2)^2}{4(\ell+1)^2(2\ell+3)^2} \\
& + \frac{(\ell+3)h(\ell+1)h(\ell+2)h(\ell+3)}{12(\ell+1)(2\ell+3)^2} + \frac{(\ell+2)(3\ell^2+2\ell-3)h(\ell)h(\ell+1)h(\ell+2)}{4\ell(\ell+1)^2(2\ell+3)^2} \\
& - \frac{(\ell-1)(3\ell^2+4\ell-2)h(\ell-1)h(\ell)h(\ell+1)}{4\ell^2(\ell+1)(2\ell-1)^2} - \frac{(\ell-2)h(\ell-2)h(\ell-1)h(\ell)}{12\ell(2\ell-1)^2} . \quad (D.3g)
\end{aligned}$$

# Bibliography

- [1] B. P. Abbott et al., *Observation of Gravitational Waves from a Binary Black Hole Merger*, [Phys. Rev. Lett. \*\*116\*\*, 061102 \(2016\)](#), [arXiv:1602.03837](#).
- [2] R. H. Dicke, *Coherence in Spontaneous Radiation Processes*, [Phys. Rev. \*\*93\*\*, 99 \(1954\)](#).
- [3] Y. B. Zel'dovich, *Generation of Waves by a Rotating Body*, [JETP Lett. \*\*14\*\*, 180 \(1971\)](#), [*Zh. Eksp. Teor. Fiz. Pis'ma Red.* **14**, 270 (1971)].
- [4] Y. B. Zel'dovich, *Amplification of Cylindrical Electromagnetic Waves Reflected from a Rotating Body*, [Sov. Phys. JETP \*\*35\*\*, 1085 \(1972\)](#), [*Zh. Eksp. Teor. Fiz.* **62**, 2076 (1972)].
- [5] A. A. Starobinsky, *Amplification of waves reflected from a rotating "black hole"*, [Sov. Phys. JETP \*\*37\*\*, 28 \(1973\)](#), [*Zh. Eksp. Teor. Fiz.* **64**, 48 (1973)].
- [6] A. A. Starobinsky and S. M. Churilov, *Amplification of electromagnetic and gravitational waves scattered by a rotating "black hole"*, [Sov. Phys. JETP \*\*38\*\*, 1 \(1974\)](#), [*Zh. Eksp. Teor. Fiz.* **65**, 3 (1973)].
- [7] N. Deruelle and R. Ruffini, *Quantum and classical relativistic energy states in stationary geometries*, [Phys. Lett. \*\*52B\*\*, 437 \(1974\)](#).
- [8] N. Deruelle and R. Ruffini, *Klein Paradox in a Kerr Geometry*, [Phys. Lett. \*\*57B\*\*, 248 \(1975\)](#).
- [9] S. A. Teukolsky, *Rotating Black Holes: Separable Wave Equations for Gravitational and Electromagnetic Perturbations*, [Phys. Rev. Lett. \*\*29\*\*, 1114 \(1972\)](#).
- [10] E. Newman and R. Penrose, *An Approach to Gravitational Radiation by a Method of Spin Coefficients*, [J. Math. Phys. \*\*3\*\*, 566 \(1962\)](#).
- [11] O. Klein, *Die Reflexion von Elektronen an einem Potentialsprung nach der relativistischen Dynamik von Dirac*, [Z. Phys. \*\*53\*\*, 157 \(1929\)](#).

- [12] F. Sauter, *Über das Verhalten eines Elektrons im homogenen elektrischen Feld nach der relativistischen Theorie Diracs*, [Z. Phys. \*\*69\*\*, 742 \(1931\)](#).
- [13] C. A. Manogue, *The Klein paradox and superradiance*, [Ann. Phys. \*\*181\*\*, 261 \(1988\)](#).
- [14] C. Itzykson and J. Zuber, [Quantum Field Theory](#), Dover Books on Physics (Dover Publications, 2012).
- [15] R. G. Winter, *Klein Paradox for the Klein-Gordon Equation*, [Am. J. Phys. \*\*27\*\*, 355 \(1959\)](#).
- [16] R. Brito, V. Cardoso and P. Pani, [Superradiance: Energy Extraction, Black-Hole Bombs and Implications for Astrophysics and Particle Physics](#), Lecture Notes in Physics, Vol. 906 (Springer International Publishing, 2015) [arXiv:1501.06570v3](#).
- [17] M. Heusler, [Black Hole Uniqueness Theorems](#), Cambridge Lecture Notes in Physics, Vol. 6 (Cambridge University Press, 1996).
- [18] R. Wald, [General Relativity](#) (University of Chicago Press, 1984).
- [19] B. Carter, *Axisymmetric Black Hole Has Only Two Degrees of Freedom*, [Phys. Rev. Lett. \*\*26\*\*, 331 \(1971\)](#).
- [20] R. P. Kerr, *Gravitational Field of a Spinning Mass as an Example of Algebraically Special Metrics*, [Phys. Rev. Lett. \*\*11\*\*, 237 \(1963\)](#).
- [21] S. A. Teukolsky, *The Kerr metric*, [Class. Quantum Grav. \*\*32\*\*, 124006 \(2015\)](#), [arXiv:1410.2130v2](#).
- [22] R. H. Boyer and R. W. Lindquist, *Maximal Analytic Extension of the Kerr Metric*, [J. Math. Phys. \*\*8\*\*, 265 \(1967\)](#).
- [23] J. D. Bekenstein, *Extraction of Energy and Charge from a Black Hole*, [Phys. Rev. \*\*D7\*\*, 949 \(1973\)](#).
- [24] S. Chandrasekhar, [The Mathematical Theory of Black Holes](#), Oxford Classic Texts in the Physical Sciences (Clarendon Press, 1998).
- [25] S. A. Teukolsky and W. H. Press, *Perturbations of a rotating black hole. III. Interaction of the hole with gravitational and electromagnetic radiation*, [Astrophys. J. \*\*193\*\*, 443 \(1974\)](#).
- [26] W. Kinnersley, *Type D Vacuum Metrics*, [J. Math. Phys. \*\*10\*\*, 1195 \(1969\)](#).

- [27] S. A. Teukolsky, *Perturbations of a rotating black hole. I. Fundamental equations for gravitational electromagnetic and neutrino field perturbations*, [Astrophys. J. \*\*185\*\*, 635 \(1973\)](#).
- [28] W. H. Press and S. A. Teukolsky, *Perturbations of a Rotating Black Hole. II. Dynamical Stability of the Kerr Metric*, [Astrophys. J. \*\*185\*\*, 649 \(1973\)](#).
- [29] E. Berti, V. Cardoso and M. Casals, *Eigenvalues and eigenfunctions of spin-weighted spheroidal harmonics in four and higher dimensions*, [Phys. Rev. \*\*D73\*\*, 02401 \(2006\)](#), [Erratum: [Phys. Rev. \*\*D73\*\*, 109902 \(2006\)](#)], [arXiv:gr-qc/0511111v4 \[gr-qc\]](#) .
- [30] J. G. Rosa, *Superradiance in the sky*, [Phys. Rev. \*\*D95\*\*, 064017 \(2017\)](#), [arXiv:1612.01826 \[gr-qc\]](#) .
- [31] J. D. Jackson, *Classical Electrodynamics*, 3rd ed. (Wiley, 1998).
- [32] J. A. H. Futterman, F. A. Handler, and R. A. Matzner, *Scattering from Black Holes*, Cambridge Monographs on Mathematical Physics (Cambridge University Press, 1988).
- [33] J. N. Goldberg, A. J. Macfarlane, E. T. Newman, F. Rohrlich, and E. C. G. Sudarshan, *Spin-s Spherical Harmonics and  $\bar{\partial}$* , [J. Math. Phys. \*\*8\*\*, 2155 \(1967\)](#).
- [34] J. J. G. Scanio, *Spin-weighted spherical harmonics and electromagnetic multipole expansions*, [Am. J. Phys. \*\*45\*\*, 173 \(1977\)](#).
- [35] G. F. Torres del Castillo, *3-D Spinors, Spin-Weighted Functions and their Applications* (Birkhäuser Boston, 2003).
- [36] E. D. Fackerell and R. G. Crossman, *Spin-weighted angular spheroidal functions*, [J. Math. Phys. \*\*18\*\*, 1849 \(1977\)](#).
- [37] E. Seidel, *A comment on the eigenvalues of spin-weighted spheroidal functions*, [Class. Quantum Grav. \*\*6\*\*, 1057 \(1989\)](#).